



OPTICAL SOLITON PROPAGATION IN METAMATERIALS; EVOLUTIONARY  
PATTERN FORMATION FOR COMPETING POPULATIONS  
UNDER SEASONAL FORCING

by

YANAN XU

A THESIS

Submitted in partial fulfillment of the requirements  
for the degree of Doctor of Philosophy in the  
Mathematics and Physics Program  
of Delaware State University

DOVER, DELAWARE  
August 2017

This thesis is approved by the following members of the Final Oral Review Committee:

Dr. Matthew C. Tanzy, Committee Chairperson, Department of Mathematical Sciences, Delaware State University

Dr. Dawn A. Lott, Committee Member, Department of Mathematical Sciences, Delaware State University

Dr. Jinjie Liu, Committee Member, Department of Mathematical Sciences, Delaware State University

Dr. Sokratis Makrogiannis, Committee Member, Department of Physics and Engineering, Delaware State University

Dr. Essaid Zerrad, External Committee Member, Department of Physics and Engineering, Delaware State University

©Yanan Xu  
All rights reserved

## DEDICATION

This thesis is dedicated to my parents, who have fostered the development of a strong work ethic and supported my never-ending curiosity throughout my life. They have provided me with a loving family and framework, from both an educational and ethical standpoint, as well as a sense of adventure upon which I have been able to build my appreciation for the natural world. Without their persistent guidance, support, and advice, the successes I have achieved to date would never have come to fruition.

## ACKNOWLEDGEMENTS

I am extremely grateful to both my supervisors, Matthew C. Tanzy and Anjan Biswas, for their insights, support and encouragement, without whom this process would not have been as smooth or as enjoyable. They always gave freely of their time, encouraged me to publish, and motivated me to work hard. Specific thanks go to Dr. Tanzy for pointing out thought-provoking questions or areas which I would not have considered, his patience and fabulous projects. I would like to thank Dr. Edwards for helping me get out of the tuff situation and planting me the wonderful teaching ideas. I would like to thank Dr. Liu for providing me meaningful advice.

My department friends have made my time here so wonderful. I extend my gratitude particularly to my lab friends, for their accompany in the long run.

I am indebted to my family for the support and encouragement I received to to the Ph.D. and throughout the whole journey. Thank my parents for everything they've done for me.

I offer thanksgiving to God for never giving up on me and for finding ways to remind me of who I've come here to be.

**Optical Soliton Propagation in Metamaterials; Evolutionary  
Pattern Formation for Competing Populations  
under Seasonal Forcing**

**Yanan Xu**

**Faculty Advisor: Dr. Matthew Tanzy**

**ABSTRACT**

Optical metamaterials is a cutting edge technology that is being studied. These Optical metamaterials possess both negative permittivity and negative permeability that cannot be found in nature; but can be engineered by using advanced processing technology. The dynamics of soliton propagation through these optical metamaterials is governed by the non-linear *Schrödinger's* equation(NLSE) with a few perturbation terms. There are a couple of ways this study can be done. One of them is to get specific values of the Super-Gaussian pulse parameters by the aid of collective variables; to recover bright 1-soliton solution by the aid of travelling wave hypothesis for bright soliton solutions of power law and dual-power law media; to obtain doubly periodic functions to the model with mapping method; to retrieve exact soliton solutions by the method of undetermined coefficients which is known as Ansatz scheme; To extract bright and exotic soliton solutions by semi-inverse variational principle; to illustrate the controllability of the Raman soliton self-frequency shift in non-linear metamaterials by numerical results.

Population models can be used to understand the Honey Bee Population Dynamics and other species at interest and also be used to understand the spread of parasites, viruses, and disease. For example, explore the impact of different death rates of forager bees on colony growth and development, evaluate the effects of artificial feeding on bee colony population dynamics, recognize the importance of pollination to our food systems and economics. In our model we describe the effects of seasonal variations on competing population dynamics. We begin with the well understood fisher's equation applied to competing species. Competition is modeled as a non-local effect through a convolution integral with an asymmetric kernel function. Seasonal variations are added by perturbing the competition term with a sinusoidal term,  $\sin(ft)$ . The extent of the non-local coupling is determined by a parameter  $\delta$ , with  $\delta = 0$  corresponding to localization; the degree of asymmetry is characterized by  $\alpha$ , so that when  $\alpha \rightarrow 0$ , the problem becomes symmetric non-local coupling, and  $p \sin(ft)$ , describing

the severity of disturbance, with  $p = 0$  corresponding to static interactions. We study the case where the model admits a stable coexistence equilibrium solution. We access stability conditions of this critical point as a function of  $\alpha$  and  $p$  and determine unstable wave number bands with  $\delta$  beyond the stability boundary. We show the evolutionary nonlinear patterns under varying seasonal forcing with sufficiently non-localization.

# TABLE OF CONTENTS

<b>LIST OF FIGURES OR ILLUSTRATIONS</b> . . . . .	<b>x</b>
<b>ABBREVIATIONS</b> . . . . .	<b>xi</b>
<b>CHAPTER 1 REVIEW OF LITERATURE</b> . . . . .	<b>1</b>
1.1 Optical soliton propagation in Metamaterials . . . . .	1
1.2 Population pattern formation under seasonal forcing . . . . .	5
<b>CHAPTER 2 SUPER-GAUSSIAN SOLITON IN OPTICAL METAMATERIALS USING COLLECTIVE VARIABLES</b> . . . . .	<b>8</b>
2.1 Introduction . . . . .	8
2.2 Mathematical formulation . . . . .	9
2.2.1 Soliton parameter dynamics . . . . .	11
2.2.2 Numerical simulation . . . . .	15
2.3 Conclusions . . . . .	15
<b>CHAPTER 3 BRIGHT SOLITON IN OPTICAL METAMATERIALS BY TRAVELING WAVE HYPOTHESIS</b> . . . . .	<b>18</b>
3.1 Governing equation . . . . .	18
3.2 Traveling wave hypothesis . . . . .	19
3.2.1 Kerr law . . . . .	20
3.2.2 Parabolic law . . . . .	22
3.2.3 Log law . . . . .	23
3.3 Conclusions . . . . .	24
<b>CHAPTER 4 SOLITON IN OPTICAL METAMATERIALS BY MAPPING METHOD</b> . . . . .	<b>25</b>
4.1 Overview of mapping method . . . . .	25
4.2 Application to metamaterials . . . . .	26
4.2.1 Kerr law . . . . .	27
4.2.2 Parabolic law . . . . .	30
4.3 Generalization . . . . .	33
<b>CHAPTER 5 SOLITON PROPAGATION THROUGH NANOSCALE WAVEGUIDES IN OPTICAL METAMATERIALS</b> . . . . .	<b>34</b>
5.1 Governing equation and mathematical analysis . . . . .	34
5.2 Kerr law . . . . .	36
5.2.1 Bright soliton . . . . .	36
5.2.2 Dark soliton . . . . .	37
5.2.3 Singular soliton (Type-I) . . . . .	37
5.2.4 Singular soliton (Type-II) . . . . .	38
5.3 Power law . . . . .	39
5.3.1 Bright soliton . . . . .	39
5.3.2 Dark soliton . . . . .	41
5.3.3 Singular soliton (Type-I) . . . . .	42

5.3.4 Singular soliton (Type-II) . . . . .	43
5.4 Parabolic law . . . . .	44
5.4.1 Bright soliton . . . . .	44
5.4.2 Dark soliton . . . . .	46
5.4.3 Singular soliton (Type-I) . . . . .	48
5.4.4 Singular soliton (Type-II) . . . . .	49
5.5 Dual-power law . . . . .	50
5.5.1 Bright soliton . . . . .	51
5.5.2 Dark soliton . . . . .	53
5.5.3 Singular soliton (Type-I) . . . . .	54
5.5.4 Singular soliton (Type-II) . . . . .	55
5.6 Log law . . . . .	56
5.7 Conclusions . . . . .	58
<b>CHAPTER 6 BRIGHT AND EXOTIC SOLITON IN OPTICAL METAMATERIALS BY SEMI-INVERSE VARIATIONAL PRINCIPLE</b>	<b>60</b>
6.1 Introduction . . . . .	60
6.2 Governing equation . . . . .	60
6.3 Semi-inverse variational principle . . . . .	61
6.3.1 Kerr law . . . . .	63
6.3.2 Power law . . . . .	68
6.3.3 Parabolic law . . . . .	72
6.3.4 Dual-power law . . . . .	74
6.3.5 Log law . . . . .	77
6.4 Conclusions . . . . .	80
<b>CHAPTER 7 RAMAN SOLITON IN NANOSCALE OPTICAL WAVEGUIDES, WITH METAMATERIALS, HAVING POLYNOMIAL LAW NON-LINEARITY</b>	<b>81</b>
7.1 Governing model . . . . .	81
7.2 Generalization . . . . .	85
7.3 Conclusions . . . . .	87
<b>CHAPTER 8 EVOLUTIONARY PATTERN FORMATION FOR COMPETING POPULATIONS WITH ASYMMETRIC NON-LOCAL COUPLING UNDER SINUSOIDAL TEMPORAL SEASONAL FORCING</b>	<b>88</b>
8.1 Governing model . . . . .	90
8.2 Stability analysis . . . . .	95
8.3 Computational Analysis . . . . .	99
8.4 Conclusions . . . . .	108
<b>CHAPTER 9 CONCLUSIONS</b>	<b>110</b>
9.1 Part I: Optical Soliton Propagation in Metamaterials . . . . .	110
9.2 Part II: Evolutionary Pattern Formation for Competing Populations under Seasonal Forcing . . . . .	113

**BIBLIOGRAPHY . . . . . 115**

## LIST OF FIGURES OR ILLUSTRATION

2.1	<i>Illustrate the parameter variation numerically with <math>m = 2</math>.</i> . . . . .	16
2.2	<i>Illustrate the parameter variation numerically with <math>m = 4</math>.</i> . . . . .	17
6.1	<i>Bright soliton with Kerr law nonlinearity.</i> . . . . .	65
6.2	<i>Cosh-Gaussian pulse with Kerr law.</i> . . . . .	67
6.3	<i>Combo-soliton with Kerr law.</i> . . . . .	69
6.4	<i>Bright soliton with Power law.</i> . . . . .	72
6.5	<i>Bright soliton with Parabolic law.</i> . . . . .	74
6.6	<i>Bright soliton with Dual-power law.</i> . . . . .	77
6.7	<i>Bright soliton (Gausson) with Log law.</i> . . . . .	79
7.1	<i>Soliton profile with Polynomial law nonlinearity.</i> . . . . .	85
7.2	<i>Soliton profile with Polynomial law nonlinearity.</i> . . . . .	87
8.1	<i><math>f(\beta)</math> and <math>\delta</math>.</i> . . . . .	100
8.2	<i><math>Ud100TWa</math> and <math>Vd100TWa</math> solutions at a fixed time.</i> . . . . .	104
8.3	<i><math>Up.3d150CIb</math> solution when time goes.</i> . . . . .	105
8.4	<i><math>Ud150CIb</math> solutions when time goes.</i> . . . . .	106
8.5	<i><math>Vp.3d100CIIB</math> solution when time goes.</i> . . . . .	107
8.6	<i><math>Vp.3d100CIIB</math> when time goes.</i> . . . . .	107

## LIST OF ABBREVIATIONS

collective variables	CV
nonlinear evolution equations	NLEEs
Nonlinear Schrödinger equation	NLSE
right-handed materials	RHM
silicon on insulator	SOI
stimulated Raman scattering	SRS
semi-inverse variational principle	SVP

# Chapter 1

## REVIEW OF LITERATURE

### 1.1 Optical soliton propagation in Metamaterials

The dynamics of soliton in optical fibers is an ongoing and active area of research in the field of nonlinear optics. This area of research has picked up momentum a few decades ago and is still burning bright. There are several aspects of this research that are visible in various publications [1, 3, 4, 29, 32, 33, 35, 36, 37, 49, 66]. These are soliton solutions, soliton perturbation theory, quasi-particle theory, quasi-stationary soliton solutions and several others.

While previously the study of optical soliton focused on optical fibers, in the current generation study of soliton the study of a new form of waveguide optical metamaterials [21] is coming into prominence. Optical metamaterials possess both negative permittivity and negative permeability properties that cannot be found in nature; but can be engineered by using advanced processing technology [23]. This material has been fabricated using nano-fabrication technology by several research groups [23, 24]. They manipulate the periodic structure of photonic crystal as well as create resonant ring for negative permeability [23, 24]. Recently, by using metamaterials, Shalaev and others demonstrate optical waveguide in visible and infrared regions [23]. One inherent property of soliton in optical metamaterials is its dissipation. Different waveguide structures are proposed using optical metamaterials [23]. As long as optical wave is guided, soliton pulses can evolve owing to delicate balance between dispersion and nonlinearity. However, it is always a challenge to compensate for the loss when engineering these types of waveguide using metamaterials. The theoretical results showed that metamaterials enhance and localize electromagnetic field in a small region that allows more light-matter interaction [22, 23, 24, 25, 26]. In metamaterials, linear and nonlinear coefficients of the propagation equation can be turned to achieve any combination of signs for permittivity and permeability that is not possible in regular materials. These properties of metamaterials lead to improved propagation of a wider variety of solitary waves, efficient phase-matching and modulational instability [25, 26, 27]. Numerical as well as analytical results of soliton propagation in several nanoscale optical waveguide were reported by several other authors [25,

26, 27]. Earlier results reveal that similar regular (positive indexed) dielectric material dispersion plays a pivotal role in supporting short duration soliton pulses. Optical waveguide with selected wavelengths can be implemented in photonic crystal partially filled with gold and nano-particles. Recently, theoretical results are reported for  $Y$ -splitter and bend waveguide structures [24].

The dynamics of soliton propagation through these optical metamaterials is governed by the nonlinear *Schrödinger's* equation (NLSE) with a few perturbation terms. This model was first reported during 2011 [21]. With the advent of such a model, a plethora of results have been reported. One important aspect is the study of the soliton parameter dynamics in a presence of perturbation terms. There are a couple of ways this study can be done. One of them is the application of variational principle. In the second chapter we make use of the collective variables (CV) principle that is often utilized in computational physics.

The third chapter recovers the bright 1-soliton solution, by the aid of travelling wave hypothesis. This integration scheme is not applicable to retrieve bright soliton solutions for power law and dual-power law media. Also, it must be noted that in the case of optical fibers there are soliton solutions that are reported earlier by the same integration scheme, namely traveling wave hypothesis applicable to five forms of nonlinearity that includes power law and dual-power law [5, 6, 7]. However, for optical metamaterials, the situation is a little different. The governing equations has parameters that obey constraint relations and prevent integrability by travelling wave hypothesis for power law and dual-power law. Another disadvantages of this scheme is that one can retrieve only bright 1-soliton solutions and not dark or singular optical soliton. Later, the focus will be on the application of additional integration techniques to retrieve dark and singular soliton along with bright-dark combo optical soliton.

The fourth chapter utilizes a different and unique approach to retrieve soliton solutions. This is the mapping method [10, 11, 12]. This scheme obtains doubly periodic functions which is of the form  $F(u, v, u_t, v_t, u_x, v_x, u_{xxx}, v_{xxx}, \dots) = 0$ , where  $u(x, t)$  and  $v(x, t)$  are traveling wave solutions. In the limiting case for modulus of ellipticity, soliton emerges from the mathematical analysis. The scheme is applied to two forms of nonlinear media, the Kerr law and the parabolic law.

In the fifth chapter we apply the method of undetermined coefficients in what is known as the Ansatz scheme [2, 49, 51, 60, 78, 79, 80], to retrieve exact soliton solutions. Bright, dark and singular soliton solutions are recovered. The method also reveals essential integrability conditions which stem from the solution structure of the model.

In the sixth chapter we study the dynamics of soliton propagation through these metamaterials. To do this we use a modified version of the usual nonlinear *Schrödinger* equation (NLSE) that normally models pulse propagation through optical fibers. It must be noted that there are several models, apart from NLSE that study soliton dynamics in non-linear optics. They are Manakov model, Lakshmanan-Porsezian-Daniel model, Sasa-Satsuma equation, Maxwell-Bloch equation and many others. The sixth chapter concentrates on the version of NLSE that is applicable to optical metamaterials [21].

The integrability aspect is the main focus of the sixth chapter. There are several tools that are available to conduct integrability of these models that fall in the category of nonlinear evolution equations (NLEEs) in mathematical physics or partial differential equations in mathematical sciences. Some of these integration schemes commonly applied to integrate NLEEs are traveling wave hypothesis [60], mapping methods [54], ansatz approach [2, 49], *F*-expansion scheme [51], collective variables method [58], simplest equation method [2], functional variable method [3] and several others [1, 2, 3, 4, 28, 29]. These algorithms yield soliton, shock waves and other solutions to the model that appear with their own integrability conditions [1, 2, 3, 4, 9]. In addition to these exact soliton solutions, very recently the semi-inverse variational principle has been applied to extract bright and exotic soliton solutions to the model [30]. This section stays away from the usual norm of seeking exact soliton solution. The semi-inverse variational principle (SVP) is applied to the model for metamaterials to obtain analytical soliton solutions to the model. Five forms of nonlinear media are studied in the sixth chapter. They are Kerr law, power law, parabolic law, dual-power law and log law nonlinearity. It is with Kerr law, that in addition to bright soliton solutions, exotic soliton solutions are retrieved. These are cosh-Gaussian pulses and bright-dark combo soliton. These results carry constraint conditions that guarantee the existence of such soliton. Finally, numerical

simulations supplement each of these analytical solutions.

The dynamics of temporal optical soliton is a treasure-trove in the area of non-linear optics [2]-[95]. The starting point is the Maxwell's equation from electromagnetic theory. Electromagnetic properties of complex materials, with simultaneous negative dielectric permittivity( $\epsilon$ ) and magnetic permeability( $\mu$ ), also known as double negative material (DNG), have attracted a lot of attention in research during recent times [21, 23, 67, 68]. Novel and interesting features of these engineered materials, are also known as metamaterials, and their possible applications to support short duration optical soliton pulses have been investigated in the seventh chapter in DNG materials in visible and infrared region by V. Shalaev and others had shown promise to manufacture optical waveguides with these materials [21, 23]. Moreover, Boardman et. al have given a lot of insight with optical metamaterials [69, 70, 71, 72, 73], i.e. developing the first comprehensive exact theory of strongly nonlinear guided waves in a double-negative planar metamaterial waveguide. For compact integration of photonic circuits, wavelength scale structures with high index contrast are a key requirement of silicon on insulator (SOI). Nanophotonic circuits appear to be the most appealing in photonic integration circuits [74, 75]. Currently, ridge silicon wire [68, 74, 75] acts as a (220 nm) waveguide in SOI structures. This structure provided higher confinement of light; so did higher non-linearity. Now-Kerr-type materials could also be used to guide lights.

Raman optical soliton pulses evolve due to a delicate balance between dispersion and non-linearity [21, 68, 76]. Soliton will dissipate in nature while propagating through DNG medium. Loss compensation is one of the challenges in engineering these types of materials. The dispersion profile of the wavelength structure is critically needed to determine the soliton pulse nature. In particular, Raman soliton self-frequency shift is induced by the stimulated Raman scattering(SRS) effect. Since the SRS effect enables the energy of the short pulse to transfer from higher to lower frequency continuously by C. V. Raman and K. S. Krishnan [76]. It is possible that the whole spectrum moved toward the longer wavelength region. The seventh chapter conducts theoretical analysis to illustrate the controllability of the Raman soliton self-frequency shift in non-linear metamaterials by numerical results.

## 1.2 Population pattern formation under seasonal forcing

My latest research field is in the field of Population modelling. Population modelling has many uses from understanding the dynamics of Honey Bee Population [96, 97, 98] and other species at interest to understanding the spread of parasites [99], viruses [100], and disease [101]. For example, exploring the impact of different death rates of forager bees on colony growth and development [102], evaluating the effects of artificial feeding on bee colony population dynamics [103], and recognizing the importance of pollination to our food systems and economics [104]. Additionally, contact and competition among different species within a community matters when it comes to the possibility of parasite disease outbreak [105], evolution of plant viruses [106] and ecology of tumors [107]. A model of competing species is developed in [108], which is based on the diffusive logistic model (Fisher's equation) and extends the scalar model to account for two competing species. In [108] a non-local competition term is used to model competition between species. This non-local competition is modelled through a convolution of a kernel,  $\phi_{\alpha,\delta}$ , with the population,  $u$ , to capture non-local interactions. The biological phenomenon of the non-local coupling can be attributed to the effect of mobility. If species compete for a sparse resource, then due to mobility the inhibiting effect of depletion of this resource should depend not just on the populations at a point but on some weighted average of the populations [108]. Additionally, the kernel,  $\phi_{\alpha,\delta}$ , used to capture non-local effects can be asymmetric. This asymmetry can be used to capture unsymmetrical terrain or other effects. Recently, there has been a growing interest in the development of predictive modeling tools to species dynamics [96, 97, 98, 109, 110, 111, 112, 113]. We add periodic variations to our model to understand how species respond to seasonal changes. The periodic variations are introduced through a sinusoidal nonlinear perturbation of the competition term.

The scalar model was in [108, 114] and then in [115, 116, 117, 118, 119, 120]. The kernel function in [108, 114] was symmetric, which meant that the non-local interaction at any specified point  $x$  weights the population symmetrically about  $x$ . In these cases we can see unstable, nonlinear effects when the interaction range of the kernel,  $\delta$ , is sufficiently large. The nonlinear effects found consist of patterns that take the form of islands of nonzero population separated by dead-zones

where the population is exponentially small. Stability analyses in [115, 116, 117] calculate the parameters under which non-linear effects occur.

Asymmetric non-local interactions, i.e., convolutions with uneven kernel function are found in [117, 118, 119]. In this case instability was still a function of the degree of non-locality,  $\delta$ , but the stability limit fluctuates depending on the degree of asymmetry in the kernel,  $\alpha$ . In these cases the nonlinear patterns are no longer stationary, but move with a velocity depending on  $\alpha$ .

In the eighth chapter, we are interested in finding persistence phenomenon in modeling competing species. In our model, we try to account for various factors including non-local competition, asymmetrical behavior, and seasonal effects. The non-local coupling is modeled through convolution integrals, which is attributed to the effect of mobility, i.e., resource should depend not just on the populations at a point but on some weighted average of the populations, due to its inhibiting effect of depletion [108, 120]. The asymmetry is introduced via the convolution integral with asymmetric kernel functions. This asymmetry can arise in many ways. In tumors it can be found as the result of complex steady-state dynamics of population distribution [121]. Within each tumor, clones can evolve that harbor selectively advantageous mutations (called drivers), neutral mutations (called passengers), and deleterious mutations. The temporal effect is via sinusoidal forcing. This is likely to become increasingly important in coming years, as the climate is expected to become more variable [111, 112, 113].

We study the case where the model admits a periodic fluctuating coexistence limit cycle solution. We show that this solution can be de-stabilized by the non-local coupling, access stability conditions of this critical point as a function of  $\alpha$ , determine unstable wave number bands with  $\delta$  beyond the stability boundary and compare results with different  $p$ . We consider the nonlinear patterns with sufficiently non-localization under varying  $p$ . Patterns consist of arrays of islands, regions of non-zero population, separated by either near dead-zones where populations are exponentially small and essentially extinct under perturbation, which is stimulated by both *Matlab* and *CLanguage*. We start with modeling and analysing the spread dynamic of coupled populations, and then focus on the impacts of population interactions on spread behavior to estimate the convo-

lutionary pattern of a relative heterogeneous environment. We have derived the stability conditions, and some nonlinear patterns under varying seasonal forcing.

## Chapter 2

# SUPER-GAUSSIAN SOLITON IN OPTICAL METAMATERIALS USING COLLECTIVE VARIABLES

This chapter studies soliton in optical metamaterials by the aid of collective variables. As an assumption, super-Gaussian soliton are selected to keep these pulses on a generalized setting. The numerical simulations of soliton parameter variation are given for specific values of the Super-Gaussian pulse parameters.

### 2.1 Introduction

The governing equation that will be considered is for optical metamaterials. In 21st century, optical fibers are transitioning its way to optical metamaterials for performance enhancement. Therefore, it is imperative to study the dynamics of soliton in optical metamaterials. This section will apply the principle of CV to address this issue. The hypothesis that will be selected is Super-Gaussian soliton.

The dynamics of soliton in optical metamaterials is governed by the model [1, 3, 4, 29, 37, 49, 66]

$$iq_t + aq_{xx} + c|q|^2q = i\alpha q_x + i\lambda(|q|^2q)_x + i\nu(|q|^2)_x q + \theta_1(|q|^2q)_{xx} + \theta_2|q|^2q_{xx} + \theta_3q^2q_{xx}^*. \quad (2.1)$$

(2.1) is the nonlinear *Schrödinger's* equation (NLSE) that is studied in the context of metamaterials. Here is (2.1),  $a$  and  $b$  are the group velocity dispersion and the self-phase modulation terms respectively. This pair produces the delicate balance between dispersion and nonlinearity that accounts for the formation of the stable soliton. On the right hand side  $\lambda$  represents the self-steepening term in order to avoid the formation of shocks and  $\nu$  is the nonlinear dispersion, while  $\alpha$  represents the intermodel dispersion. Then finally,  $\theta_j$  for  $j = 1, 2, 3$  are the perturbation terms that appears in the context of metamaterials [49].

## 2.2 Mathematical formulation

In the algorithm for CV, the solution of the NLSE is assumed to be split into two components. The first component constitutes soliton solution while the second one represents the residual radiation that is commonly known as small amplitude dispersive waves. The hypothesis is that the soliton solution depends on a collection of variables that possibly represent soliton amplitude, inverse width, frequency, chirp, center position and others. Introduction of CV increases the phase space of the dynamical system of the soliton parameters. The residual field is set to zero approximately. The constraint relations result in a nonlinear dynamical system of the field variables which are going to be studied numerically.

The soliton field  $q(t, x)$  decomposed into two parts as

$$q(x, t) = f(x, t) + g(x, t), \quad (2.2)$$

where  $f$  represents the pulse configuration while  $g$  represents the residual field. Next, the soliton field is assumed to be a function of  $N$  independent variables  $x_j$  for  $1 \leq j \leq N$  which are called CVs. Again, each of these CVs in turn are dependent on the variables  $t$  and  $x$ . Thus one can rewrite (2.2) as

$$q(x, t) = f(x_1, x_2, \dots, x_N, t) + g(x, t). \quad (2.3)$$

With these  $N$  CVs for the function  $f$  increases the degrees of freedom. This gives an expansion of the available phase-space of the system. In order for the system to remain in the original phase space, certain constraints are imposed. These constraints are obtained by configuring function  $f$  so that it is the best fit for the static solution. The residual free energy (RFE) is

$$E = \int_{-\infty}^{\infty} |g|^2 dt = \int_{-\infty}^{\infty} |q - f(x_1, x_2, \dots, x_N, t)|^2 dt. \quad (2.4)$$

From this definition, let  $C_j$  denote the rate of change of RFE with respect to the  $j$ th CV  $x_j$  so that

$$C_j = \frac{\partial E}{\partial x_j} = \frac{\partial}{\partial x_j} \int_{-\infty}^{\infty} |g|^2 dt = \int_{-\infty}^{\infty} \left( \frac{\partial g}{\partial x_j} g^* + \frac{\partial g^*}{\partial x_j} g \right) dt. \quad (2.5)$$

Again from

$$g(x, t) = q(x, t) - f(x_1(x, t), x_2(x, t), \dots, x_N(x, t)), \quad (2.6)$$

one can rewrite (2.5) as

$$C_j = \left\langle \frac{\partial f^*}{\partial x_j}, g \right\rangle + \left\langle \frac{\partial f}{\partial x_j}, g^* \right\rangle, \quad (2.7)$$

where the notation

$$\langle u, v \rangle = \int_{-\infty}^{\infty} u(t)v(t)dt, \quad (2.8)$$

was introduced. Next, the rate of change of  $C_j$  with respect to the normalized distance is defined as

$$\dot{C}_j = \frac{dC_j}{dx} = 2\Re \frac{d}{dx} \left( \int_{-\infty}^{\infty} \frac{\partial f^*}{\partial x_j} g dt \right) = 2\Re \left( \int_{-\infty}^{\infty} \frac{\partial f^*}{\partial x_j} \frac{\partial g}{\partial x} dt + \sum_{k=1}^N \int_{-\infty}^{\infty} \frac{\partial^2 f^*}{\partial x_j \partial x_k} \frac{\partial x_k}{\partial x} g dt \right), \quad (2.9)$$

$\Re$  represents the real part. Thus,

$$\dot{C}_j = 2\Re \left( \left\langle \frac{\partial f^*}{\partial x_j}, \frac{\partial g}{\partial x} \right\rangle + \left\langle \frac{\partial^2 f^*}{\partial x_j \partial x_k}, \frac{\partial x_k}{\partial x} \right\rangle g \right). \quad (2.10)$$

Now, Dirac's principle states that if a function is approximately zero, one cannot be set equal to zero until its variations with respect to all its parameters are made [32, 33, 34, 35, 36]. Hence the system will evolve so that  $C_j$  are minimum and the equations of the constraints are  $C_j \approx 0, \dot{C}_j \approx 0$ .

Substituting (2.2) into (2.1), leads to the equations of motion of the residual field  $g(x, t)$  which upon substitution into (2.9) gives

$$-\dot{C}_j = 2\Re \sum_{k=1}^N \left[ \int_{-\infty}^{\infty} \frac{\partial f^*}{\partial x_j} \frac{\partial f}{\partial x_k} dt - \int_{-\infty}^{\infty} \frac{\partial^2 f^*}{\partial x_j \partial x_k} dt \right] \frac{dx_k}{dt} + R_j, \quad (2.11)$$

for  $1 \leq j \leq N$ . This is equivalent to the matrix equation

$$\dot{\mathbf{C}} = \frac{\partial \mathbf{C}}{\partial \mathbf{X}} \dot{\mathbf{X}} + \mathbf{R}, \quad (2.12)$$

where

$$\mathbf{X} = \begin{pmatrix} x_1 \\ x_2 \\ \dots \\ x_N \end{pmatrix}, \quad (2.13)$$

and

$$\mathbf{R} = \begin{pmatrix} R_1 \\ R_2 \\ \dots \\ R_N \end{pmatrix}. \quad (2.14)$$

While the  $N \times N$  Jacobian matrix is given by

$$\frac{\partial \mathbf{C}}{\partial \mathbf{X}} = \frac{\partial(C_1, C_2, \dots, C_N)}{\partial(x_1, x_2, \dots, x_N)} = \left( \frac{\partial C_j}{\partial x_k} \right)_{N \times N}, \quad (2.15)$$

with

$$\frac{\partial C_j}{\partial x_k} = 2\Re \left( \int_{-\infty}^{\infty} \frac{\partial f^*}{\partial x_j} \frac{\partial f}{\partial x_k} dt - \int_{-\infty}^{\infty} \frac{\partial^2 f^*}{\partial x_j \partial x_k} dt \right), \quad (2.16)$$

for  $1 \leq j, k \leq N$ . One can now solve (2.12) for  $\dot{\mathbf{X}}$  that will lead to adiabatic parameter dynamics of the CVs (soliton parameters) in presence of perturbation terms. The process of solving for  $\dot{\mathbf{X}}$  from (2.12) requires the inversion of the Jacobian matrix given by (2.15).

### 2.2.1 Soliton parameter dynamics

In this section the adiabatic parameter dynamics of soliton in optical metamaterials will be obtained by CV method. For soliton,  $N=6$  as will be illustrated. The equations for all CVs are going to be obtained by lowest order CV theory [32, 33, 34, 35, 36] that is alternatively referred to

as *bare approximation*. When dressing of the soliton and soliton radiation are negligible, the bare approximation is applied by which the residual field is set to zero. Thus,  $g(t, x)$  is set to zero.

For super-Gaussian soliton ansatz, one can take the chirped soliton pulse as

$$f(x_1, x_2, x_3, x_4, x_5, x_6; t) = x_1 e^{-\frac{(t-x_2)^{2m}}{x_3^2}} e^{i[\frac{x_4}{2}(t-x_2)^2 + x_5(t-x_2) + x_6]}, \quad (2.17)$$

where  $x_1$  is the soliton amplitude,  $x_2$  is the center position of the soliton,  $x_3$  is the inverse width of the pulse,  $x_4$  is the soliton chirp,  $x_5$  is the soliton frequency and  $x_6$  is the soliton phase. Also  $m$  is the super-Gaussian parameter, where  $m > 0$ . In this case, with  $N=6$ ,

$$\frac{\partial C}{\partial x} = \begin{pmatrix} \frac{\partial C_1}{\partial x_1} & \frac{\partial C_1}{\partial x_2} & \frac{\partial C_1}{\partial x_3} & \frac{\partial C_1}{\partial x_4} & \frac{\partial C_1}{\partial x_5} & \frac{\partial C_1}{\partial x_6} \\ \frac{\partial C_2}{\partial x_1} & \frac{\partial C_2}{\partial x_2} & \frac{\partial C_2}{\partial x_3} & \frac{\partial C_2}{\partial x_4} & \frac{\partial C_2}{\partial x_5} & \frac{\partial C_2}{\partial x_6} \\ \frac{\partial C_3}{\partial x_1} & \frac{\partial C_3}{\partial x_2} & \frac{\partial C_3}{\partial x_3} & \frac{\partial C_3}{\partial x_4} & \frac{\partial C_3}{\partial x_5} & \frac{\partial C_3}{\partial x_6} \\ \frac{\partial C_4}{\partial x_1} & \frac{\partial C_4}{\partial x_2} & \frac{\partial C_4}{\partial x_3} & \frac{\partial C_4}{\partial x_4} & \frac{\partial C_4}{\partial x_5} & \frac{\partial C_4}{\partial x_6} \\ \frac{\partial C_5}{\partial x_1} & \frac{\partial C_5}{\partial x_2} & \frac{\partial C_5}{\partial x_3} & \frac{\partial C_5}{\partial x_4} & \frac{\partial C_5}{\partial x_5} & \frac{\partial C_5}{\partial x_6} \\ \frac{\partial C_6}{\partial x_1} & \frac{\partial C_6}{\partial x_2} & \frac{\partial C_6}{\partial x_3} & \frac{\partial C_6}{\partial x_4} & \frac{\partial C_6}{\partial x_5} & \frac{\partial C_6}{\partial x_6} \end{pmatrix}, \quad (2.18)$$

while

$$\mathbf{X} = \begin{pmatrix} x_1 \\ x_2 \\ x_3 \\ x_4 \\ x_5 \\ x_6 \end{pmatrix}, \quad (2.19)$$

and

$$\mathbf{R} = \begin{pmatrix} R_1 \\ R_2 \\ R_3 \\ R_4 \\ R_5 \\ R_6 \end{pmatrix}. \quad (2.20)$$

Here

$$R_1 = 2^{\frac{m-1}{m}} X_1^3 X_3^{\frac{1}{m}} X_4 (\theta_1 - \theta_2 + \theta_3) \Gamma(1 + \frac{1}{2m}), \quad (2.21)$$

$$\begin{aligned} R_2 = & \frac{1}{m} 2^{-\frac{m+3}{m}} X_1^2 X_3^{\frac{3}{m}} [4\Gamma(\frac{3}{2m}) X_4^2 (2^{\frac{3}{2m}} (\alpha - 3aX_5) + X_1^2 (\lambda + 3X_5(\theta_1 + \theta_2 + \theta_3)))] + \\ & 2^{\frac{7}{2m}} m^2 \Gamma(2 - \frac{1}{2m}) X_3^{-\frac{4}{m}} [4(\alpha - 3aX_5) + 2^{\frac{1}{2m}} X_1^2 (3\lambda + 2\nu + X_5)(9\theta_1 + 5\theta_2 + \theta_3)] - \\ & 4^{1+\frac{1}{2m}} X_3^{-\frac{2}{m}} X_5 [2^{\frac{1}{2m}} X_5 (aX_5 - \alpha) - X_1^2 (b + X_5(\lambda + X_5(\theta_1 + \theta_2 + \theta_3)))]], \end{aligned} \quad (2.22)$$

$$R_3 = \frac{1}{m} 2^{\frac{m+1}{m}} X_1^2 X_3^{\frac{1-m}{m}} X_4 \Gamma(1 + \frac{1}{2m}) (X_1^2 (\theta_1 (6m + 1) + (\theta_2 - \theta_3)(2m - 1)) - 2^{3+\frac{1}{2m}} am), \quad (2.23)$$

$$\begin{aligned} R_4 = & \frac{1}{16m} 2^{-\frac{5}{m}} X_1^2 X_3^{\frac{5}{m}} (16\Gamma(\frac{5}{2m}) X_4^2 (2^{\frac{5}{2m}} a - X_1^2 (\theta_1 + \theta_2 + \theta_3)) 16^{\frac{1}{m}} \Gamma(\frac{1}{2m}) X_3^{-\frac{4}{m}} \\ & (2^{2+\frac{1}{2m}} a(2m - 3) + X_1^2 (\theta_1 (21 - 6m) - (\theta_2 + \theta_3)(6m - 5))) \\ & - 4^{2+\frac{1}{m}} \Gamma(\frac{3}{2m}) X_3^{-\frac{2}{m}} (2^{\frac{3}{2m}} X_5 (\alpha - aX_5) + X_1^2 (b + X_5(\lambda + X_5(\lambda + X_5(\theta_1 + \theta_2 + \theta_3))))), \end{aligned} \quad (2.24)$$

$$R_5 = -\frac{2}{m} 2^{-\frac{3}{m}} \Gamma(\frac{3}{2m}) X_1^2 X_3^{\frac{3}{m}} X_4 (2^{\frac{3}{2m}} (\alpha - 2aX_5) + X_1^2 (\lambda + 2X_5(\theta_1 + \theta_2 + \theta_3))), \quad (2.25)$$

$$\begin{aligned} R_6 = & \frac{1}{m} 2^{-\frac{m+3}{m}} X_1^2 X_3^{\frac{3}{m}} (4\Gamma(\frac{3}{2m}) X_4^2 (2^{\frac{3}{2m}} a) - X_1^2 (\theta_1 + \theta_2 + \theta_3)) - 2^{\frac{7}{2m}} m^2 \Gamma(2 - \frac{1}{2m}) \\ & X_3^{-\frac{4}{m}} (32^{\frac{1}{2m}} X_1^2 (\theta_1 + \theta_2 + \theta_3) - 4a) - 4^{1+\frac{1}{m}} \Gamma(\frac{1}{2m}) X_3^{-\frac{2}{m}} (2^{\frac{1}{2m}} X_5 (\alpha - aX_5) + \\ & X_1^2 (b + X_5(\theta_1 + \theta_2 + \theta_3))). \end{aligned} \quad (2.26)$$

Thus, the nonlinear dynamical system (DS) reduces to

$$\dot{x}_1 = \frac{1}{8m} 2^{1+\frac{1}{2m}} X_1 X_4 (X_1 (\theta_1 (2m - 1) + (\theta_2 - \theta_3)(6m + 1)) - 2^{\frac{1}{2m}+3} am), \quad (2.27)$$

$$\dot{x}_2 = -\alpha + 2aX_5 - 2^{\frac{1}{2m}-2}X_1^2(3\lambda + 2\nu + 2X_5(3\theta_1 + \theta_2 - \theta_3)), \quad (2.28)$$

$$\dot{x}_3 = 2^{-\frac{1}{2m}-2}X_3X_4(2^{\frac{1}{2m}+3}am + X_1^2(\theta_1(1 - 6m) - (\theta_2 - \theta_3)(2m + 1))), \quad (2.29)$$

$$\dot{x}_4 = 15\frac{\xi_1}{\xi_2}, \quad (2.30)$$

where

$$\begin{aligned} \xi_1 = & 32^{\frac{2}{m}-3}m\Gamma(1 - \frac{1}{2m})\Gamma(\frac{3}{2m})X_3^{-\frac{4}{m}}(32^{\frac{1}{2m}}X_1^2(\theta_1 + \theta_2 + \theta_3) - 4a) + \\ & 32^{\frac{3}{2m}-4}\Gamma(1 + \frac{1}{2m})\Gamma(\frac{1}{2m})X_3^{-\frac{4}{m}}(2^{\frac{1}{2m}+2}a(2m - 3) + X_1^2(\theta_1(21 - 6m) - (\theta_2 + \theta_3)(6m - 5))) \\ & - 2^{-\frac{3}{2m}}\Gamma(1 + \frac{3}{2m})\Gamma(\frac{3}{2m})X_4^2(2^{\frac{3}{2m}}a - X_1^2(\theta_1 + \theta_2 + \theta_3)) \\ & + 482^{-\frac{5}{2m}-4}\Gamma(1 + \frac{1}{2m})\Gamma(\frac{5}{2m})X_4^2(2^{\frac{5}{2m}}a - X_1^2(\theta_1 + \theta_2 + \theta_3)) \\ & + 2^{-\frac{1}{2m}}(2^{\frac{1}{m}} - 1)X_1^2\Gamma(1 + \frac{3}{2m})\Gamma(\frac{1}{2m})X_3^{-\frac{2}{m}}(b + X_5(\lambda + X_5(\theta_1 + \theta_2 + \theta_3))), \end{aligned}$$

and

$$\xi_2 = 5m\Gamma(\frac{3}{2m} + 1)^2 - \frac{9}{2}\Gamma(\frac{5}{2m} + 1)\Gamma(\frac{1}{2m}),$$

$$\dot{x}_5 = 2^{-\frac{3}{2m}-2}X_1^2X_4(4(\lambda + 2X_5(\theta_1 + \theta_2 + \theta_3)) - 4^{\frac{1}{m}}(3\lambda + 2\nu + 2X_5(3\theta_1 + \theta_2 - \theta_3))), \quad (2.31)$$

where

$$\begin{aligned} \chi_1 = & -\frac{9}{2m}2^{-\frac{1}{2m}}\Gamma(1 + \frac{5}{2m})\Gamma(\frac{1}{2m})(2^{\frac{1}{2m}}X_5(\alpha - aX_5) + X_1^2(b + X_5(\lambda + X_5(\theta_1 + \theta_2 + \theta_3)))) \\ & - \frac{45}{16}2^{-\frac{1}{m}}X_3^{-\frac{2}{m}}\Gamma(2 - \frac{1}{2m})\Gamma(\frac{5}{2m})(3(\theta_1 + \theta_2 + \theta_3)2^{\frac{1}{2m}}X_1^2 - 4a) \\ & + \frac{9}{2m}2^{-\frac{5}{2m}}X_3^{\frac{2}{m}}X_4^2\Gamma(1 + \frac{5}{2m})\Gamma(\frac{3}{2m})(2^{\frac{3}{2m}}a - (\theta_1 + \theta_2 + \theta_3)X_1^2), \\ \chi_2 = & \frac{15}{2m}2^{-\frac{3}{2m}}\Gamma(\frac{3}{2m})(2^{\frac{2}{3m}}X_5(\alpha - aX_5) + X_1^2(b + X_5(\theta_1 + \theta_2 + \theta_3))) \\ & + \frac{15}{2m}2^{-\frac{7}{2m}}X_3^{\frac{2}{m}}X_4^2\Gamma(\frac{5}{2m})((\theta_1 + \theta_2 + \theta_3)X_1^2 - 2^{\frac{5}{2m}}a) + \\ & \frac{15}{2m}2^{\frac{1}{2m}}X_3^{-\frac{2}{m}}\Gamma(\frac{1}{2m})(X_1^2(3\theta_1(2m - 7) + (\theta_2 + \theta_3)(6m - 5)) - 2^{\frac{1}{2m}+2}(2m - 3)a). \end{aligned}$$

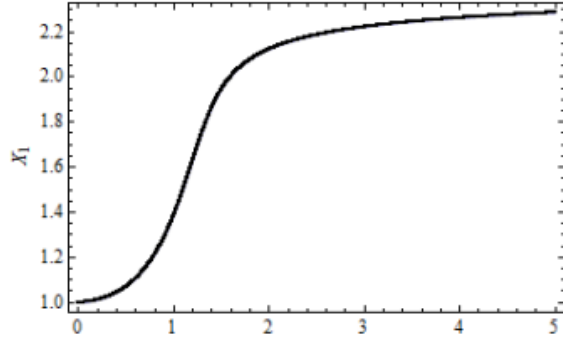
$$\begin{aligned} \dot{x}_6 = & \frac{\chi_1 + \Gamma(1 + \frac{3}{2m})\chi_2}{5\Gamma(1 + \frac{3}{2m})^2 - 9\Gamma(1 + \frac{1}{2m})\Gamma(1 + \frac{5}{2m})} + 2aX_5^2 - \alpha X_5 \\ & - 2^{\frac{1}{2m}-2} X_1^2 X_5 (2\lambda + 2\nu + 2(\theta_1 + \theta_2 - \theta_3)X_5). \end{aligned} \quad (2.32)$$

### 2.2.2 Numerical simulation

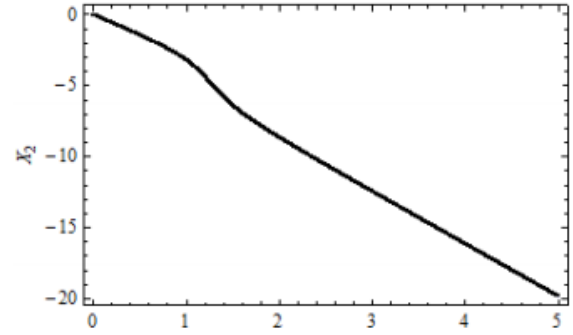
The nonlinear dynamical system developed in the previous section will now be plotted to illustrate the parameter variation numerically. There are two sets of plots with super-Gaussian pulses. There are with  $m = 2$  in **Fig. 2.1** and  $m = 4$  in **Fig. 2.2** respectively. The parameter values chosen, for both cases, are as follows:  $c_1 = 0.001$ ,  $c_2 = 0.25$ ,  $c_3 = 0.001$ ,  $\alpha = 2.5$ ,  $\theta_1 = 0.1$ ,  $\theta_2 = 0.1$ ,  $\theta_3 = 0.1$ ,  $a = 0.1$ ,  $b = 0.1$ ,  $\lambda = 0.1$ ,  $\nu = 0.1$ .

### 2.3 Conclusions

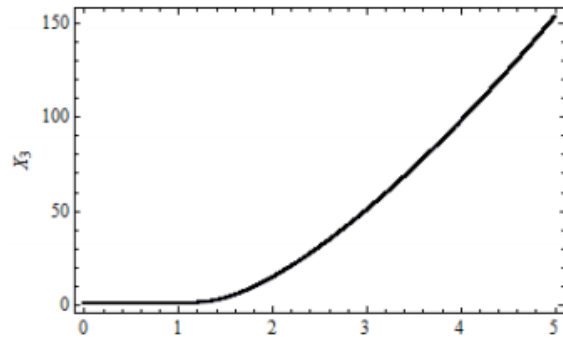
The dynamics of soliton parameters are studied numerically in this chapter by the aid of CV approach. Super-Gaussian soliton are considered. The two cases where  $m = 2$  and  $m = 4$  are studied numerically. This chapter stands on a strong foundation for further future work. While this chapter addresses Kerr law nonlinearity, later parabolic law nonlinearity will be studied. The results of those researches will be available soon.



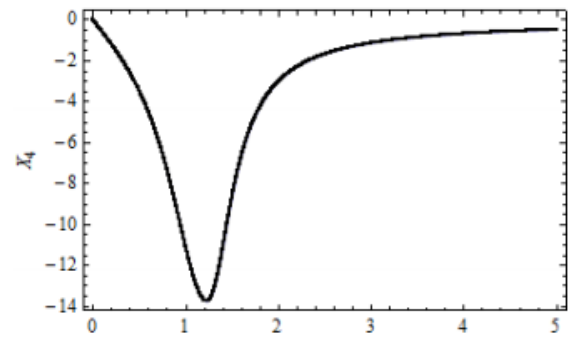
(a)  $m = 2$  Soliton amplitude variation



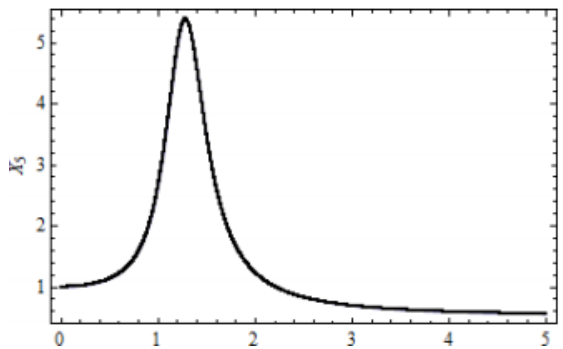
(b)  $m = 2$  SSoliton center-position variation



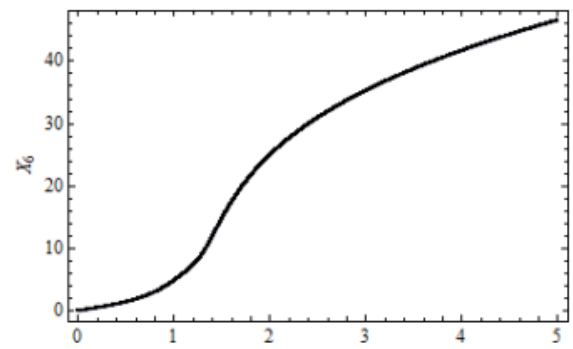
(c)  $m = 2$  Soliton inverse-width variation



(d)  $m = 2$  Soliton chirp variation

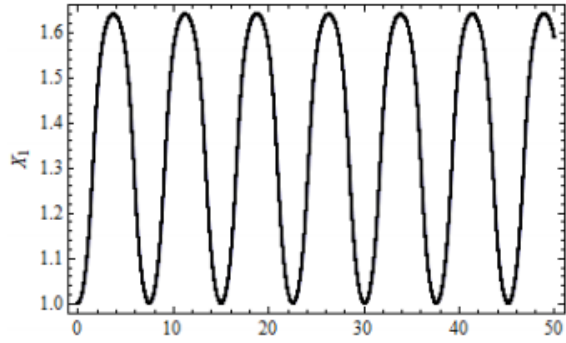


(e)  $m = 2$  Soliton frequency variation

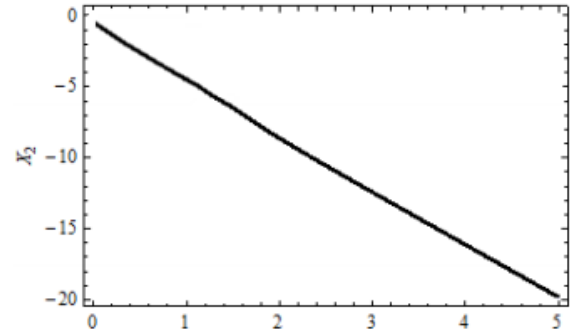


(f)  $m = 2$  Soliton phase variation

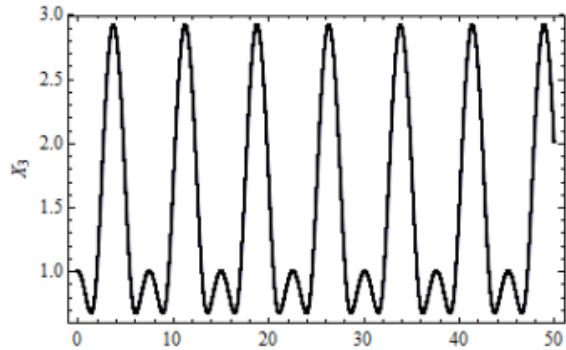
Figure 2.1: Illustrate the parameter variation numerically with  $m = 2$ .



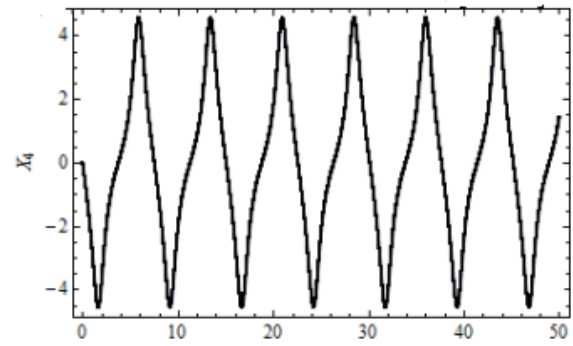
(a)  $m = 4$  Soliton amplitude variation



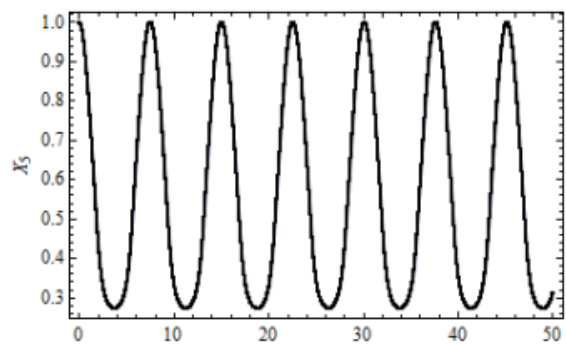
(b)  $m = 4$  Soliton center-position variation



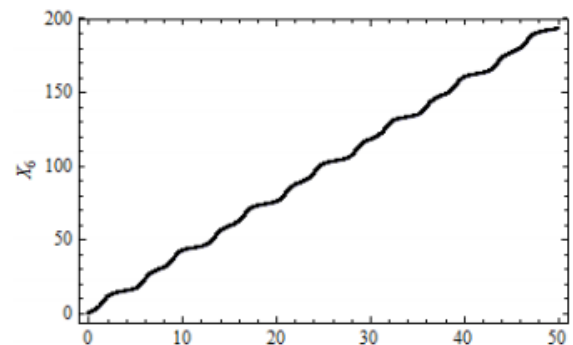
(c)  $m = 4$  Soliton inverse-width variation



(d)  $m = 4$  Soliton chirp variation



(e)  $m = 4$  Soliton frequency variation



(f)  $m = 4$  Soliton phase variation

Figure 2.2: Illustrate the parameter variation numerically with  $m = 4$ .

# Chapter 3

## BRIGHT SOLITON IN OPTICAL METAMATERIALS BY TRAVELING WAVE HYPOTHESIS

This chapter obtains bright 1-soliton solutions in optical metamaterials by the aid of traveling wave hypothesis. There are three types of nonlinear media that are considered. They are Kerr law, parabolic law and log law nonlinearity. There are several constraint relations there obtained for soliton solutions to exist.

### 3.1 Governing equation

The dimensionless form of NLSE in optical metamaterials is given by [1, 2, 3, 4, 21, 29, 78, 79, 80]:

$$iq_t + aq_{xx} + F(|q|^2)q = iaq_x + i\lambda(|q|^2)_x q + i\nu(|q|^2)_x q + \theta_1(|q|^2)_{xx} q + \theta_2|q|^2q_{xx} + \theta_3q^2q_{xx}^*. \quad (3.1)$$

The independent variables are  $x$  and  $t$  that respectively represent the spatial and temporal variables, while the dependent variable is  $q(x, t)$  which represents the complex valued wave envelope. Also,  $a$  is the coefficient of group velocity dispersion (GVD). The functional  $F$  represents the nonlinear term. On the right hand side,  $\alpha$  is due to inter-modal dispersion,  $\lambda$  represents the self-steepening term to avoid formation of shock waves,  $\nu$  is the nonlinear dispersion. The  $\theta_j$  for  $j = 1, 2, 3$  terms appear in the context of metamaterials [1]-[4].

The function  $F$  represents, in general, non-Kerr law nonlinear media and is a real-valued algebraic function and the smoothness of the complex function  $F(|q|^2)q : C \mapsto C$  is needed. Considering the complex plane  $C$  as a two-dimensional linear space  $R^2$ , the function  $F(|q|^2)q$  is  $k$  times continuously differentiable, so that [6, 7]

$$F(|q|^2)q \in \bigcup_{m,n=1}^{\infty} C^k((-n, n) \times (-m, m); R^2). \quad (3.2)$$

The traveling wave hypothesis will be introduced in the following section and 1-soliton solution will

be obtained for three forms of the nonlinear function  $F$ .

### 3.2 Traveling wave hypothesis

The starting hypothesis to address (3.1) is given by [5, 6, 7]

$$q(x, t) = g(x - vt) e^{i(-\kappa x + \omega t + \sigma)}, \quad (3.3)$$

where  $v$  represents the speed of the soliton and the function  $g$  is the amplitude component of the complex valued function  $q(x, t)$ . From the phase component,  $\kappa$  is the soliton frequency,  $\omega$  is the soliton wave number and  $\sigma$  is the phase constant. Substituting (3.3) into (3.1) and decomposing into real and imaginary parts lead to

$$\begin{aligned} ag'' - (\omega + a\kappa + a\kappa^2)g + \{F(g^2) - \lambda\kappa g^2 + (\theta_1 + \theta_2 + \theta_3)\kappa^2 g^2\}g - (3\theta_1 + \theta_2 + \theta_3)g^2 g'' \\ - 6\theta_1 g (g')^2 = 0, \end{aligned} \quad (3.4)$$

and

$$(\nu + a + 2a\kappa)g' + \{3\lambda + 2\nu - 2(3\theta_1 + \theta_2 + \theta_3)\kappa\}g^2 g' = 0. \quad (3.5)$$

In (3.4) and (3.5), the notations  $g' = dg/ds$  and  $g'' = d^2g/ds^2$  are used where

$$s = x - vt. \quad (3.6)$$

From the real part equation, setting the coefficients of linearly independent functions to zero gives

$$\theta_1 = 0, \quad (3.7)$$

and

$$\theta_2 + \theta_3 = 0. \quad (3.8)$$

Consequently, from the imaginary part equation it follows from the coefficients of linearly independent functions

$$3\lambda + 2\nu = 0, \quad (3.9)$$

and the speed of the soliton falls out to be

$$v = -a - 2a\kappa, \quad (3.10)$$

which is valid for all forms of nonlinear media. Therefore with these parameter settings, the governing equation (3.1) modifies to

$$iq_t + aq_{xx} + F(|q|^2)q = iaq_x + i\lambda(|q|^2q)_x + i\nu(|q|^2)_x q + \theta_2|q|^2q_{xx} - \theta_2q^2q_{xx}^*, \quad (3.11)$$

and the real part equation simplifies to

$$ag'' - (\omega + a\kappa + a\kappa^2)g + \{F(g^2) - \lambda\kappa g^2\}g = 0. \quad (3.12)$$

The traveling wave hypothesis of this equation will now be studied. Multiplying both sides of (3.12) by  $g'$  and integrating leads to

$$2a(g')^2 - 2(\omega + a\kappa + a\kappa^2)g^2 - \lambda\kappa g^4 + 4 \int_0^g F(h^2)hh' dh = 0, \quad (3.13)$$

upon simplification after choosing the integration constant to be zero, since the search is for a soliton solution. The next three subsections will focus on the linearity of the ordinary differential equation (ODE) given by (3.13) for Kerr law, Parabolic law and Log law where the functional  $F$  is known.

### 3.2.1 Kerr law

For Kerr law nonlinearity [1],

$$F(u) = bu, \quad (3.14)$$

for a real constant  $b$  so that (3.11) reduces to

$$iq_t + aq_{xx} + b|q|^2q = iaq_x + i\lambda(|q|^2q)_x + i\nu(|q|^2)_x q + \theta_2|q|^2q_{xx} - \theta_2q^2q_{xx}^*, \quad (3.15)$$

and hence the real part ODE gives

$$2a(g')^2 - 2(\omega + a\kappa + a\kappa^2)g^2 + (b - \lambda\kappa)g^4 = 0. \quad (3.16)$$

After separating variables in (3.16) and integrating leads to

$$g(s) = g(x - vt) = A \operatorname{sech}[B(x - vt)], \quad (3.17)$$

where

$$A = \sqrt{\frac{2(\omega + a\kappa + a\kappa^2)}{b - \lambda\kappa}}, \quad (3.18)$$

and

$$B = \sqrt{\frac{2(\omega + a\kappa + a\kappa^2)}{a}}. \quad (3.19)$$

Hence, bright 1-soliton solution to (3.15) is given by

$$q(x, t) = A \operatorname{sech}[B(x - vt)]e^{i(-\kappa x + \omega t + \sigma)}, \quad (3.20)$$

where the amplitude  $A$  of the soliton and the inverse width  $B$  of the soliton and given by (3.18) and (3.19), respectively. It must be noted that these bright soliton exist provided the constraints

$$(b - \lambda\kappa)(\omega + a\kappa + a\kappa^2) > 0, \quad (3.21)$$

and

$$a(\omega + a\kappa + a\kappa^2) > 0. \quad (3.22)$$

### 3.2.2 Parabolic law

In this case,

$$F(u) = b_1 u + b_2 u^2, \quad (3.23)$$

where  $b_1$  and  $b_2$  are real-valued constants [5, 6, 7, 9]. Therefore, (3.11) takes the form

$$iq_t + aq_{xx} + (b_1|q|^2 + b_2|q|^4)q = iaq_x + i\lambda(|q|^2q)_x + i\nu(|q|^2)_x q + \theta_2|q|^2q_{xx} - \theta_2q^2q_{xx}^*, \quad (3.24)$$

and hence the real part ODE gives

$$6a(g')^2 - 6(\omega + a\kappa + a\kappa^2)g^2 + 3(b_1 - \lambda\kappa)g^4 + 2b_2g^6 = 0. \quad (3.25)$$

After separating variables in (3.25) and integrating leads to

$$g(s) = g(x - vt) = \frac{A}{\sqrt{D + \cos h[B(x - vt)]}}, \quad (3.26)$$

where

$$A = \frac{2\sqrt{6}(\omega + a\kappa + a\kappa^2)}{\sqrt{3(b_1 - \lambda\kappa)^2 + 16b_1(\omega + a\kappa + a\kappa^2)}}, \quad (3.27)$$

and

$$B = 2\sqrt{\frac{(\omega + a\kappa + a\kappa^2)}{a}}, \quad (3.28)$$

and

$$D = \frac{\sqrt{3}(b_1 - \lambda\kappa)}{\sqrt{3(b_1 - \lambda\kappa)^2 + 16b_1(\omega + a\kappa + a\kappa^2)}}. \quad (3.29)$$

Hence, bright 1-soliton solution to (3.24) is given by

$$q(x, t) = \frac{A}{\sqrt{D + \cos h[B(x - vt)]}} e^{i(-\kappa x + \omega t + \sigma)}, \quad (3.30)$$

where the amplitude  $A$  of the soliton and the inverse width  $B$  of the soliton are given by (3.27) and (3.28), respectively. This case introduces a new parameter  $D$  that is given by (3.29). The condition for the existence of the bright soliton is guaranteed for

$$3(b_1 - \lambda\kappa)^2 + 16b_1(\omega + a\kappa + a\kappa^2) > 0, \quad (3.31)$$

and (3.22) which follows from (3.27) or (3.29) and (3.28).

### 3.2.3 Log law

Here,

$$F(s) = b \ln(s), \quad (3.32)$$

for real valued constant  $b$ , so that equation (3.11) reduces to [5, 6, 7]

$$iq_t + aq_{xx} + bq \ln |q|^2 = iaq_x + i\lambda(|q|^2 q)_x + i\nu(|q|^2)_x q + \theta_2 |q|^2 q_{xx} - \theta_2 q^2 q_{xx}^*, \quad (3.33)$$

and hence the real part ODE gives

$$2a(g')^2 - (2\omega + 2a\kappa + 2a\kappa^2 + b)g^2 - 2bg^2 \ln g = 0. \quad (3.34)$$

After separating variables in (3.34) and integrating leads to

$$g(s) = g(x - vt) = Ae^{-B^2(x-vt)^2}, \quad (3.35)$$

where

$$A = \exp\left(\frac{\omega + a\kappa + a\kappa^2 + b}{2b}\right), \quad (3.36)$$

and

$$B = \sqrt{\frac{b}{2a}}. \quad (3.37)$$

Hence, Gausson solution to (3.33) is given by

$$q(x, t) = Ae^{-B^2(x-vt)^2} e^{i(-\kappa x + \omega t + \sigma)}, \quad (3.38)$$

where the amplitude  $A$  of the Gausson and the inverse width  $B$  of the Gausson are given by (3.36) and (3.37), respectively. It must be noted that these bright soliton exist provided the constraints

$$b \neq 0, \quad (3.39)$$

$$ab > 0, \quad (3.40)$$

hold respectively for (3.36) and (3.37). The equation (3.40) implies that both GVD and nonlinearity must maintain the same sign for Gausson to exist.

### 3.3 Conclusions

This chapter recovers bright 1-soliton solution, in optical metamaterials, by the aid of travelling wave hypothesis. This integration scheme is not applicable to retrieve bright soliton solutions for power law and dual-power law media. Also, it must be noted that there are soliton solutions that are reported earlier by this same integration scheme, namely traveling wave hypothesis applicable to five forms of nonlinearity that includes powers law and dual-power law [5, 6, 7]. However, for optical metamaterials, the situation is a little different. The governing equations have parameters that obey constraint relations, as discussed in Section-3, and thus prevent integrability by traveling wave hypothesis for power law and dual-power law.

Another disadvantage of this scheme is that one can retrieve only bright 1-soliton solutions and not dark or singular optical soliton. Later, the focus will be on the application of additional integration techniques to retrieve dark and singular soliton along with bright-dark combo optical soliton. The results of those research will be applied soon. Additionally, soliton perturbation theory as well as quasi-stationary soliton solutions will be obtained. Finally, the quasi-particle theory, for suppression of intra-channel collision, will also be developed and reported.

# Chapter 4

## SOLITON IN OPTICAL METAMATERIALS BY MAPPING METHOD

This chapter studies soliton in optical metamaterials by the aid of mapping method. There are two types of nonlinear media taken into consideration. They are Kerr law and parabolic law nonlinearity. The constraint conditions, on the parameters, that need to hold for the soliton to exist, are also listed.

### 4.1 Overview of mapping method

In this section, we give an analysis of mapping methods which was employed in [10, 11, 12]. The analysis given below is in general for a system of partial differential equations (PDE)s [13] but in this chapter we have applied it for a single PDE.

Consider a nonlinear coupled PDE with two dependent variables  $u$  and  $v$  and two independent variables  $x$  and  $t$  given by

$$F(u, v, u_t, v_t, u_x, v_x, u_{xxx}, v_{xxx}, \dots) = 0, \quad (4.1)$$

where subscripts denote partial derivatives with respect to the corresponding independent variables and  $F$  is a polynomial function of the indicated variables.

Step-1: Assume that (4.1) has a traveling wave solution in the form

$$u(x, t) = u(\xi) = \sum_{i=0}^{l_1} A_i f^i(\xi); v(x, t) = v(\xi) = \sum_{i=0}^{l_2} B_i f^i(\xi), \quad (4.2)$$

where  $\xi = x - \lambda t$ ,  $A_i$ ,  $B_i$  and  $\lambda$  are arbitrary constants,  $l_1$  and  $l_2$  are integers and  $i$  represents integer powers of  $f$ . The first derivative of  $f$  with respect to  $\xi$  denoted by  $f'$  can be expressed in powers of  $f$  in the form

$$f'^2 = pf^2 + \frac{1}{2}qf^4 + r, \quad (4.3)$$

where  $p$ ,  $q$  and  $r$  are arbitrary constants. The motivation for (4.3) was that the squares of the first derivatives of Jacobi elliptic functions JEFs can be expressed in even powers of themselves.

Step–2: Substituting (4.2) into (4.1), the PDE reduces to an ODE. Balancing the highest order derivative term and the highest order nonlinear term of the ODE, the values of  $l_1$  and  $l_2$  can be found.

Step–3: Substituting for  $u$  and  $v$  and using (4.3), the ODE gives rise to a set of algebraic equations by setting the coefficients of various powers of  $f$  to zero.

Step–4: From the values of the parameters  $A_i$ ,  $B_i$ ,  $p$ ,  $q$  and  $r$ , the solution of (4.1) can be derived.

Thus a mapping relation is established through (4.2) between the solution to (4.3) and that of (4.1). It is to be noted that if the values of  $l_1$  and  $l_2$  are integers, we can use the method directly to get a variety of solutions in terms of hyperbolic functions or JEFs. If they are nonintegers, the equation may still have solutions are rational expressions involving hyperbolic functions or JEFs.

## 4.2 Application to metamaterials

The mapping scheme described above will be applied to optical metamaterials. The governing equation for optical metamaterials is given by the nonlinear *Schrödinger's* equation(NLSE) below

$$iq_t + aq_{xx} + F(|q|^2)q = i\alpha q_x + i\lambda(|q|^2)_x q + i\nu(|q|^2)_x q + \theta_1(|q|^2)_{xx} + \theta_2|q|^2 q_{xx} + \theta_3 q^2 q_{xx}^*. \quad (4.4)$$

In (4.4), the dependent variable that represents the complex valued wave profile is denoted by  $q$  and its complex conjugate is  $q^*$ . The independent variables are  $x$  and  $t$  which represent spatial and temporal variables. Next the first term on the left hand side is linear evolution. The coefficient of  $a$  is the group velocity dispersion(GVD) and the nonlinearity is represented by the functional  $F$ . On the right hand side,  $\alpha$  is the coefficient of inter-model dispersion, while  $\lambda$  is the self-steepening term to avoid the formation of shock waves and  $\nu$  gives the coefficient of nonlinear dispersion. Finally the coefficients of  $\theta_j$  for  $j = 1, 2, 3$  are accounted for metamaterials [1, 2, 3, 4, 9].

Also in (4.4),  $F$  is a real-valued algebraic function and it is necessary to have the smoothness

of the complex function  $F(|q|^2)q : C \mapsto C$ . Considering the complex plane  $C$  as a two-dimensional linear space  $R^2$ , the function  $F(|q|^2)q$  is  $k$  times continuously differentiable, so that

$$F(|q|^2)q \in \bigcup_{m,n=1}^{\infty} C^k((-n, n) \times (-m, m); R^2). \quad (4.5)$$

This chapter will consider only two forms of nonlinearity. They are Kerr law and parabolic law that are discussed in details in the next two subsections.

### 4.2.1 Kerr law

This law arises when the refractive index of light is intensity dependent. For Kerr law nonlinearity,  $F(s) = s$  and therefore this form of nonlinearity is also referred to as cubic nonlinearity. Most commercial optical fibers obey this Kerr law of nonlinearity. For Kerr law medium, the NLSE given by (4.4) modifies to

$$iq_t + aq_{xx} + b|q|^2q = i\alpha q_x + i\lambda(|q|^2q)_x + i\nu(|q|^2)_x q + \theta_1(|q|^2q)_{xx} + \theta_2|q|^2q_{xx} + \theta_3q^2q_{xx}^*. \quad (4.6)$$

To derive soliton solutions, the starting hypothesis is

$$q(x, t) = P(x, t)e^{i\varphi}, \varphi = -\kappa x + \omega t + \theta, \quad (4.7)$$

where  $\kappa$  is the wave number,  $\omega$  is the soliton frequency and  $\theta$  is the phase constant. Substituting (4.7) into (4.6) and separating them into real and imaginary parts, we obtain

$$\begin{aligned} (\omega + \alpha\kappa + a\kappa^2)P + [\kappa(\lambda - \kappa\theta_1 - \kappa\theta_2 - \kappa\theta_3) - b]P^3 - a\frac{\partial^2 P}{\partial x^2} + 6P\left(\frac{\partial P}{\partial x}\right)^2\theta_1 \\ + (3\theta_1 + \theta_2 + \theta_3)P^2\frac{\partial^2 P}{\partial x^2} = 0, \end{aligned} \quad (4.8)$$

and

$$\frac{\partial P}{\partial t} - (\alpha + 2a\kappa)\frac{\partial P}{\partial x} = (3\lambda + 2\nu - 6\theta_1\kappa - 2\theta_2\kappa + 2\theta_3\kappa)P^2\frac{\partial P}{\partial x}, \quad (4.9)$$

respectively.

Next, considering the traveling wave solution  $P(x, t) = P(\tau)$  where  $\tau = B(x - vt)$ , where  $B$  and  $v$  are constant, (4.9) becomes

$$\begin{aligned} (\omega + \alpha\kappa + a\kappa^2)P + [\kappa(\lambda - \kappa\theta_1 - \kappa\theta_2 - \kappa\theta_3) - b]P^3 - aB^2P'' + 6PP'^2B^2\theta_1 \\ + (3\theta_1 + \theta_2 + \theta_3)P^2B^2P'' = 0, \end{aligned} \quad (4.10)$$

where prime denotes differentiation with respect to  $\tau$ . The imaginary part leads to the relations

$$v = -\alpha - 2a\kappa, \quad (4.11)$$

and

$$3\lambda + 2\nu - 2\kappa(3\theta_1 + \theta_2 - \theta_3) = 0, \quad (4.12)$$

(4.11) gives the speed of the soliton and (4.12) is the constraint relation that must be valid in order for the soliton to exist.

Now, (4.10) can be written in the form

$$P'' = A_1P + A_2P^3 + A_3PP'^2 + A_4P^2P'', \quad (4.13)$$

where,

$$\begin{aligned} A_1 &= \frac{\omega + \alpha\kappa + a\kappa^2}{aB^2}, \\ A_2 &= \frac{\kappa(\lambda - \kappa(\theta_1 + \theta_2 + \theta_3) - b)}{aB^2}, \\ A_3 &= \frac{6\theta_1}{a}, \\ A_4 &= \frac{3\theta_1 + \theta_2 + \theta_3}{a}. \end{aligned} \quad (4.14)$$

Applying the mapping method, we can assume the solution structure of (4.13) in the form [10, 11, 12]

$$P(\tau) = a_0 + a_1f(\tau), \quad (4.15)$$

where  $f$  satisfies (4.3). Substituting (4.15) into (4.13) and using (4.3), we obtain a polynomial in  $f$

given by

$$\begin{aligned}
a_1 p f + a_1 q f^3 &= A_1(a_0 + a_1 f) + A_2(a_0^3 + 3a_0^2 a_1 f + 3a_0 a_1^2 f^2 + a_1^3 f^3) \\
&+ A_3(a_0 a_1^2 \tau + a_1^3 \tau f + a_0 a_1^2 p f^2 + a_1^3 p f^3 + \frac{1}{2} a_0 a_1^2 q f^4) \\
&+ A_4(a_0^2 a_1 p f + 2a_0 a_1^2 p f^2 + (a_0^2 a_1 q + a_1^3 p) f^3 + 2a_0 a_1^2 q f^4 + a_1^3 q f^5). \tag{4.16}
\end{aligned}$$

Equating the coefficients of different powers of  $f$  in (4.16), we arrive at the following algebraic equations:

$$f^5 : \frac{1}{2} a_1^3 q A_3 + a_1^3 q A_4 = 0 \Rightarrow \frac{1}{2} A_3 + A_4 = 0, \tag{4.17}$$

$$f^4 : \frac{1}{2} a_0 a_1^2 q A_3 + 2a_0 a_1^2 q A_4 = 0 \Rightarrow \frac{1}{2} A_3 + 2A_4 = 0, \tag{4.18}$$

(4.17) and (4.18) lead us to  $A_3 = 0$  and  $A_4 = 0$ . This gives rise to  $\theta_1 = \theta_2 = \theta_3 = 0$ . From the coefficients of  $f^3$ ,  $f^2$  and the constant term, we obtain

$$a_0 = 0, a_1 = \pm \sqrt{\frac{q}{A_2}}, A_1 = p. \tag{4.19}$$

So, we can easily see that  $a_1$  can be written as

$$a_1 = \pm \sqrt{\frac{q(\omega + \alpha\kappa + a\kappa^2)}{p(\kappa\lambda - b)}}. \tag{4.20}$$

Case-1:  $p = -(1 + m^2)$ ,  $q = 2m^2$ ,  $\tau = 1$ .

Here, (4.3) gives  $f(\tau) = sn(\tau)$ . In this case, (4.4) gives rise to the periodic wave solution [14]

$$q(x, t) = \pm \sqrt{\frac{2m^2(\omega + \alpha\kappa + a\kappa^2)}{(1 + m^2)(b - \kappa\lambda)}} \times sn[B(x - vt)]e^{i(-\kappa x + \omega t + \theta)}. \tag{4.21}$$

As  $m \rightarrow 1$ , one recovers dark soliton solution from (4.21)

$$q(x, t) = \pm \sqrt{\frac{\omega + \alpha\kappa + a\kappa^2}{b - \kappa\lambda}} \times \tanh[B(x - vt)]e^{i(-\kappa x + \omega t + \theta)}. \tag{4.22}$$

Case-2:  $p = 2m^2 - 1, q = -2m^2, \tau = 1 - m^2$ .

So, (4.3) yields  $f(\tau) = cn(\tau)$ . In this case, (4.4) gives rise to the periodic wave solution [14]

$$q(x, t) = \pm \sqrt{\frac{2m^2(\omega + \alpha\kappa + a\kappa^2)}{(2m^2 - 1)(b - \kappa\lambda)}} \times cn[B(x - vt)]e^{i(-\kappa x + \omega t + \theta)}. \quad (4.23)$$

As  $m \rightarrow 1$ , one obtains bright soliton solution from (4.23)

$$q(x, t) = \pm \sqrt{\frac{2(\omega + \alpha\kappa + a\kappa^2)}{b - \kappa\lambda}} \times \operatorname{sech}[B(x - vt)]e^{i(-\kappa x + \omega t + \theta)}. \quad (4.24)$$

Case-3:  $p = -(1 + m^2), q = 2, \tau = m^2$ .

Here, (4.3) gives  $f(\tau) = ns(\tau)$ . Therefore, (4.4) gives rise to the periodic wave solution [14]

$$q(x, t) = \pm \sqrt{\frac{2(\omega + \alpha\kappa + a\kappa^2)}{(1 + m^2)(b - \kappa\lambda)}} \times ns[B(x - vt)]e^{i(-\kappa x + \omega t + \theta)}. \quad (4.25)$$

As  $m \rightarrow 1$ , (4.25) leads us to the singular soliton solution

$$q(x, t) = \pm \sqrt{\frac{2(\omega + \alpha\kappa + a\kappa^2)}{b - \kappa\lambda}} \times \operatorname{coth}[B(x - vt)]e^{i(-\kappa x + \omega t + \theta)}. \quad (4.26)$$

These soliton and doubly periodic solutions, listed in (4.21)-(4.26) immediately introduce the constraint condition

$$(b - \kappa\lambda)(\omega + \alpha\kappa + a\kappa^2) > 0. \quad (4.27)$$

Thus, the soliton and doubly periodic functions will exist provided the constraint relation of the parameters hold.

## 4.2.2 Parabolic law

The equation under consideration, for this law of nonlinearity, is

$$iq_t + aq_{xx} + (b_1|q|^2 + b_2|q|^4)q = i\alpha q_x + i\lambda \left(|q|^2 q\right)_x + i\nu \left(|q|^2\right)_x q + \theta_1 \left(|q|^2 q\right)_{xx} + \theta_2 |q|^2 q_{xx} + \theta_3 q^2 q_{xx}^*. \quad (4.28)$$

This law is commonly known as the cubic-quintic nonlinearity. The second term of nonlinearity on the left hand side of (4.28) is large for the case of p-toluene sulfonate crystals. This law arises in the nonlinear interaction between Langmuir waves and electrons. It describes the nonlinear interaction between the high frequency Langmuir waves and the ion–acoustic waves by ponderomotive forces.

Substituting (4.25) into (4.28) and considering the traveling wave solution as in section3, the imaginary part remains the same as before and the real part becomes

$$P'' = A_1P + A_2P^3 + A_3PP'^2 + A_4P^2P'' + A_5P^5, \quad (4.29)$$

where,  $A_1, A_2, A_3$  and  $A_4$  are as in (4.14) with  $b$  replaced by  $b_1$  and  $A_5 = -b_2/(aB^2)$ .

Assuming the solution of (4.29) in the form of (4.15) and using (4.3), we get a fifth degree polynomial in  $f$ . The coefficients of different powers of  $f$  give rise to a set of algebraic equations whose solutions give

$$a_0 = 0, a_1 = \sqrt{\frac{apB^2 - \omega - \alpha\kappa - a\kappa^2}{6B^2\tau\theta_1}}, \quad (4.30)$$

and get the constraint condition

$$q\tau A_3^2 + 2q\tau A_3A_4 - 2A_1A_5 + 2pA_5 = 0, \quad (4.31)$$

Case-1:  $p = -(1 + m^2), q = 2m^2, \tau = 1$ .

Here, (4.3) gives  $f(\tau)sn(\tau)$ . In this case, (4.28) gives rise to the periodic wave solution [14]

$$q(x, t) = \pm \sqrt{-\frac{a(1 + m^2)B^2 + \omega + \alpha\kappa + a\kappa^2}{6B^2\theta_1}} \times sn[B(x - vt)]e^{i(-\kappa x + \omega t + \theta)}, \quad (4.32)$$

As  $m \rightarrow 1$ , (4.32) leads us dark soliton solution

$$q(x, t) = \pm \sqrt{-\frac{2aB^2 + \omega + \alpha\kappa + a\kappa^2}{6B^2\theta_1}} \times tanh[B(x - vt)]e^{i(-\kappa x + \omega t + \theta)}. \quad (4.33)$$

Case-2:  $p = 2m^2 - 1, q = -2m^2, \tau = 1 - m^2$ .

So, (4.3) yields  $f(\tau) = cn(\tau)$ . In this case, (4.28) gives rise to the periodic wave solution [14]

$$q(x, t) = \pm \sqrt{-\frac{a(2m^2 - 1)B^2 - \omega - \alpha\kappa - a\kappa^2}{6B^2\theta_1}} \times cn[B(x - vt)]e^{i(-\kappa x + \omega t + \theta)}. \quad (4.34)$$

As  $m \rightarrow 1$ , (4.34) does not give rise to a solitary wave solution.

Case-3:  $p = -(1 + m^2)$ ,  $q = 2$ ,  $\tau = m^2$ .

Here, (4.3) gives  $f(\tau) = ns(\tau)$ . In this case, (4.28) gives rise to the periodic wave solution [14]

$$q(x, t) = \pm \sqrt{-\frac{a(1 + m^2)B^2 + \omega + \alpha\kappa + a\kappa^2}{6B^2m^2\theta_1}} \times ns[B(x - vt)]e^{i(-\kappa x + \omega t + \theta)}. \quad (4.35)$$

As  $m \rightarrow 1$ , (4.35) leads us to the singular solitary wave solution

$$q(x, t) = \pm \sqrt{-\frac{2aB^2 + \omega + \alpha\kappa + a\kappa^2}{6B^2m^2\theta_1}} \times \coth[B(x - vt)]e^{i(-\kappa x + \omega t + \theta)}. \quad (4.36)$$

It needs to be noted that the doubly periodic functions, for this law of nonlinearity, given by (4.32) and (4.35) will exist provided

$$\theta_1[a(1 + m^2)B^2 + \omega + \alpha\kappa + a\kappa^2] < 0. \quad (4.37)$$

Consequently, dark soliton and singular soliton will exist if

$$\theta_1(2aB^2 + \omega + \alpha\kappa + a\kappa^2) < 0. \quad (4.38)$$

Finally, the periodic wave solution given by (4.34) will exist with constraint condition

$$\theta_1[a(2m^2 - 1)B^2 - \omega - \alpha\kappa + a\kappa^2] > 0. \quad (4.39)$$

### 4.3 Generalization

This chapter retrieved soliton solutions to the NLSE in optical metamaterials with Kerr and parabolic law nonlinearity. The mapping method is applied to obtain these solutions. The results of this chapter came with certain constraints that must hold for these soliton to exist. These soliton solutions are recovered after a limiting process applied to doubly periodic functions when the modulus of ellipticity approached unity. This approach is therefore a very unique method to derive soliton solutions.

Later the results will be extended to the case when several perturbation terms will be considered. Better yet, soliton perturbation theory will be applied to give the adiabatic variation of these soliton parameters. Several other integration tools will be adopted to obtain soliton and other solutions. The results of those researches are awaited at this time.

## Chapter 5

# SOLITON PROPAGATION THROUGH NANOSCALE WAVEGUIDES IN OPTICAL METAMATERIALS

This chapter studies the dynamics of soliton propagation through optical metamaterials. The proposed model will be studied with five forms of nonlinearity. They are Kerr law, power law, parabolic law, dual-power law and log-law. The integration scheme that will be adopted is the method of undetermined coefficients. Bright, dark and singular soliton solutions will be obtained. The essential conditions for the existence of these soliton will naturally emerge.

### 5.1 Governing equation and mathematical analysis

The dynamics of soliton in optical metamaterials is governed by the nonlinear *Schrödinger's* equation (NLSE) which in the dimensionless form is given by [1, 2, 3, 4, 6, 7, 9, 15, 16, 17, 18, 19, 20, 21, 23, 24, 25, 27, 26, 28, 29, 30, 49, 51, 60, 78, 79, 80]:

$$iq_t + aq_{xx} + F(|q|^2)q = i\alpha q_x + i\lambda(|q|^2q)_x + i\nu(|q|^2)_x q + \theta_1(|q|^2q)_{xx} + \theta_2|q|^2q_{xx} + \theta_3q^2q_{xx}^*. \quad (5.1)$$

(5.1) is the NLSE that is studied in the context of metamaterials. Here in (5.1),  $a$  is the group velocity dispersion. This section produces the delicate balance between dispersion and nonlinearity that accounts for the formation of the stable soliton. On the right-hand side  $\lambda$  represents the self-steepening term in order to avoid the formation of shocks and  $\nu$  is the nonlinear dispersion, while  $\alpha$  represents the inter-modal dispersion. This arises from the fact that group velocity of light in multi-mode fibers depends on chromatic dispersion as well as the propagation mode involved. Next,  $\theta_j$  for  $j = 1, 2, 3$  are the perturbation terms that appear in the context of metamaterials [17, 20, 21, 23, 25, 26, 66]. Finally, the independent variables are  $x$  and  $t$  that represent spatial and temporal variables respectively with the dependent variable  $q(x, t)$  being the complex-valued wave profile.

The real-valued algebraic functional  $F$  must possess smoothness of the complex-valued function

$F(|q|^2)q : C \mapsto C$ . Treating the complex plane  $C$  as two-dimensional linear space  $R^2$ , the function  $F(|q|^2)q$  is  $k$  times continuously differentiable provided

$$F(|q|^2)q \in \bigcup_{m,n=1}^{\infty} C^k((-n, n) \times (-m, m); R^2). \quad (5.2)$$

In order to start with the analysis of (5.1), the starting hypothesis is

$$q(x, t) = P(x, t) e^{i\phi}. \quad (5.3)$$

In (5.3),  $P(x, t)$  represents amplitude portion of the wave while  $\phi(x, t)$  is the phase component that is given by

$$\phi = -\kappa x + \omega t + \theta, \quad (5.4)$$

where  $\kappa$  gives the soliton frequency and  $\omega$  being the soliton wave number while  $\theta$  represent the phase constant. After substituting (5.3) into (5.1) and decomposing into real and imaginary parts lead to

$$\begin{aligned} & (\omega + a\kappa + a\kappa^2) P - a \frac{\partial^2 P}{\partial x^2} + 6\theta_1 P \left( \frac{\partial P}{\partial x} \right)^2 - \\ & P^3 \{ b - \lambda\kappa + \kappa^2 (\theta_1 + \theta_2 + \theta_3) \} + P^2 \frac{\partial^2 P}{\partial x^2} (3\theta_1 + \theta_2 + \theta_3) = 0, \end{aligned} \quad (5.5)$$

and

$$\frac{\partial P}{\partial t} - (a + 2a\kappa) \frac{\partial P}{\partial x} = (3\lambda + 2\nu - 6\theta_1\kappa - 2\theta_2\kappa + 3\theta_3\kappa) P^2 \frac{\partial P}{\partial x}, \quad (5.6)$$

respectively. The imaginary part equation (5.6) implies the relations

$$\nu = -a - 2a\kappa, \quad (5.7)$$

and

$$3\lambda + 2\nu = 2\kappa (3\theta_1 + \theta_2 - \theta_3). \quad (5.8)$$

This follows from the fact that the amplitude portion  $P(x, t)$  can be written in terms of the wave  $g(x - vt)$  with  $v$  being the speed of the wave. The two relations (5.7) and (5.8) are obtained by setting the coefficients of linearly independent functions from (5.6) to zero. These two expressions serve as the existence condition for the soliton that is commonly referred to as constraint relation.

The speed of the soliton stays the same for all laws of non-linearity, namely for all forms of the function  $F$  introduced in (5.1) and for all kinds of soliton. The constraint relation (5.8) however modifies with power and dual-power laws. It is the real part equation that will be further analyzed in detail for various nonlinear forms of  $F$  in the following sections.

## 5.2 Kerr law

This law is also known as the cubic nonlinearity and is considered to be the simplest known form of nonlinearity. Most optical fibers that are commercially available nowadays obey this Kerr law of nonlinearity. Therefore, in this first section the attention will be on optical metamaterials with cubic nonlinearity. In this case  $F(u) = bu$  for some non-zero constants [18]. Therefore, the governing equation given by (5.1) with Kerr law nonlinearity reduces to [49].

$$iq_t + aq_{xx} + b|q|^2q = i\alpha q_x + i\lambda(|q|^2q)_x + i\nu(|q|^2)_x q + \theta_1(|q|^2q)_{xx} + \theta_2|q|^2q_{xx} + \theta_3q^2q_{xx}^*. \quad (5.9)$$

For Kerr law nonlinearity the results of bright, dark and singular soliton have been already reported in the past [2, 49]. Therefore, this section will just list the results from these earlier published [2, 49]. It is only the singular soliton of the second type that will be derived in detail.

### 5.2.1 Bright soliton

For Kerr law nonlinear medium, bright 1-soliton solution in optical metamaterials is given by [49]

$$q(x, t) = A \operatorname{sech}[B(x - vt)] e^{i(-\kappa x + \omega t + \theta)}, \quad (5.10)$$

where  $A$  is the amplitude and  $B$  is the inverse width of the soliton. The relation between amplitude and width is given by

$$(b - \lambda\kappa - 5\theta_1\kappa^2) A^2 - 3\theta_1 A^2 B^2 - 2aB^2 = 0. \quad (5.11)$$

The soliton frequency is

$$\omega = aB^2 - a\kappa^2 - a\kappa, \quad (5.12)$$

and the additional constraint condition is

$$6\theta_1 + \theta_2 + \theta_3 = 0. \quad (5.13)$$

### 5.2.2 Dark soliton

For Kerr law, dark soliton solution is given by [49]

$$q(x, t) = A \tanh[B(x - vt)] e^{i(-\kappa x + \omega t + \theta)}. \quad (5.14)$$

In this case, the parameters  $A$  and  $B$  are referred to as free parameters and these are connected as

$$(b - \lambda\kappa - 5\theta_1\kappa^2) A^2 + 6\theta_1 A^2 B^2 + 2aB^2 = 0, \quad (5.15)$$

and the wave number is

$$\omega = -(\alpha\kappa + a\kappa^2 + 2aB^2 + 6\theta_1 A^2 B^2). \quad (5.16)$$

together with the constraint condition (5.13) that also remains valid here.

### 5.2.3 Singular soliton (Type-I)

In this case, singular soliton solution of first kind is [2]

$$q(x, t) = A \operatorname{csch}[B(x - vt)] e^{i(-\kappa x + \omega t + \theta)}, \quad (5.17)$$

where the free parameters  $A$  and  $B$  are connected as in (5.11). The wave number is also located in (5.12) while the same constraint (5.13) holds here.

#### 5.2.4 Singular soliton (Type-II)

In this case, the starting hypothesis is given by [6, 7]

$$P(x, t) = A \coth^p \tau, \quad (5.18)$$

where

$$\tau = B(x - vt). \quad (5.19)$$

In this case,  $A$  and  $B$  are free parameters and  $p$  is unknown exponent. Substituting this hypothesis into (5.5) and (5.6), the real and imaginary parts are

$$\begin{aligned} & ap(p-1)B^2 \coth^{p-2} \tau - \{2ap^2B^2 + (\omega + a\kappa + a\kappa^2)\} \coth^p \tau + ap(p+1)B^2 \coth^{p+2} \tau \\ & + A^2 [\{b - \lambda\kappa + \kappa^2(\theta_1 + \theta_2 + \theta_3)\} + 12\theta_1 p^2 B^2 + 2p^2 B^2 (3\theta_1 + \theta_2 + \theta_3)] \coth^{3p} \tau \\ & - A^2 B^2 \{6\theta_1 p^2 + p(p-1)(3\theta_1 + \theta_2 + \theta_3)\} \coth^{3p-2} \tau \\ & - A^2 B^2 \{6\theta_1 p^2 + p(p+1)(3\theta_1 + \theta_2 + \theta_3)\} \coth^{3p+2} \tau = 0, \end{aligned} \quad (5.20)$$

and

$$\nu + a + 2a\kappa + A^2(3\lambda + 2\nu - 6\theta_1\kappa - 2\theta_2\kappa + 3\theta_3\kappa) \coth^{2p} \tau = 0, \quad (5.21)$$

respectively. By virtue of balancing principle for optical soliton, equating the exponents  $3p$  and  $p+2$  from real part equation (5.20) gives

$$p = 1. \quad (5.22)$$

Next, setting the coefficients of undetermined coefficients or linearly independent functions, from (5.20) to zero yields the constraint relation (5.13), the wave number given by (5.12) and the relation between the free parameters  $A$  and  $B$  as in (5.11). The imaginary part equation leads to (5.7) and (5.8).

Therefore, singular 1-soliton solution of Type-II in Kerr law medium is

$$q(x, t) = A \coth[B(x - vt)]e^{i(-\kappa x + \omega t + \theta)}. \quad (5.23)$$

where the definition of parameters and their respective constraints are all in place.

### 5.3 Power law

This law of nonlinearity also arises in nonlinear plasmas that solves the problem of small  $K$ -condensation in weak turbulence theory. It also arises in the context of nonlinear optics. Physically, various materials, including semiconductors, exhibit power law nonlinearities. For power,  $F(u) = bu^n$ , where  $n$  is the power law nonlinearity parameter. It is important to note that  $0 < n < 2$  to prevent wave collapse and in particular  $n \neq 2$  to prevent self-focusing singularity [18]. In this case, NLSE given by (5.1) modifies to

$$iq_t + aq_{xx} + b|q|^{2n}q = i\alpha q_x + i\lambda(|q|^2q)_x + i\nu(|q|^2)_x q + \theta_1(|q|^2q)_{xx} + \theta_2|q|^2q_{xx} + \theta_3q^2q_{xx}^*. \quad (5.24)$$

This equation will now be further analyzed in the following sections to obtain four forms of soliton.

#### 5.3.1 Bright soliton

The starting hypothesis for bright soliton is given by [6, 7, 18]

$$P(x, t) = A \operatorname{sech}^p \tau, \quad (5.25)$$

which upon substitution, simplifies real and imaginary part equations (5.5) and (5.6) to

$$\begin{aligned} ap^2B^2 - (\omega + a\kappa + a\kappa^2) - ap(p+1)B^2\operatorname{sech}^2\tau + (b - \lambda\kappa)A^{2n}\operatorname{sech}^{2np}\tau \\ A^2\{(\theta_1 + \theta_2 + \theta_3)\kappa^2 - p^2B^2(9\theta_1 + \theta_2 + \theta_3)\}\operatorname{sech}^{2p}\tau \\ + A^2B^2\{6\theta_1p^2 + p(p+1)(3\theta_1 + \theta_2 + \theta_3)\}\operatorname{sech}^{2np}\tau = 0, \end{aligned} \quad (5.26)$$

and

$$\nu + a + 2a\kappa + A^{2n} ((2n + 1) \lambda + 2n\nu) \operatorname{sech}^{2np} \tau - A^2 \{2\kappa (3\theta_1 + \theta_2 - \theta_3)\} \operatorname{sech}^{2np} \tau = 0, \quad (5.27)$$

respectively. From balancing principle, equating the exponents  $2np$  and  $2$ , from real part (5.26) gives

$$p = \frac{1}{n}. \quad (5.28)$$

Next, setting the coefficients of linearly independent functions, in (5.26), to zero reveals the wave number

$$\omega = \frac{1}{n^2} \{aB^2 - n^2 (a\kappa + a\kappa^2)\}, \quad (5.29)$$

width of the soliton

$$B = n\kappa \sqrt{\frac{\theta_1 + \theta_2 + \theta_3}{9\theta_1 + \theta_2 + \theta_3}}, \quad (5.30)$$

and the amplitude-width relation as

$$n^2 (b - \lambda\kappa) A^{2n} = a(n + 1)B^2. \quad (5.31)$$

From (5.30) and (5.31), the amplitude of the soliton is

$$A = \left[ \frac{a(n + 1)\kappa^2 (\theta_1 + \theta_2 + \theta_3)}{(b - \lambda\kappa) (9\theta_1 + \theta_2 + \theta_3)} \right]^{1/2n}. \quad (5.32)$$

The amplitude and width of the soliton will exist provided

$$(\theta_1 + \theta_2 + \theta_3) (9\theta_1 + \theta_2 + \theta_3) > 0, \quad (5.33)$$

and

$$a(b - \lambda\kappa) > 0, \quad (5.34)$$

which follows from (5.30) and (5.32) respectively. The next constraint relation that stems out from the coefficient of  $sech^{2p+2}\tau$  in (5.26) is

$$6\theta_1 + (n+1)(3\theta_1 + \theta_2 + \theta_3) = 0. \quad (5.35)$$

The imaginary part equation given by (5.27) leads to the speed  $v$  given by (5.7) as well as the following set of constraints:

$$(2n+1)\lambda + 2n\nu = 0, \quad (5.36)$$

and

$$3\theta_1 + \theta_2 - \theta_3 = 0. \quad (5.37)$$

Thus, bright 1-soliton solution in optical metamaterials with power law nonlinearity is

$$q(x, t) = Asech^{1/n}[B(x - vt)]e^{i(-\kappa x + \omega t + \theta)}, \quad (5.38)$$

with the definition of parameters and necessary constraints in place, as indicated.

### 5.3.2 Dark soliton

For dark soliton solution, the starting hypothesis is given by [6, 7, 18]

$$P(x, t) = A \tanh^p \tau, \quad (5.39)$$

which upon substituting into the real and imaginary part equations (5.5) and (5.6) simplifies to

$$\begin{aligned} & ap(p-1)B^2 \tanh^{p-2}\tau - \{\omega + a\kappa + a\kappa^2 + 2ap(p+1)B^2\} \tanh^p \tau \\ & + ap(p+1)B^2 \tanh^{p+2}\tau + (b - \lambda\kappa)A^{2n} \tanh^{(2n+1)p}\tau \\ & - A^2 B^2 p \{6\theta_1 p + (p-1)(3\theta_1 + \theta_2 + \theta_3)\} \tanh^{3p-2}\tau \\ & + A^2 [12p^2 B^2 \theta_1 + p(2p+1)B^2(3\theta_1 + \theta_2 + \theta_3) + \kappa^2(\theta_1 + \theta_2 + \theta_3)] \tanh^{3p}\tau \\ & - pA^2 B^2 \{6p\theta_1 + (p+1)(3\theta_1 + \theta_2 + \theta_3)\} \tanh^{3p+2}\tau = 0, \end{aligned} \quad (5.40)$$

and

$$\nu + a + 2a\kappa + A^{2n} \{(2n + 1) \lambda + 2n\nu\} \tanh^{2np}\tau - 2\kappa A^2 (3\theta_1 + \theta_2 - \theta_3) \tanh^{2p}\tau = 0, \quad (5.41)$$

respectively. Now, setting the coefficient of stand-alone linearly independent function  $\tanh^{p-2}\tau$  to (5.22). Again from balancing principle, equating the exponents  $(2n + 1)p$  and  $p + 2$  gives (5.28). From (5.22) and (5.28),

$$n = 1. \quad (5.42)$$

Thus, dark soliton with power law nonlinearity condenses to Kerr law nonlinearity. The imaginary part equation (5.41) leads to (5.7), (5.36) and (5.37) with (5.42).

Therefore, dark 1-soliton solution for power law nonlinearity is also given by (5.14) with the wave number as in (5.16) and the relation between the free parameters as in (5.15). The constraint (5.13) remains valid, in this case.

### 5.3.3 Singular soliton (Type-I)

The starting hypothesis for singular soliton (Type-I) is given by [6, 7]

$$P(x, t) = A \operatorname{csch}^p \tau, \quad (5.43)$$

which upon substitution, simplifies (5.5) and (5.6) respectively to

$$\begin{aligned} ap^2 B^2 - (\omega + a\kappa + a\kappa^2) - ap(p + 1) B^2 \csc h^2 \tau + (b - \lambda\kappa) A^{2n} \operatorname{csh} h^{2np} \tau \\ A^2 \{(\theta_1 + \theta_2 + \theta_3) \kappa^2 - p^2 B^2 (9\theta_1 + \theta_2 + \theta_3)\} \operatorname{csch}^{2p} \tau \\ + A^2 B^2 \{6\theta_1 p^2 + p(p + 1) (3\theta_1 + \theta_2 + \theta_3)\} \operatorname{csch}^{2p+2} \tau = 0, \end{aligned} \quad (5.44)$$

and

$$\nu + a + 2a\kappa + A^{2n} \{(2n + 1) \lambda + 2n\nu\} \operatorname{csch}^{2np} \tau - 2\kappa A^2 (3\theta_1 + \theta_2 - \theta_3) \operatorname{csch}^{2p} \tau = 0. \quad (5.45)$$

From balancing principle applied to real part equation (5.44) equating the exponents  $2np$  and 2 gives the same value  $p$  as in (5.28). Next, from the linearly independent functions, similarly as in bright soliton, the same results (5.29)-(5.35) fall out.

The imaginary part equation (5.45) leads to (5.7), (5.36) and (5.37), namely the speed and necessary constraints.

Thus, singular 1-soliton solution in optical metamaterials with power law nonlinearity is

$$q(x, t) = A \operatorname{csc} h^{1/n} [B(x - vt)] e^{i(-\kappa x + \omega t + \theta)}, \quad (5.46)$$

with the definition of parameters and necessary constraints in place.

### 5.3.4 Singular soliton (Type-II)

With Kerr law nonlinear medium, singular soliton hypothesis is given by [6, 7]

$$P(x, t) = A \operatorname{coth}^p \tau, \quad (5.47)$$

which upon substituting into (5.17) and (5.18), the real and imaginary part equations reduce to

$$\begin{aligned} & ap(p-1)B^2 \operatorname{coth}^{p-2} \tau - \{\omega + a\kappa + a\kappa^2 + 2ap(p+1)B^2\} \operatorname{coth}^p \tau \\ & + ap(p+1)B^2 \operatorname{coth}^{p+2} \tau + (b - \lambda\kappa) A^{2n} \operatorname{coth}^{(2n+1)p} \tau \\ & - A^2 B^2 p \{6\theta_1 p + (p-1)(3\theta_1 + \theta_2 + \theta_3)\} \operatorname{coth}^{3p-2} \tau \\ & + A^2 [12p^2 B^2 \theta_1 + p(2p+1)B^2(3\theta_1 + \theta_2 + \theta_3) + \kappa^2(\theta_1 + \theta_2 + \theta_3)] \operatorname{coth}^{3p} \tau \\ & - pA^2 B^2 \{6p\theta_1 + (p+1)(3\theta_1 + \theta_2 + \theta_3)\} \operatorname{coth}^{3p+2} \tau = 0, \end{aligned} \quad (5.48)$$

and

$$\nu + a + 2a\kappa + A^{2n} \{(2n+1)\lambda + 2n\nu\} \operatorname{coth}^{2np} \tau - 2\kappa A^2 (3\theta_1 + \theta_2 - \theta_3) \operatorname{coth}^{2p} \tau = 0, \quad (5.49)$$

respectively. Similarly, as in dark soliton solutions relation (5.42) falls out. Therefore, singular soliton of the second type, with power law nonlinearity, will exist if power law nonlinearity boils

down to Kerr law.

The imaginary part equation (5.6) which leads to (5.7), (5.36) and (5.37) along with (5.40). Therefore, singular 1-soliton solution for power law nonlinearity is also given by (5.23) with parameter definitions and constraints as in dark soliton with Kerr law.

## 5.4 Parabolic law

This law is alternatively known as the cubic-quintic nonlinearity and is studied in nonlinear interaction between Langmuir waves and electrons. It describes the nonlinear interaction between the high frequency Langmuir wave and the ion-acoustic waves by pondermotive forces. It takes the form  $F(u) = b_1 u + b_2 u^2$  for non-zero constants  $b_1$  and  $b_2$ . For parabolic law medium, the NLSE given by (5.1) changes to

$$iq_t + aq_{xx} + \left(b_1|q|^2 + b_2|q|^4\right)q = i\alpha q_x + i\lambda\left(|q|^2q\right)_x + i\nu\left(|q|^2\right)_x q + \theta_1\left(|q|^2q\right)_{xx} + \theta_2|q|^2q_{xx} + \theta_3q^2q_{xx}^*. \quad (5.50)$$

The rest of this section will focus on the details of retrieving soliton solutions to this model along with their conditions for existence.

### 5.4.1 Bright soliton

For bright soliton with parabolic law, the starting hypothesis is [6,27,28]

$$p(x, t) = \frac{A}{(D + \cosh \tau)^p}, \quad (5.51)$$

where  $A$  is the amplitude of the soliton and  $D$  is a newly introduced parameter and the usual definition of  $\tau$  is carried over from (5.19) with the unknown exponent  $p$ . Substituting (5.50) into

(5.5) and (5.6) gives

$$\begin{aligned}
& \frac{\omega + a\kappa + a\kappa^2 - ap^2B^2}{(D + \cosh \tau)^p} - \frac{A^2 \{b_1 - \lambda\kappa + \kappa^2 (\theta_1 + \theta_2 + \theta_3) - p^2B^2 (9\theta_1 + \theta_2 + \theta_3)\}}{(D + \cosh \tau)^{3p}} \\
& + \frac{ap(2p+1)B^2D}{(D + \cosh \tau)^{p+1}} - \frac{A^2B^2 \{12\theta_1p^2D + p(2p+1)D(3\theta_1 + \theta_2 + \theta_3)\}}{(D + \cosh \tau)^{3p+1}} - \frac{b_2A^4}{(D + \cosh \tau)^{5p}} \\
& - \frac{ap(p+1)B^2(D^2-1)}{(D + \cosh \tau)^{p+2}} + \frac{A^2B^2(D^2-1) \{6p^2\theta_1B^2 + p(p+1)(3\theta_1 + \theta_2 + \theta_3)\}}{(D + \cosh \tau)^{3p+2}} = 0,
\end{aligned} \tag{5.52}$$

and

$$\nu + a + 2a\kappa + \frac{A^2 \{3\lambda + 2\nu - 2\kappa(3\theta_1 + \theta_2 + \theta_3)\}}{(D + \cosh \tau)^{2p}} = 0, \tag{5.53}$$

respectively. By balancing principle, applied to (5.52), equating the exponents  $3p$  and  $p+1$  or the pair  $5p$  and  $p+2$  leads to

$$p = \frac{1}{2}, \tag{5.54}$$

Next, from the undetermined coefficients of linearly independent functions, one recovers the wave number

$$\omega = \frac{1}{4} (aB^2 - 4a\kappa^2 - 4a\kappa), \tag{5.55}$$

and the constraint

$$5\theta_1 + \theta_2 + \theta_3 = 0. \tag{5.56}$$

From the remaining linearly independent functions, the amplitude and the width are

$$\begin{aligned}
A = & \left\{ \frac{1}{2b_2\theta_1} [-D(\theta_1(b_1 - \lambda\kappa - 4\theta_1\kappa^2) + ab_2) \right. \\
& \left. \pm \sqrt{D^2\{\theta_1(b_1 - \lambda\kappa - 4\theta_1\kappa^2) + ab_2\}^2 - 3ab_2\theta_1(D^2-1)(b_1 - \lambda\kappa - 4\theta_1\kappa^2)}] \right\}^{1/2},
\end{aligned} \tag{5.57}$$

subject to the conditions

$$\begin{aligned}
& b_2\theta_1 [-D(\theta_1(b_1 - \lambda\kappa - 4\theta_1\kappa^2) + ab_2) \\
& \pm \sqrt{D^2\{\theta_1(b_1 - \lambda\kappa - 4\theta_1\kappa^2) + ab_2\}^2 - 3ab_2\theta_1(D^2-1)(b_1 - \lambda\kappa - 4\theta_1\kappa^2)}] > 0,
\end{aligned} \tag{5.58}$$

and

$$D^2\{\theta_1 (b_1 - \lambda\kappa - 4\theta_1\kappa^2) + ab_2\}^2 - 3ab_2\theta_1 (D^2 - 1) (b_1 - \lambda\kappa - 4\theta_1\kappa^2) > 0. \quad (5.59)$$

The width of the soliton is connected to the amplitude by the relation

$$B = A\sqrt{\frac{b_1 - \lambda\kappa - 4\theta_1\kappa^2}{aD + \theta_1 A^2}}. \quad (5.60)$$

Now the imaginary part equation (5.53) in this case gives (5.7) and (5.8). Finally, bright 1-soliton solution to optical metamaterials with parabolic law nonlinearity is

$$q(x, t) = \frac{A}{\sqrt{D + \cosh [B(x - vt)]}} e^{i(-\kappa x + \omega t + \theta)}, \quad (5.61)$$

where the parameter definitions and constraints are all in place.

#### 5.4.2 Dark soliton

For dark optical soliton [6, 7],

$$P(x, t) = (A + B \tanh \tau)^p, \quad (5.62)$$

where, in this case

$$\tau = \mu(x - vt). \quad (5.63)$$

Here  $A$ ,  $B$  and  $\mu$  are all free parameters. With (5.62), (5.5) and (5.6) respectively reduce to

$$\begin{aligned}
& ap(p-1)\mu^2(A^2 - B^2)^2(A + B \tanh \tau)^{p-2} - 2p(p-1)Aa\mu^2(A^2 - B^2)(A + B \tanh \tau)^{p-1} \\
& - \{B^2(\omega + a\kappa + a\kappa^2) - 2ap^2\mu^2(3A^2 - B^2)\}(A + B \tanh \tau)^p + ap(p+1)\mu^2(A + B \tanh \tau)^{p+2} \\
& + [2\mu^2p^2(B^2 - 3A^2)(9\theta_1 + \theta_2 + \theta_3) + B^2\{b_1 - \lambda\kappa + \kappa^2(\theta_1 + \theta_2 + \theta_3)\}](A + B \tanh \tau)^{3p} \\
& \quad - \mu^2p(A^2 - B^2)^2\{p(9\theta_1 + \theta_2 + \theta_3) - (3\theta_1 + \theta_2 + \theta_3)\}(A + B \tanh \tau)^{3p-2} \\
& + 2\mu^2pA(A^2 - B^2)\{2p(9\theta_1 + \theta_2 + \theta_3) - (3\theta_1 + \theta_2 + \theta_3)\}(A + B \tanh \tau)^{3p-1} \\
& \quad + 2\mu^2pA\{2p(9\theta_1 + \theta_2 + \theta_3) + (3\theta_1 + \theta_2 + \theta_3)\}(A + B \tanh \tau)^{3p+1} \\
& \quad - 2Aa\mu^2p(2p+1)(A + B \tanh \tau)^{p+1} + b_2B^2(A + B \tanh \tau)^{5p} \\
& - \mu^2p\{p(9\theta_1 + \theta_2 + \theta_3) + (3\theta_1 + \theta_2 + \theta_3)\}(A + B \tanh \tau)^{3p+2} = 0,
\end{aligned} \tag{5.64}$$

and

$$\nu + a + 2a\kappa - \{3\lambda + 2\nu - 2\kappa(3\theta_1 + \theta_2 + \theta_3)\}(A + B \tanh \tau)^{2p} = 0. \tag{5.65}$$

Again balancing exponents  $3p + 1$  with  $p + 2$ , from (5.64), leads to the same value of  $p$  as given by (5.54). There are more exponent pairs in (5.64) that will lead to (5.54) by virtue of the same principle. The coefficient of stand-alone linearly independent function  $(A + B \tanh \tau)^p$  gives

$$A = \pm B. \tag{5.66}$$

The undetermined coefficients of the remaining linearly independent functions from (5.64) yield the same constraint (5.4.3) along with the wave number

$$\omega = a\mu^2 - a\kappa - a\kappa^2, \tag{5.67}$$

and the relation between the free parameters

$$A = \frac{2a\mu^2}{b_1 - \lambda\kappa - 4\theta_1(\mu^2 + \kappa^2)}, \tag{5.68}$$

which stays valid as long as

$$\lambda\kappa + 4\theta_1(\mu^2 + \kappa^2) \neq b_1. \quad (5.69)$$

Next the imaginary part equation (5.65), relations (5.7) and (5.8) are valid.

Therefore, dark 1-soliton solution with parabolic law is given by

$$q(x, t) = \sqrt{A \{1 \pm \tanh [\mu (x - vt)]\}} e^{i(-\kappa x + \omega t + \theta)}, \quad (5.70)$$

with the respective parameters and constraints as indicated.

### 5.4.3 Singular soliton (Type-I)

For first type of singular soliton, the starting hypothesis is [6, 7],

$$P(x, t) = \frac{A}{(D + \sinh \tau)^p}, \quad (5.71)$$

where  $A$  and consequently  $D$  are free parameters. With the hypothesis (5.5) and (5.6) respectively transform to

$$\begin{aligned} & \frac{\omega + a\kappa + a\kappa^2 - ap^2B^2}{(D + \sinh \tau)^p} + \frac{ap(2p+1)B^2D}{(D + \sinh \tau)^{p+1}} - \frac{ap(p+1)B^2(D^2+1)}{(D + \sinh \tau)^{p+2}} \\ & - \frac{A^2 \{b_1 - \lambda\kappa + \kappa^2(\theta_1 + \theta_2 + \theta_3) - 6\theta_1p^2B^2 - p^2B^2(3\theta_1 + \theta_2 + \theta_3)\}}{(D + \sinh \tau)^{3p}} \\ & - \frac{A^2B^2 \{12\theta_1p^2D + p(2p+1)D(3\theta_1 + \theta_2 + \theta_3)\}}{(D + \sinh \tau)^{3p+1}} - \frac{b_2A^4}{(D + \sinh \tau)^{5p}} \\ & + \frac{A^2B^2(D^2+1) \{6p^2\theta_1B^2 + p(p+1)(3\theta_1 + \theta_2 + \theta_3)\}}{(D + \sinh \tau)^{3p+2}} = 0, \end{aligned} \quad (5.72)$$

and

$$\nu + a + 2a\kappa + \frac{A^2 \{3\lambda + 2\nu - 2\kappa(3\theta_1 + \theta_2 - \theta_3)\}}{(D + \sinh \tau)^{2p}} = 0. \quad (5.73)$$

Proceeding in the same way as in bright soliton, from real part equation (5.72), relations - are all recovered. The free parameter  $A$  in this case is

$$A = \left\{ \frac{1}{2b_2\theta_1} \left[ D (\theta_1 (b_1 - \lambda\kappa - 4\theta_1\kappa^2) + ab_2) \pm \sqrt{D^2 \{ \theta_1 (b_1 - \lambda\kappa - 4\theta_1\kappa^2) + ab_2 \}^2 + 3ab_2\theta_1 (D^2 + 1) (b_1 - \lambda\kappa - 4\theta_1\kappa^2)} \right] \right\}^{1/2}, \quad (5.74)$$

subject to the conditions

$$\pm \sqrt{D^2 \{ \theta_1 (b_1 - \lambda\kappa - 4\theta_1\kappa^2) + ab_2 \}^2 - 3ab_2\theta_1 (D^2 + 1) (b_1 - \lambda\kappa - 4\theta_1\kappa^2)} > 0, \quad (5.75)$$

and

$$D^2 \{ \theta_1 (b_1 - \lambda\kappa - 4\theta_1\kappa^2) + ab_2 \}^2 + 3ab_2\theta_1 (D^2 + 1) (b_1 - \lambda\kappa - 4\theta_1\kappa^2) > 0, \quad (5.76)$$

The parameters  $A$  and  $B$  are related as

$$B = A \sqrt{\frac{b_1 - \lambda\kappa - 4\theta_1\kappa^2}{aD - \theta_1 A^2}}. \quad (5.77)$$

Next, the imaginary part equation (5.73), relations (5.7) and (5.8) are obtained.

Finally, singular 1-soliton solution to optical metamaterials with parabolic law nonlinearity is given by

$$q(x, t) = \frac{A}{\sqrt{D + \sinh [B (x - vt)]}} e^{i(-\kappa x + \omega t + \theta)}, \quad (5.78)$$

where the parameter definitions and constraints are all in place.

#### 5.4.4 Singular soliton (Type-II)

For singular soliton of second type [6, 7],

$$P(x, t) = (A + B \coth \tau)^P, \quad (5.79)$$

with the same definition of  $\tau$  as in (5.63). Substitution of (5.79) into (5.5) and (5.6) implies

$$\begin{aligned}
& ap(p-1)\mu^2(A^2-B^2)^2(A+B\coth\tau)^{p-2} - 2p(2p-1)Aa\mu^2(A^2-B^2)(A+B\coth\tau)^{p-1} \\
& - \{B^2(\omega+a\kappa+a\kappa^2) - 2ap^2\mu^2(3A^2-B^2)\}(A+B\coth\tau)^p + ap(p+1)\mu^2(A+B\coth\tau)^{p+2} \\
& + [2\mu^2p^2(B^2-3A^2)(9\theta_1+\theta_2+\theta_3) + B^2\{b_1-\lambda\kappa+\kappa^2(\theta_1+\theta_2+\theta_3)\}](A+B\coth\tau)^{3p} \\
& \quad - \mu^2p(A^2-B^2)^2\{p(9\theta_1+\theta_2+\theta_3) - (3\theta_1+\theta_2+\theta_3)\}(A+B\coth\tau)^{3p-2} \\
& + 2\mu^2pA(A^2-B^2)\{2p(9\theta_1+\theta_2+\theta_3) - (3\theta_1+\theta_2+\theta_3)\}(A+B\coth\tau)^{3p-1} \\
& \quad + 2\mu^2pA\{2p(9\theta_1+\theta_2+\theta_3) + (3\theta_1+\theta_2+\theta_3)\}(A+B\coth\tau)^{3p+1} \\
& \quad - \mu^2p\{p(9\theta_1+\theta_2+\theta_3) + (3\theta_1+\theta_2+\theta_3)\}(A+B\coth\tau)^{3p+2} \\
& \quad - 2Aa\mu^2p(2p+1)(A+B\coth\tau)^{p+1} + b_2B^2(A+B\coth\tau)^{5p} = 0,
\end{aligned} \tag{5.80}$$

and

$$\nu + \alpha + 2a\kappa - \{3\lambda+2\nu - 2\kappa(3\theta_1+\theta_2+\theta_3)\}(A+B\coth\tau)^{2p} = 0, \tag{5.81}$$

respectively. These expressions lead to (5.7)-(5.9) as well as (5.66)-(5.69).

Therefore, singular 1-soliton solution of Type-II with parabolic law in optical metamaterials is given by

$$q(x, t) = \sqrt{A(1 \pm \coth(\mu(x-vt)))} e^{i(-\kappa x + \omega t + \theta)}, \tag{5.82}$$

with the respective parameters and constraints are discussed.

## 5.5 Dual-power law

This model describes saturation on nonlinear refractive index and its exact soliton solutions are known. The effective NLSE, with this form of nonlinearity, serve as a basic model to describe spatial soliton in photovoltaic-photo refractive materials such as LiNbO<sub>3</sub>. Optical nonlinearities in many organic and polymer materials are governed with such form of nonlinearity. The governing

NLSE in optical metamaterials for dual-power nonlinearity is

$$\begin{aligned}
& iq_t + aq_{xx} + \left( b_1|q|^{2n} + b_2|q|^{4n} \right) q \\
& = i\alpha q_x + i\lambda \left( |q|^2 q \right)_x + i\nu \left( |q|^2 \right)_x q + \theta_1 \left( |q|^2 q \right)_{xx} + \theta_2 |q|^2 q_{xx} + \theta_3 q^2 q_{xx}^*,
\end{aligned} \tag{5.83}$$

for  $F(u) = b_1|u|^{2n} + b_2|u|^{4n}$ , with non-zero  $b_1$  and  $b_2$ , where  $n$  is the power law parameter. This section will now comprehensively derive the soliton solutions to NLSE in the following subsections.

### 5.5.1 Bright soliton

With the same starting hypothesis as given by (5.51), the real part (5.5) and (5.6) reduce to

$$\begin{aligned}
& \frac{\omega + a\kappa + \alpha\kappa^2 - \alpha p^2 B^2}{(D + \cosh \tau)^p} - \frac{A^2 \{ \kappa^2 (\theta_1 + \theta_2 + \theta_3) - p^2 B^2 (9\theta_1 + \theta_2 + \theta_3) \}}{(D + \cosh \tau)^{3p}} \\
& + \frac{ap(2p+1)B^2 D}{(D + \cosh \tau)^{p+1}} - \frac{A^2 B^2 \{ 12\theta_1 p^2 D + p(2p+1)D(3\theta_1 + \theta_2 + \theta_3) \}}{(D + \cosh \tau)^{3p+1}} \\
& + \frac{A^2 B^2 (D^2 - 1) \{ 6p^2 \theta_1 B^2 + p(p+1)(3\theta_1 + \theta_2 + \theta_3) \}}{(D + \cosh \tau)^{3p+2}} \\
& - \frac{ap(p+1)B^2(D^2 - 1)}{(D + \cosh \tau)^{p+2}} - \frac{(b_1 - \lambda\kappa)A^{2n}}{(D + \cosh \tau)^{(2n+1)p}} - \frac{b_2 A^{4n}}{(D + \cosh \tau)^{(4n+1)p}} = 0,
\end{aligned} \tag{5.84}$$

and

$$\omega + a\kappa + 2\alpha\kappa + \frac{\{(2n+1)\lambda + 2n\nu\}A^{2n}}{(D + \cosh \tau)^{2np}} - \frac{2\kappa(3\theta_1 + \theta_2 - \theta_3)A^2}{(D + \cosh \tau)^{2p}} = 0, \tag{5.85}$$

respectively. The imaginary part equation leads to the constraints given by (5.7), (5.36) and (5.37).

By balancing principle applied to real part (5.84) equating the exponents,  $(4n+1)p$  and  $p+2$ , implies

$$p = \frac{1}{2n}. \tag{5.86}$$

Next, from the undetermined coefficients of linearly independent functions, one covers the wave number

$$\omega = \frac{1}{4n^2} (\alpha B^2 - 4n^2 \alpha n^2 - 4n^2 a\kappa), \tag{5.87}$$

and the constraint

$$3(2n+3)\theta_1 + (2n+1)(\theta_2 + \theta_3) = 0. \quad (5.88)$$

From the remaining linearly independent functions, the amplitude of the soliton is

$$A = \left[ -\frac{(2n+1)(D^2-1)(b_1-\lambda\kappa)}{2(n+1)b_2D} \right]^{1/2n}, \quad (5.89)$$

provided

$$b_2D(D^2-1)(b_1-\lambda\kappa) < 0, \quad (5.90)$$

and the width is

$$B = \frac{n(b_1-\lambda\kappa)}{D(n+1)} \sqrt{-\frac{(2n+1)(D^2-1)}{ab_2}}, \quad (5.91)$$

that stays valid for

$$b_2D(D^2-1) < 0. \quad (5.92)$$

Finally, bright 1-soliton solution to optical metamaterials with dual-power law nonlinearity is given by

$$q(x, t) = \frac{A}{(D + \cosh[B(x-vt)])^{1/2n}} e^{i(-\kappa x + \omega t + \theta)}, \quad (5.93)$$

where the parameter definitions and constraints are all in place.

### 5.5.2 Dark soliton

With the same starting hypothesis given by (5.62), the real and imaginary part (5.5) and (5.6) are

$$\begin{aligned}
& ap(p-1)\mu^2(A^2 - B^2)^2(A + B \tanh \tau)^{p-2} - 2p(2p-1)Aa\mu^2(A^2 - B^2)(A + B \tanh \tau)^{p-1} \\
& - \{B^2(\omega + a\kappa + a\kappa^2) - 2ap^2\mu^2(3A^2 - B^2)\}(A + B \tanh \tau)^p + ap(p+1)\mu^2(A + B \tanh \tau)^{p+2} \\
& + [2\mu^2p^2(B^2 - 3A^2)(9\theta_1 + \theta_2 + \theta_3) + B^2\kappa^2(\theta_1 + \theta_2 + \theta_3)](A + B \tanh \tau)^{3p} \\
& - \mu^2p(A^2 - B^2)^2\{p(9\theta_1 + \theta_2 + \theta_3) - (3\theta_1 + \theta_2 + \theta_3)\}(A + B \tanh \tau)^{3p-2} \\
& - 2\mu^2pA(B^2 - A^2)\{2p(9\theta_1 + \theta_2 + \theta_3) - (3\theta_1 + \theta_2 + \theta_3)\}(A + B \tanh \tau)^{3p-1} \\
& + 2\mu^2pA\{2p(9\theta_1 + \theta_2 + \theta_3) + (3\theta_1 + \theta_2 + \theta_3)\}(A + B \tanh \tau)^{3p+1} - \\
& \mu^2p\{p(9\theta_1 + \theta_2 + \theta_3) + (3\theta_1 + \theta_2 + \theta_3)\}(A + B \tanh \tau)^{3p+2} + (b_1 - \lambda\kappa)B^2(A + B \tanh \tau)^{(2n+1)p} \\
& - 2Aa\mu^2p(2p+1)(A + B \tanh \tau)^{p+1} + b_2B^2(A + B \tanh \tau)^{(4n+1)p} = 0,
\end{aligned} \tag{5.94}$$

and

$$\nu + a + 2a\kappa - \{(2n+1)\lambda + 2n\nu\}(A + B \tanh \tau)^{2np} - 2\kappa(3\theta_1 + \theta_2 + \theta_3)(A + B \tanh \tau)^{2p} = 0. \tag{5.95}$$

Again balancing exponents  $3p+1$  with  $p+2$  leads to the same value of  $p$  as given by (5.54). Next, equating the exponents  $(2n+1)p$  and  $p+2$  leads to (5.42). This shows that dark soliton for dual-power law collapse to the case of parabolic law. Therefore, all results from parabolic law dark soliton given by (5.4.3) and (5.66)-(5.69) remain valid. In addition, the imaginary part equation leads to (5.7) and (5.8). Finally, dark 1-soliton solution to dual-power law nonlinearity is given by (5.70), with all definition of parameters and their respective constraints in place.

### 5.5.3 Singular soliton (Type-I)

In this case, substituting the starting hypothesis given by (5.71) into (5.5) and (5.6) gives

$$\begin{aligned}
& \frac{\omega + a\kappa + \alpha\kappa^2 - \alpha p^2 B^2}{(D + \sinh \tau)^p} + \frac{ap(2p+1)B^2 D}{(D + \sinh \tau)^{p+1}} - \frac{ap(p+1)B^2(D^2+1)}{(D + \sinh \tau)^{p+2}} \\
& \quad - \frac{A^2 \{ \kappa^2 (\theta_1 + \theta_2 + \theta_3) - p^2 B^2 (9\theta_1 + \theta_2 + \theta_3) \}}{(D + \sinh \tau)^{3p}} \\
& \quad - \frac{A^2 B^2 \{ 12\theta_1 p^2 D + p(2p+1)D(3\theta_1 + \theta_2 + \theta_3) \}}{(D + \sinh \tau)^{3p+1}} \\
& \quad + \frac{A^2 B^2 (D^2 + 1) \{ 6p^2 \theta_1 B^2 + p(p+1)(3\theta_1 + \theta_2 + \theta_3) \}}{(D + \sinh \tau)^{3p+2}} \\
& \quad - \frac{(b_1 - \lambda\kappa) A^{2n}}{(D + \sinh \tau)^{(2n+1)p}} - \frac{b_2 A^{4n}}{(D + \sinh \tau)^{(4n+1)p}} = 0,
\end{aligned} \tag{5.96}$$

and

$$\nu + \alpha + 2a\kappa + \frac{\{(2n+1)\lambda + 2n\vartheta\} A^{2n}}{(D + \sinh \tau)^{2np}} - \frac{2\kappa(3\theta_1 + \theta_2 - \theta_3) A^2}{(D + \sinh \tau)^{2p}} = 0, \tag{5.97}$$

respectively. The imaginary part equation clear leads to (5.7), (5.26) and (5.37).

While the balancing principle from real part (5.96) yields (5.86), the remaining undetermined coefficients lead to (5.87) and (5.88) as well. The free parameters  $A$  and  $B$  are now

$$A = \left[ -\frac{(2n+1)(D^2+1)(b_1 - \lambda\kappa)}{2(n+1)b_2 D} \right]^{1/2n}, \tag{5.98}$$

provided

$$b_2 D (b_1 - \lambda\kappa) < 0, \tag{5.99}$$

and

$$B = \frac{n(b_1 - \lambda\kappa)}{D(n+1)} \sqrt{-\frac{(2n+1)(D^2+1)}{ab_2}}, \tag{5.100}$$

only if

$$ab_2 < 0, \tag{5.101}$$

Finally, singular 1-soliton solution to optical metamaterials with dual-power law nonlinearity is

$$q(x, t) = \frac{A}{(D + \sinh [B (x - vt)])^{1/2n}} e^{i(-\kappa x + \omega t + \theta)}, \quad (5.102)$$

where the parameter definitions and constraints are all in place.

#### 5.5.4 Singular soliton (Type-II)

With the starting hypothesis given by (5.79), the real and imaginary parts (5.5) and (5.6) are

$$\begin{aligned} & ap(p-1)\mu^2(A^2 - B^2)^2(A + B \coth \tau)^{p-2} - 2p(2p-1)Aa\mu^2(A^2 - B^2)(A + B \tanh \tau)^{p-1} \\ & - \{B^2(\omega + a\kappa + a\kappa^2) - 2ap^2\mu^2(3A^2 - B^2)\}(A + B \coth \tau)^p \\ & + [2\mu^2p^2(B^2 - 3A^2)(9\theta_1 + \theta_2 + \theta_3) + B^2\kappa^2(\theta_1 + \theta_2 + \theta_3)](A + B \coth \tau)^{3p} \\ & - \mu^2p(A^2 - B^2)^2\{p(9\theta_1 + \theta_2 + \theta_3) - (3\theta_1 + \theta_2 + \theta_3)\}(A + B \coth \tau)^{3p-2} \\ & - 2\mu^2pA(B^2 - A^2)\{2p(9\theta_1 + \theta_2 + \theta_3) - (3\theta_1 + \theta_2 + \theta_3)\}(A + B \coth \tau)^{3p-1} \\ & + 2\mu^2pA\{2p(9\theta_1 + \theta_2 + \theta_3) + (3\theta_1 + \theta_2 + \theta_3)\}(A + B \coth \tau)^{3p+1} \\ & - \mu^2p\{p(9\theta_1 + \theta_2 + \theta_3) + (3\theta_1 + \theta_2 + \theta_3)\}(A + B \coth \tau)^{3p+2} \\ & - 2Aa\mu^2p(2p+1)(A + B \coth \tau)^{p+1} + (b_1 - \lambda\kappa)B^2(A + B \coth \tau)^{(2n+1)p} \\ & + ap(p+1)\mu^2(A + B \coth \tau)^{p+2} + b_2B^2(A + B \coth \tau)^{(4n+1)p} = 0, \end{aligned} \quad (5.103)$$

and

$$\begin{aligned} & \nu + \alpha + 2a\kappa + ((2n+1)\lambda + 2n\nu)(A + B \coth \tau)^{2np} \\ & - 2\kappa(3\theta_1 + \theta_2 + \theta_3)(A + B \coth \tau)^{2p} = 0. \end{aligned} \quad (5.104)$$

Once again, proceeding along the same lines as in the case of dark soliton, (5.54) and (5.42) are recovered. Thus, this form of the singular soliton of Type-II exists whenever dual-power law reduces to parabolic law nonlinearity. Hence, all results from (5.7), (5.36), (5.37) and (5.66)-(5.69) hold. Finally, singular 1-soliton solution for dual power law is given by

(5.82) along with the parameters and constraints as described.

## 5.6 Log law

In this case  $F(u) = b \ln u$  for non-zero constant  $b$ . This law permits closed form exact expressions Gaussian beams. The advantage of this model is that the radiation from the periodic soliton is absent as the linearized problem contains discrete spectrum only [18]. For log-law medium, the model given by (5.1) modifies to

$$iq_t + aq_{xx} + F(\ln |q|^2) q = i\alpha q_x + i\lambda(|q|^2 q)_x + i\nu(|q|^2)_x q + \theta_1(|q|^2 q)_{xx} + \theta_2 |q|^2 q_{xx} + \theta_3 q^2 q_{xx}^*. \quad (5.105)$$

The solutions of NLSE in log-law nonlinear medium lead to Gaussian soliton that are occasionally referred to as Gausson [6, 7]. Therefore, the starting hypothesis for (5.105) is given by [6, 7]

$$P(x, t) = Ae^{-\tau^2}, \quad (5.106)$$

where  $A$  is the amplitude and  $B$  is the inverse width of the Gausson. Substituting this hypothesis into (5.5) and (5.6), the real and imaginary parts respectively simplify to

$$\begin{aligned} & -(4aB^2 - 2b)\tau^2 + A^2(\lambda\kappa - \kappa^2(\theta_1 + \theta_2 + \theta_3) - 2B^2(3\theta_1 + \theta_2 + \theta_3))e^{-2\tau^2} \\ & + (\omega + \alpha\kappa + a\kappa^2 + 2aB^2 - 2b \ln A) + A^2(24B^2\theta_1 + 4B^2(3\theta_1 + \theta_2 + \theta_3))\tau^2 e^{-2\tau^2} = 0, \end{aligned} \quad (5.107)$$

and

$$\nu + \alpha + 2a\kappa + A(3\lambda + 2\vartheta - 2\kappa(3\theta_1 + \theta_2 + \theta_3)) = 0. \quad (5.108)$$

From the undetermined coefficients of linearly independent functions in (5.107), the wave number is

$$\omega = -\alpha\kappa - 2a\kappa^2 - 2aB^2 + 2b \ln A, \quad (5.109)$$

and the width of Gausson is given by

$$B = \sqrt{\frac{\lambda\kappa - \kappa^2 (\theta_1 + \theta_2 + \theta_3)}{2(3\theta_1 + \theta_2 + \theta_3)}}, \quad (5.110)$$

with the condition

$$(\lambda\kappa - \kappa^2 (\theta_1 + \theta_2 + \theta_3)) (3\theta_1 + \theta_2 + \theta_3) > 0. \quad (5.111)$$

Substituting the width B from (5.110), the wave number from (5.109) reduces to

$$\omega = -\frac{a\lambda\kappa + 2a\kappa^2\theta_1 + (3\theta_1 + \theta_2 + \theta_3)(\alpha\kappa - 2b \ln A)}{3\theta_1 + \theta_2 + \theta_3}, \quad (5.112)$$

which holds provided

$$3\theta_1 + \theta_2 + \theta_3 \neq 0. \quad (5.113)$$

Next, setting the coefficient of the fourth linearly independent function in (5.106), namely  $\tau^2 e^{-2\tau^2}$  to zero, gives

$$9\theta_1 + \theta_2 + \theta_3 = 0. \quad (5.114)$$

Finally, the coefficient of  $\tau^2$  from (5.107) leads to the width of Gaussian as

$$B = \sqrt{\frac{b}{2a}}, \quad (5.115)$$

which shows that these Gausson will exist provided

$$ab > 0. \quad (5.116)$$

This means that GVD and the nonlinear term in (5.105) must both carry the same sign for Gaussons to exist. This imaginary part equation (5.108) yields (5.7) and (5.8). Equating the two values of the width B of the soliton from (5.110) and (5.115) leads to another constraint

between the frequency and coefficients of the model (5.105) as follows:

$$\alpha\lambda\kappa - 2b\theta_1 = (b + \alpha\kappa^2)(3\theta_1 + \theta_2 + \theta_3). \quad (5.117)$$

From (5.111) and (5.114), one can recover

$$\theta_1\kappa(\lambda + 8\theta_1\kappa) < 0, \quad (5.118)$$

which can be treated as another constraint. Next substituting (5.115) into (5.109) leads to an alternate expression to the wave number:

$$\omega = b(2\ln A - 1) - \kappa(\alpha + a\kappa). \quad (5.119)$$

Thus, the Gausson solution to optical metamaterials with log-law nonlinearity is given by

$$q(x, t) = Ae^{-B^2(x-vt)^2} e^{i(-\kappa x + \omega t + \theta)}, \quad (5.120)$$

where the parameter definitions and constraints are all listed above.

## 5.7 Conclusions

This chapter obtained soliton solutions in optical metamaterials with five forms of nonlinear media. For Kerr law nonlinearity, there are three forms of soliton that are already reported earlier; therefore this paper derived only singular soliton (Type-II). For the remaining laws all soliton solutions and their derivations are comprehensively reported in this chapter. These solutions come with respective integrability criteria that are listed as constraint conditions. These solutions will be immensely useful in the literature of optical metamaterials.

These soliton solutions will be a great asset in all future investigations in this area of nonlinear

optics. In the presence of perturbation terms these soliton will dictate the adiabatic parameter dynamics and other such features that will be obtained. The quasi-particle theory of optical soliton interaction will be reported. Later bifurcation analysis of soliton in optical metamaterials will be carried out. Other integration schemes will be applied to these models and those will reveal additional solutions, such as plane waves and periodic singular solutions. The semi-inverse variational principle will extract exotic soliton such as cosh-Gaussian pulses and bright-dark combo optical soliton. All of these are currently under investigation. The results of those research will be reported gradually and sequentially. Finally, the study will be extended to DWDM systems so that efficient soliton transmission can be conducted in parallel, thus improving performance enhancement. These just form a tip of the iceberg.

## Chapter 6

# BRIGHT AND EXOTIC SOLITON IN OPTICAL METAMATERIALS BY SEMI-INVERSE VARIATIONAL PRINCIPLE

This chapter addresses soliton in optical metamaterials. The semi-inverse variational principle is utilized to secure bright soliton solutions to the governing model. There are five forms of nonlinearity that are studied in this paper. They are Kerr law, power law, parabolic law, dual-power law and finally the log law nonlinearity. In particular for Kerr law nonlinearity, there are two additional forms of soliton solutions obtained. They are cosh-Gaussian pulses and bright-dark combo soliton and these are collectively being referred to as exotic soliton. There are several constraint conditions that naturally emerge for these soliton to exist.

### 6.1 Introduction

The semi-inverse variational principle (SVP) will be applied to the model for metamaterials to obtain analytical soliton solutions to the model. There are five forms of nonlinear media that will be studied in this paper. They are Kerr law, power law, parabolic law, dual-power law and log law nonlinearity. It is only for Kerr law, that in addition to bright soliton solutions, exotic soliton solutions will be retrieved by the application of SVP. These are cosh-Gaussian pulses and bright-dark combo soliton. These results will carry constraint conditions that will guarantee the existence of such soliton. Finally, numerical simulations supplement each of these analytical solutions.

### 6.2 Governing equation

The dimensionless form NLSE that governs the propagation of soliton through optical metamaterials is given by [78, 79]

$$iq_t + aq_{xx} + F(|q|^2)q = i\alpha q_x + i\lambda(|q|^2q)_x + i\nu(|q|^2)_x q + \theta_1(|q|^2q)_{xx} + \theta_2|q|^2q_{xx} + \theta_3q^2q_{xx}^*. \quad (6.1)$$

In this model  $q(x, t)$  represents the complex valued wave function with the independent variables being  $x$  and  $t$  that represent spatial and temporal variables respectively. The first term represents the temporal evolution of nonlinear wave, while the coefficient  $a$  is the group velocity dispersion (GVD). The functional  $F$ , which is the source of nonlinearity, is a real-valued algebraic function where it is necessary to have the smoothness of the complex function  $F(|q|^2)q : C \mapsto C$ . Treating the complex plane  $C$  as a two-dimensional linear space  $R^2$ , the function  $F(|q|^2)q$  is  $k$  times continuously differentiable, so that

$$F(|q|^2)q \in \bigcup_{m,n=1}^{\infty} C^k((-n, n) \times (-m, m); R^2). \quad (6.2)$$

From the right hand side of (6.1),  $\alpha$  represents the coefficient of inter-modal dispersion. This arises when the group velocity of light propagating through a metamaterial is dependent on propagation mode in addition to chromatic dispersion. The factors  $\lambda$  and  $\nu$  are accounted for self-steepening for preventing shock-waves, and nonlinear dispersion. Finally, the terms with  $\theta_j$  for  $j = 1, 2, 3$  arise in the context of optical metamaterials [21].

This model equation will now be studied for five forms of nonlinear media as indicated earlier. The subsequent section now introduces SVP in a succinct manner which will be applied to the model to retrieve soliton solutions.

### 6.3 Semi-inverse variational principle

To apply the SVP to (6.1), the starting hypothesis is the traveling wave argument given by

$$q(x, t) = g(s)e^{i\phi}, \quad (6.3)$$

where  $g(s)$  represents the shape of the wave profile, and

$$s = x - vt, \quad (6.4)$$

with  $v$  being the speed of the wave. The phase component  $\phi(x, t)$  is defined as

$$\phi(x, t) = -\kappa x + \omega t + \theta, \quad (6.5)$$

where  $\kappa$  represents the soliton frequency, and  $\omega$  the wave number while  $\theta$  the phase constant. Therefore by substituting the hypothesis (6.3) into (6.1) and decomposing into real and imaginary parts one gets for the real portion

$$(\omega + \alpha\kappa + a\kappa^2)g - [\kappa^2(\theta_1 + \theta_2 + \theta_3) - \kappa\lambda]g^3 - cF(g^2)g - ag'' + 6\theta_1g(g')^2 + (3\theta_1 + \theta_2 + \theta_3)g^2g'' = 0, \quad (6.6)$$

and for the imaginary part

$$(v + \alpha + 2a\kappa)g' + \{3\lambda + 2\nu - 2\kappa(3\theta_1 + \theta_2 + \theta_3)\}g^2g' = 0, \quad (6.7)$$

the notations  $g' = dg/ds$ ,  $g'' = d^2g/ds^2$  and so on, are introduced in (6.6) and (6.7) for convenience. From the imaginary part equation given in (6.7), setting the coefficients of the linearly independent functions to zero yield the constraint condition

$$3\lambda + 2\nu = 2\kappa(3\theta_1 + \theta_2 + \theta_3), \quad (6.8)$$

and consequently the soliton speed, irrespective of the nonlinearity under consideration, falls out to be

$$v = -(\alpha + 2a\kappa). \quad (6.9)$$

Then, the 1-soliton solution hypothesis is, in general, taken to be

$$g(s) = Af(Bs), \quad (6.10)$$

where  $A$  is the amplitude,  $B$  is the inverse width of the soliton or Gausson, and  $s$  is as defined in (6.4). The functional  $f$  in (6.10) depends on the nonlinearity to be considered in the following

sections. The SVP states that the amplitude can be retrieved from the coupled system of equations given by

$$\frac{\partial J}{\partial A} = 0, \quad (6.11)$$

$$\frac{\partial J}{\partial B} = 0, \quad (6.12)$$

where  $J$  represents the stationary integral. In the next sections, SVP will be applied to (6.1) for Kerr law, power law, parabolic law, dual-power law and log-law nonlinearities in order to obtain bright and exotic soliton solutions.

### 6.3.1 Kerr law

For Kerr law nonlinearity  $F(u) = u$ . Thus, with this nonlinearity the NLSE (6.1) is rewritten as

$$iq_t + aq_{xx} + c \ln |q|^2 q = \beta \alpha q_x + i\lambda(|q|^2 q)_x + i\nu(|q|^2)_x q + \theta_1(|q|^2 q)_{xx} + \theta_2 |q|^2 q_{xx} + \theta_3 q^2 q_{xx}^*. \quad (6.13)$$

In this scenario, the real part (6.6) becomes

$$(\omega + \alpha\kappa + a\kappa^2) g - \{c + \kappa^2(\theta_1 + \theta_2 + \theta_3) - \kappa\lambda\} g^3 - ag'' + 6\theta_1 g (g')^2 + (3\theta_1 + \theta_2 + \theta_3) g^2 g'' = 0. \quad (6.14)$$

Now, multiplying the last equation by  $g'$  and integrating once leads to

$$2(\omega + \alpha\kappa + a\kappa^2) g^2 - (c + 4\kappa^2\theta_1 - \kappa\lambda) g^4 - 2a (g')^2 + 12\theta_1 g^2 (g')^2 = K, \quad (6.15)$$

whenever

$$3\theta_1 = \theta_2 + \theta_3. \quad (6.16)$$

In (6.15),  $K$  represents the arbitrary constant of integration, thus the stationary integral is defined as

$$J = \int_{\mathbb{R}} K ds, \quad (6.17)$$

where  $K$  is given by

$$K = \left\{ 2(\omega + \alpha\kappa + a\kappa^2)g^2 - (c + 4\kappa^2\theta_1 - \kappa\lambda)g^4 - 2a(g')^2 + 12\theta_1g^2(g')^2 \right\}. \quad (6.18)$$

The study for Kerr law nonlinearity will be now split into three subsections. These are on bright soliton and exotic soliton. There are two kinds of exotic soliton that will be considered. They are cosh-Gaussian pulses as well as combo soliton. The details are described in the following subsections.

### Bright soliton

For Kerr law nonlinearity, the hypothesis to be taken is

$$g(s) = A \operatorname{sech}(Bs). \quad (6.19)$$

Then, after substituting (6.19) into (6.18) the integration leads to

$$J = \frac{4(\omega + \alpha\kappa + a\kappa^2)A^2}{B} - \frac{4(c + 4\kappa^2\theta_1 - \kappa\lambda)A^4}{3B} - \frac{4aA^2B}{3} + \frac{16\theta_1A^4B}{5}. \quad (6.20)$$

Consequently, (6.11) and (6.12), after simplification are given by

$$5(c + 4\kappa^2\theta_1 - \kappa\lambda)A^2 + 10aB^2 - 36\theta_1A^2B^2 = 0, \quad (6.21)$$

which, upon solving, reveals the relation between the amplitude and inverse width of the soliton as

$$B = A \sqrt{\frac{5(c + 4\kappa^2\theta_1 - \kappa\lambda)}{36\theta_1A^2 - 10a}}, \quad (6.22)$$

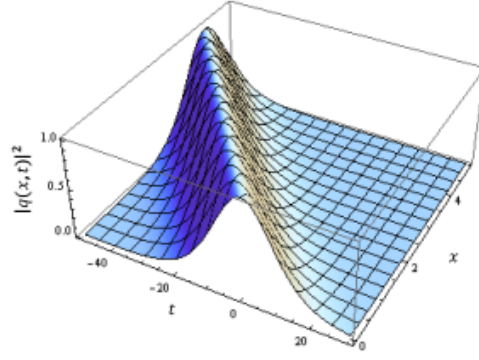


Figure 6.1: *Bright soliton with Kerr law nonlinearity.*

whenever

$$(c + 4\kappa^2\theta_1 - \kappa\lambda) (18\theta_1 A^2 - 5a) > 0. \quad (6.23)$$

Therefore the bright soliton solution for NLSE (6.1) with Kerr law nonlinearity (6.13) is given by

$$q(x, t) = A \operatorname{sech}[B(x - vt)] e^{i(-\kappa x + \omega t + \theta)}, \quad (6.24)$$

where the amplitude  $A$  and inverse width of the soliton  $B$  are associated by (6.22) while the speed is defined by the expression (6.9). In this case the solution is possible whenever (6.8), (6.16), and (6.23) are satisfied.

The figure in **Fig. 6.1** shows a surface plot of a single bright soliton solution in optical meta-materials. Here,  $a = 0.1$ ,  $c = 1$ ,  $\alpha = 0.1$ ,  $\lambda = -0.1$ ,  $\nu = 0.21$ ,  $\theta_1 = 0.1$ ,  $\theta_2 = 0.2$ ,  $\theta_3 = 0.1$ .

### Cosh-Gaussian pulses

For cosh-Gaussian pulse solution, we assume a solution of the form

$$g(s) = A e^{-B^2 s^2} \cosh(Bs). \quad (6.25)$$

Then, after substituting (6.25) into (6.18) the integration leads to

$$J = \gamma\left(\frac{1}{2}\right) \left[ \frac{\sqrt{2}(1+e^{\frac{1}{2}})(\omega+\alpha\kappa+a\kappa^2)A^2}{2B} - \frac{(3+e+e^{\frac{1}{4}})(c-\kappa\lambda+4\theta_1\kappa^2)\kappa^2 A^4}{16B} - \frac{e^{\frac{1}{4}}\sqrt{2}A^2B}{2} - \frac{3(1+e+2e^{\frac{1}{4}})\theta_1 A^4 B}{8} \right]. \quad (6.26)$$

As a consequence, (6.11) and (6.12), after simplification are given by

$$4\sqrt{2}\left(1+e^{\frac{1}{2}}\right)(\omega+\alpha\kappa+a\kappa^2) - \left(3+e+4e^{\frac{1}{4}}\right)(c-\kappa\lambda+4\theta_1\kappa^2)\kappa^2 A^2 - 4e^{\frac{1}{2}}\sqrt{2}aB^2 - 6\left(1+e+2e^{\frac{1}{4}}\right)\theta_1 A^2 B^2 = 0, \quad (6.27)$$

and

$$8\sqrt{2}\left(1+e^{\frac{1}{2}}\right)(\omega+\alpha\kappa+a\kappa^2) - \left(3+e+4e^{\frac{1}{4}}\right)(c-\kappa\lambda+4\theta_1\kappa^2)\kappa^2 A^2 - 8e^{\frac{1}{2}}\sqrt{2}aB^2 + 6\left(1+e+2e^{\frac{1}{4}}\right)\theta_1 A^2 B^2 = 0, \quad (6.28)$$

respectively. Then, uncoupling the last two equations leads to the inverse width of the pulse as

$$B = \left[ -\frac{\sqrt{2}\left(1+e^{\frac{1}{2}}\right)(\omega+\alpha\kappa+a\kappa^2)}{3\left\{\sqrt{2}e^{\frac{1}{2}}a + \left(1+e+2e^{\frac{1}{4}}\right)\right\}} \right]^{\frac{1}{2}}, \quad (6.29)$$

subject to domain restriction

$$(\omega+\alpha\kappa+a\kappa^2)\left\{\sqrt{2}e^{\frac{1}{2}}a + \left(1+e+2e^{\frac{1}{4}}\right)\right\} < 0. \quad (6.30)$$

Therefore we conclude that the cosh-Gaussian pulse soliton solution for NLSE (6.1) is given by

$$q(x, t) = A e^{-B^2(x-vt)^2} \cosh[B(x-vt)] e^{i(-\kappa x + \omega t + \theta)}, \quad (6.31)$$

where parameters  $A$  and  $B$  are associated by (6.29) while the speed is defined by the expression (6.9). The solution is possible whenever the constraint conditions (6.8), (6.16), and (6.30) are satisfied.

The figure in **Fig. 6.2** shows a surface plot of a single cosh-Gaussian pulse in optical meta-

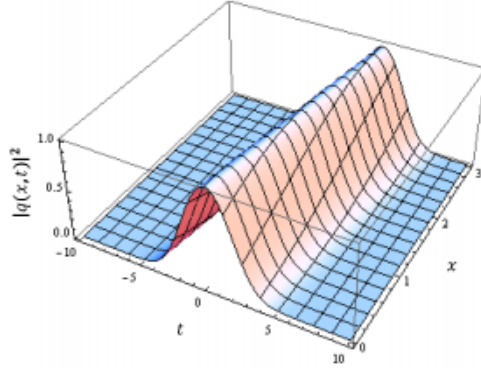


Figure 6.2: *Cosh-Gaussian pulse with Kerr law.*

materials. Here,  $a = 0.5$ ,  $c = 1$ ,  $\alpha = -0.1$ ,  $\lambda = 1$ ,  $\nu = -0.9$ ,  $\theta_1 = 0.1$ ,  $\theta_2 = 0.2$ ,  $\theta_3 = 0.1$ .

### Combo soliton

To retrieve combo soliton solutions from (6.1) the hypothesis to be considered is

$$g(s) = A \operatorname{sech}(Bs) \tanh(Bs). \quad (6.32)$$

Thus, by substituting this ansatz into (6.18) and carrying out the corresponding integration, the stationary integral yields

$$J = \frac{4(\omega + \alpha\kappa + a\kappa^2)A^2}{3B} - \frac{4(c - \kappa\lambda + 4\theta_1\kappa^2)\kappa^2A^4}{35B} - \frac{28aA^2B}{15} + \frac{16\theta_1A^4B}{21}. \quad (6.33)$$

Consequently, the expressions (6.11) and (6.12), in this case, take the form

$$35(\omega + \alpha\kappa + a\kappa^2) - 6(c - \kappa\lambda + 4\theta_1\kappa^2)\kappa^2A^2 - 49aB^2 + 10\theta_1A^2B^2 = 0, \quad (6.34)$$

and

$$35(\omega + \alpha\kappa + a\kappa^2) - 3(c - \kappa\lambda + 4\theta_1\kappa^2)\kappa^2A^2 + 49aB^2 - 20\theta_1A^2B^2 = 0. \quad (6.35)$$

Upon subtraction, one recovers

$$3(c - \kappa\lambda + 4\theta_1\kappa^2)\kappa^2 A^2 + 98aB^2 - 30\theta_1 A^2 B^2 = 0. \quad (6.36)$$

This relation gives

$$B = \sqrt{\frac{3(c - \kappa\lambda + 4\theta_1\kappa^2)\kappa^2 A^2}{30\theta_1 A^2 - 98a}}, \quad (6.37)$$

subject to the constraint condition

$$(c - \kappa\lambda + 4\theta_1\kappa^2)(15\theta_1 A^2 - 49a) > 0. \quad (6.38)$$

Finally, the combo soliton solution for NLSE (6.1) is given by

$$q(x, t) = A \operatorname{sech}[B(x - vt)] \tanh[B(x - vt)] e^{i(-\kappa x + \omega t + \theta)}, \quad (6.39)$$

where the parameters  $A$  and  $B$  are associated by (6.37) while the speed is defined by the expression (6.9). The solution is possible whenever the constraint conditions (6.8), (6.16), and (6.38) are satisfied.

The figure in **Fig. 6.3** shows a surface plot of a single combo soliton solution in optical meta-materials. Here,  $a = -0.5$ ,  $c = 1$ ,  $\alpha = -0.1$ ,  $\lambda = 0.1$ ,  $\nu = -0.75$ ,  $\theta_1 = 0.1$ ,  $\theta_2 = 0.2$ ,  $\theta_3 = 0.1$ .

### 6.3.2 Power law

For power law nonlinearity  $F(u) = u^n$ , whenever

$$0 < n < 2, \quad (6.40)$$

to prevent wave collapse. Next, to avoid self-focusing singularity, it is also needed to have

$$n \neq 2. \quad (6.41)$$

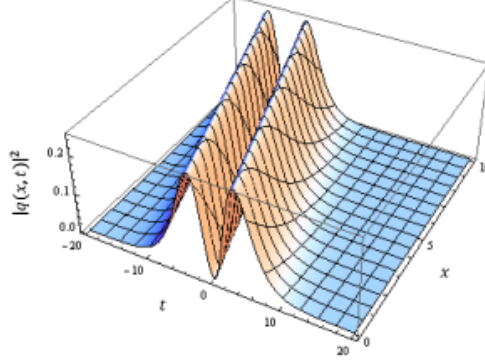


Figure 6.3: *Combo-soliton with Kerr law.*

Thus, with this nonlinearity NLSE (6.1) is rewritten as

$$iq_t + aq_{xx} + c|q|^{2n}q = i\alpha q_x + i\lambda \left(|q|^2 q\right)_x + i\nu \left(|q|^2\right)_x q + \theta_1 \left(|q|^2 q\right)_{xx} + \theta_2 |q|^2 q_{xx} + \theta_3 q^2 q_{xx}^*. \quad (6.42)$$

For this nonlinearity (6.6) becomes

$$(\omega + \alpha\kappa + a\kappa^2)g - \{\kappa^2(\theta_1 + \theta_2 + \theta_3) - \kappa\lambda\}g^3 - cg^{2n+1} - ag'' + 6\theta_1g(g')^2 + (3\theta_1 + \theta_2 + \theta_3)g^2g'' = 0. \quad (6.43)$$

So that the corresponding stationary integral (6.17) is

$$J = \int_{\mathbb{R}} \left\{ 2(\omega + \alpha\kappa + a\kappa^2)g^2 - (4\kappa^2\theta_1 - \kappa\lambda)g^4 - 2c\frac{g^{2(n+1)}}{n+1} - 2a(g')^2 + 12\theta_1g^2(g')^2 \right\} ds. \quad (6.44)$$

Then, by substituting the hypothesis

$$g(s) = A \operatorname{sech}^{\frac{1}{n}}(Bs), \quad (6.45)$$

into (6.44) and integrating over the entire real line, whenever the condition (6.16) is satisfied, the stationary integral reduces to

$$J = \frac{2(\omega + \alpha\kappa + a\kappa^2)A^2}{B}P_1 - \frac{(4\kappa^2\theta_1 - \kappa\lambda)A^4}{B}P_2 - \frac{4cA^{2n+2}}{B}P_3 - 4aA^2BP_4 + 24\theta_1A^4BP_5, \quad (6.46)$$

where

$$P_1 = \frac{\Gamma\left(\frac{1}{2}\right)\Gamma\left(\frac{1}{n}\right)}{\Gamma\left(\frac{1}{2} + \frac{1}{n}\right)}, \quad (6.47)$$

$$P_2 = \frac{\Gamma\left(\frac{1}{2}\right)\Gamma\left(\frac{2}{n}\right)}{\Gamma\left(\frac{1}{2} + \frac{2}{n}\right)}, \quad (6.48)$$

$$P_3 = \frac{\Gamma\left(\frac{1}{2}\right)\Gamma\left(\frac{1}{n}\right)}{(n+1)(n+2)\Gamma\left(\frac{1}{2} + \frac{1}{n}\right)}, \quad (6.49)$$

$$P_4 = \frac{1}{n^2 2^{\frac{2}{n}}} \times {}_2F_1\left(2 + \frac{2}{n}, \frac{2}{n}; \frac{3}{2} + \frac{2}{n}; \frac{1}{2}\right) \times B\left(\frac{2}{n}, \frac{3}{2}\right), \quad (6.50)$$

$$P_5 = \frac{1}{n^2 2^{\frac{4}{n}}} \times {}_2F_1\left(2 + \frac{4}{n}, \frac{4}{n}; \frac{3}{2} + \frac{4}{n}; \frac{1}{2}\right) \times B\left(\frac{4}{n}, \frac{3}{2}\right). \quad (6.51)$$

Here  ${}_2F_1(c_1, c_2; c_3; z)$  is the Gauss' hypergeometric function usually defined in terms of power series as

$${}_2F_1(c_1, c_2; c_3; z) = 1 + \frac{c_1 c_2}{1! c_3} z + \frac{c_1(c_1+1)c_2(c_2+1)}{2! c_3(c_3+1)} z^2 + \dots = \sum_{n=0}^{\infty} \frac{(c_1)_n (c_2)_n}{(c_3)_n} \frac{z^n}{n!}, \quad (6.52)$$

which converges inside the unit disk

$$|z| < 1. \quad (6.53)$$

The term  $\Gamma(z)$  represents the *Gamma* function and is defined by the Euler integral

$$\Gamma(z) = \int_{\mathbb{R}_{\geq 0}} t^{z-1} e^{-t} dt, \quad (6.54)$$

and  $B(l, m)$  is the *Beta* function which is generally defined as

$$B(l, m) = \int_0^1 x^{l-1} (1-x)^{m-1} dx. \quad (6.55)$$

Then, equations (6.11) and (6.12), in this case, after simplification, are

$$(\omega + \alpha\kappa + a\kappa^2) P_1 - (4\kappa^2\theta_1 - \kappa\lambda) A^2 P_2 - 2c(n+1)A^{2n} P_3 - 2aB^2 P_4 + 24\theta_1 A^2 B^2 P_5 = 0, \quad (6.56)$$

and

$$2(\omega + \alpha\kappa - a\kappa^2) P_1 - (4\kappa^2\theta_1 - \kappa\lambda) A^2 P_2 - 4cA^{2n} P_3 + 4aB^2 P_4 - 24\theta_1 A^2 B^2 P_5 = 0. \quad (6.57)$$

From (6.56) and (6.57) one can get the relation between the amplitude and inverse width of the soliton as

$$B = \sqrt{\frac{(\omega + \alpha\kappa + a\kappa^2) P_1 + 2c(n-1)A^{2n} P_3}{48\theta_1 A^2 P_5 - 6aP_4}}, \quad (6.58)$$

whenever

$$\{(\omega + \alpha\kappa + a\kappa^2) P_1 + 2c(n-1)A^{2n} P_3\} (8\theta_1 A^2 P_5 - aP_4) > 0. \quad (6.59)$$

Thus, the soliton solution for NLSE (6.1) with power law nonlinearity (6.42) is

$$q(x, t) = A \operatorname{sech}^{\frac{1}{n}} [B(x - vt)] e^{i(-\kappa x + \omega t + \theta)}, \quad (6.60)$$

where the amplitude  $A$  and inverse width of the soliton  $B$  are related by (6.58) while the speed is defined by the expression (6.9). The bright soliton solution in this case is possible when the solvability conditions (6.8), (6.16), and (6.59) are satisfied.

The figure in **Fig. 6.4** shows a surface plot of a single bright soliton solution in optical metamaterials. Here,  $a = 0.1$ ,  $c = 1$ ,  $\alpha = 0.1$ ,  $\lambda = 1$ ,  $\nu = -0.9$ ,  $\theta_1 = 0.1$ ,  $\theta_2 = 0.2$ ,  $\theta_3 = 0.1$ , with  $n = 1/2$ .

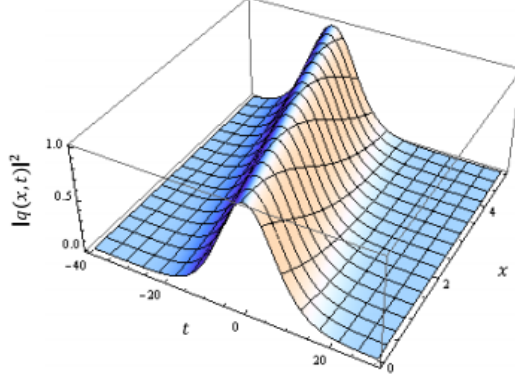


Figure 6.4: *Bright soliton with Power law.*

### 6.3.3 Parabolic law

The parabolic law is also known as the cubic-quintic form of nonlinearity and is given by  $F(u) = c_1 u + c_2 u^2$ . Thus, NLSE with parabolic law nonlinearity becomes

$$iq_t + aq_{xx} + (c_1 |q|^2 + c_2 |q|^4) q = i\alpha q_x + i\lambda (|q|^2 q)_x + i\nu (|q|^2)_x q + \theta_1 (|q|^2 q)_{xx} + \theta_2 |q|^2 q_{xx} + \theta_3 q^2 q_{xx}^*. \quad (6.61)$$

The real part (6.6) for parabolic law takes the form

$$\begin{aligned} & (\omega + \alpha\kappa + a\kappa^2) g \\ & - \{c_1 + \kappa^2 (\theta_1 + \theta_2 + \theta_3) - \kappa\lambda\} g^3 + c_2 g^5 - ag'' + 6\theta_1 g (g')^2 + (3\theta_1 + \theta_2 + \theta_3) g^2 g'' = 0. \end{aligned} \quad (6.62)$$

and the corresponding stationary integral is

$$J = \int_{\mathbb{R}} \left\{ 6 (\omega + \alpha\kappa + a\kappa^2) g^2 - 3 (c_1 + 4\kappa^2\theta_1 - \kappa\lambda) g^4 + 2c_2 g^6 - 6a (g')^2 + 36\theta_1 g^2 (g')^2 \right\} ds. \quad (6.63)$$

For parabolic law the ansatz to be consider is of the form

$$g(s) = \frac{A}{\sqrt{D + \cosh(Bs)}}, \quad (6.64)$$

where  $D$  is an arbitrary constant. By substituting this hypothesis into (6.63) and carrying out the integration the stationary integral takes the form

$$J = \frac{12(\omega + \alpha + a\kappa^2)A^2}{B}M_1 - \frac{2(c_1 + 4\kappa^2\theta_1 - \kappa\lambda)A^4}{B}M_2 + \frac{2c_2A^6}{5B}M_3 - aA^2BM_4 + \frac{3\theta_1A^4B}{5}M_5, \quad (6.65)$$

where

$$M_1 = {}_2F_1\left(1, 1; \frac{3}{2}; \frac{1-D}{2}\right), \quad (6.66)$$

$$M_2 = {}_2F_1\left(2, 2; \frac{5}{2}; \frac{1-D}{2}\right), \quad (6.67)$$

$$M_3 = {}_2F_1\left(3, 3; \frac{7}{2}; \frac{1-D}{2}\right), \quad (6.68)$$

$$M_4 = {}_2F_1\left(3, 1; \frac{5}{2}; \frac{1-D}{2}\right), \quad (6.69)$$

$$M_5 = {}_2F_1\left(4, 2; \frac{7}{2}; \frac{1-D}{2}\right), \quad (6.70)$$

for

$$-1 < D < 3. \quad (6.71)$$

This restriction for parameter  $D$  follows from (6.66) by virtue of (6.53). Then identities (6.11) and (6.12) in this case, after simplification, become

$$60(\omega + \alpha + a\kappa^2)M_1 - 20(c_1 + 4\kappa^2\theta_1 - \kappa\lambda)A^2M_2 + 6c_2A^4M_3 - 5aB^2M_4 + 6\theta_1A^2B^2M_5 = 0, \quad (6.72)$$

and

$$60(\omega + \alpha + a\kappa^2)M_1 - 10(c_1 + 4\kappa^2\theta_1 - \kappa\lambda)A^2M_2 + 2c_2A^4M_3 + 5aB^2M_4 - 3\theta_1A^2B^2M_5 = 0, \quad (6.73)$$

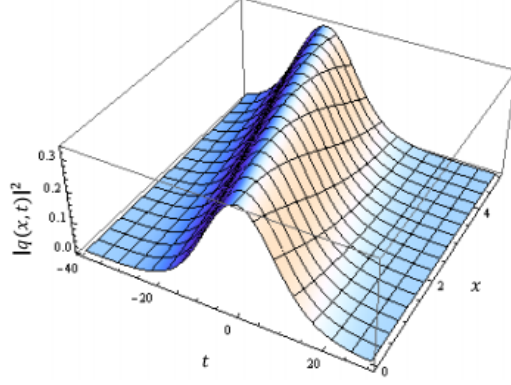


Figure 6.5: *Bright soliton with Parabolic law.*

respectively. From (6.72) and (6.73) one obtains

$$B = A \sqrt{\frac{4c_2 A^2 M_3 - 10(c_1 + 4\kappa^2 \theta_1 - \kappa \lambda) M_2}{10aM_4 - 9\theta_1 A^2 M_5}}, \quad (6.74)$$

whenever

$$\{2c_2 A^2 M_3 - 5(c_1 + 4\kappa^2 \theta_1 - \kappa \lambda) M_2\} (10aM_4 - 9\theta_1 A^2 M_5) > 0. \quad (6.75)$$

Thus for parabolic law nonlinearity, 1-soliton solution is given by

$$q(x, t) = \frac{A}{\sqrt{D + \cosh[B(x - vt)]}} e^{i(-\kappa x + \omega t + \theta)}, \quad (6.76)$$

with the parameters as defined.

The figure in **Fig. 6.5** shows a surface plot of a single bright soliton solution in optical metamaterials. Here,  $a = 0.1$ ,  $c_1 = c_2 = 0.1$ ,  $\alpha = 0.1$ ,  $\lambda = 1$ ,  $\nu = -0.9$ ,  $\theta_1 = 0.1$ ,  $\theta_2 = 0.2$ ,  $\theta_3 = 0.1$  and  $D = 2$ .

### 6.3.4 Dual-power law

The dual-power law nonlinearity is a generalization of the parabolic law and is generally represented as  $F(u) = c_1 u^n + c_2 u^{2n}$  with nonzero constants  $c_1$  and  $c_2$ . Notice that when  $n = 1$

this model condenses to parabolic law. Thus, NLSE model in this case is given by

$$\begin{aligned}
& iq_t + aq_{xx} + (c_1 |q|^{2n} + c_2 |q|^{4n}) q = \\
& i\alpha q_x + i\lambda (|q|^2 q)_x + i\nu (|q|^2)_x q + \theta_1 (|q|^2 q)_{xx} + \theta_2 |q|^2 q_{xx} + \theta_3 q^2 q_{xx}^*.
\end{aligned} \tag{6.77}$$

For dual-power law, the real part (6.6) takes the form

$$\begin{aligned}
& (\omega + \alpha\kappa + a\kappa^2) g - \{\kappa^2 (\theta_1 + \theta_2 + \theta_3) - \kappa\lambda\} g^3 \\
& - ag'' + 6\theta_1 g (g')^2 + (3\theta_1 + \theta_2 + \theta_3) g^2 g'' - c_1 g^{2n+1} - c_2 g^{4n+1} = 0.
\end{aligned} \tag{6.78}$$

Thus, the stationary integral (6.17) modifies to

$$J = \int_{\mathbb{R}} K ds, \tag{6.79}$$

where

$$K = 2(\omega + a\kappa + \alpha\kappa^2)g^2 - (4\kappa^2\theta_1 - \kappa\lambda)g^4 - 2a(g')^2 + 12\theta_1 g^2 (g')^2 - \frac{2c_1}{n+1}g^{2n+2} - \frac{2c_2}{2n+1}g^{4n+2}.$$

For dual power law the hypothesis to be considered is of the form

$$g(s) = \frac{A}{[D + \cosh(Bs)]^{\frac{1}{2n}}}, \tag{6.80}$$

where  $D$  is an arbitrary constant. By substituting this hypothesis into (6.79) and carrying out the integration, the stationary integral takes the form

$$\begin{aligned}
J = & \frac{4(\omega + \alpha + a\kappa^2)A^2}{B}Q_1 - \frac{2(c_1 + 4\kappa^2\theta_1 - \kappa\lambda)A^4}{B}Q_2 - aA^2BQ_3 + 6\theta_1A^4BQ_4 - \frac{2c_1A^{2n+2}}{(n+1)B}Q_5 \\
& - \frac{c_2A^{4n+2}}{(2n+1)B}Q_6,
\end{aligned} \tag{6.81}$$

where

$$Q_1 = \frac{1}{2^{\frac{1}{n}}} \times {}_2F_1 \left( \frac{1}{n}, \frac{1}{n}; \frac{1}{2} + \frac{1}{n}; \frac{1-D}{2} \right) \times B \left( \frac{1}{n}, \frac{1}{2} \right), \quad (6.82)$$

$$Q_2 = \frac{1}{4^{\frac{1}{n}}} \times {}_2F_1 \left( \frac{2}{n}, \frac{2}{n}; \frac{1}{2} + \frac{2}{n}; \frac{1-D}{2} \right) \times B \left( \frac{2}{n}, \frac{1}{2} \right), \quad (6.83)$$

$$Q_3 = \frac{1}{n^2 2^{\frac{1}{n}}} \times {}_2F_1 \left( 2 + \frac{1}{n}, \frac{1}{n}; \frac{3}{2} + \frac{1}{n}; \frac{1-D}{2} \right) \times B \left( \frac{1}{n}, \frac{3}{2} \right), \quad (6.84)$$

$$Q_4 = \frac{1}{n^2 4^{\frac{1}{n}}} \times {}_2F_1 \left( 2 + \frac{2}{n}, \frac{2}{n}; \frac{3}{2} + \frac{2}{n}; \frac{1-D}{2} \right) \times B \left( \frac{2}{n}, \frac{3}{2} \right), \quad (6.85)$$

$$Q_5 = \frac{1}{2^{\frac{1}{n}}} \times {}_2F_1 \left( 1 + \frac{1}{n}, 1 + \frac{1}{n}; \frac{3}{2} + \frac{1}{n}; \frac{1-D}{2} \right) \times B \left( 1 + \frac{1}{n}, \frac{1}{2} \right), \quad (6.86)$$

$$Q_6 = \frac{1}{2^{\frac{1}{n}}} \times {}_2F_1 \left( 2 + \frac{1}{n}, 2 + \frac{1}{n}; \frac{5}{2} + \frac{1}{n}; \frac{1-D}{2} \right) \times B \left( 2 + \frac{1}{n}, \frac{1}{2} \right). \quad (6.87)$$

Then, by finding (6.11) and (6.12) of  $J$  given by (6.81) one get after simplification

$$\begin{aligned} & 4(\omega + \alpha + a\kappa^2) Q_1 - 4(4\kappa^2\theta_1 - \kappa\lambda) A^2 Q_2 - aB^2 Q_3 \\ & + 12\theta_1 A^2 B^2 Q_4 - 2c_1 A^{2n} Q_5 - c_2 A^{4n} Q_6 = 0, \end{aligned} \quad (6.88)$$

and

$$\begin{aligned} & 4(\omega + \alpha + a\kappa^2) Q_1 - 2(\kappa^2\theta_1 - \kappa\lambda) A^2 Q_2 + aB^2 Q_3 \\ & - 6\theta_1 A^2 B^2 Q_4 - \frac{2c_1 A^{2n}}{n+1} Q_5 - \frac{c_2 A^{4n}}{2n+1} Q_6 = 0. \end{aligned} \quad (6.89)$$

After adding (6.88) and (6.89) and solving for  $B$  one get

$$B = \sqrt{\frac{(n+1)(2n+1)(4\kappa^2\theta_1 - \kappa\lambda) A^2 Q_2 + c_1 n A^{2n} Q_5 + c_2 n A^{4n} Q_6}{(n+1)(2n+1)(9\theta_1 A^2 Q_4 - aQ_3)}}, \quad (6.90)$$

which forces the condition

$$\{(n+1)(2n+1)(4\kappa^2\theta_1 - \kappa\lambda) A^2 Q_2 + c_1 n A^{2n} Q_5 + c_2 n A^{4n} Q_6\} (9\theta_1 A^2 Q_4 - aQ_3) > 0, \quad (6.91)$$

in order for the soliton to exist. The final form of 1-soliton solution in metamaterials with dual-power law nonlinearity is given by

$$q(x, t) = \frac{A}{\{D + \cosh[B(x - vt)]\}^{\frac{1}{2n}}} e^{i(-\kappa x + \omega t + \theta)}, \quad (6.92)$$

with the definition of its appropriate parameters.

The figure in **Fig. 6.6** shows a surface plot of a single bright soliton solution in optical metamaterials. Here,  $a = 0.1$ ,  $c_1 = c_2 = 0.1$ ,  $\alpha = 0.1$ ,  $\lambda = 1$ ,  $\nu = -0.9$ ,  $\theta_1 = 0.1$ ,  $\theta_2 = 0.2$ ,  $\theta_3 = 0.1$  and  $D = 2$  with  $n = 2$  and  $n = 2$ , respectively .

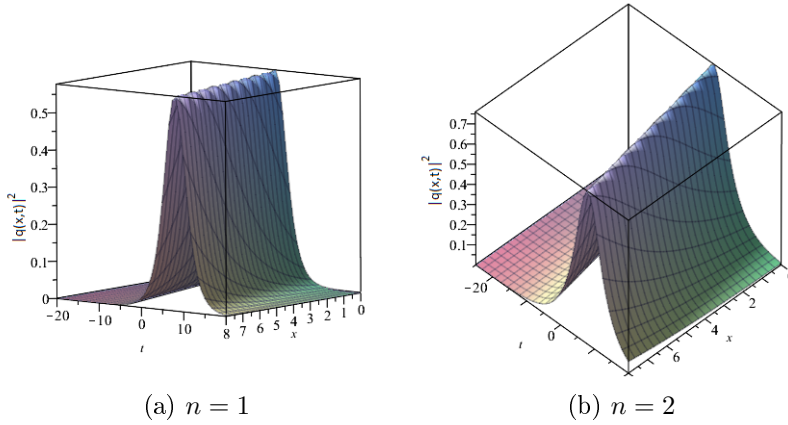


Figure 6.6: *Bright soliton with Dual-power law.*

### 6.3.5 Log law

In the case of log law nonlinearity,  $F(u) = \ln u$ . The logarithmic law of nonlinearity has an edge over the usual Kerr law nonlinearity. Thus, NLSE (6.1) for this nonlinearity is given by

$$\begin{aligned} & iq_t + aq_{xx} + c \ln |q|^2 q \\ &= i\alpha q_x + i\lambda (|q|^2 q)_x + i\nu (|q|^2)_x q + \theta_1 (|q|^2 q)_{xx} + \theta_2 |q|^2 q_{xx} + \theta_3 q^2 q_{xx}^*. \end{aligned} \quad (6.93)$$

Hence (6.6) modifies to

$$\begin{aligned} & (\omega + \alpha\kappa + a\kappa^2)g - \{\kappa^2(\theta_1 + \theta_2 + \theta_3) - \kappa\lambda\}g^3 - cg \ln g \\ & - ag'' + 6\theta_1g(g')^2 + (3\theta_1 + \theta_2 + \theta_3)g^2g'' = 0, \end{aligned} \quad (6.94)$$

and the stationary integral (6.17) takes the form

$$J = \int_{\mathbb{R}} \left\{ 2(\omega + \alpha\kappa + a\kappa^2)g^2 - (4\kappa^2\theta_1 - \kappa\lambda)g^4 + cg^2 - 2cg^2 \ln g - 2a(g')^2 + 12\theta_1g^2(g')^2 \right\} ds. \quad (6.95)$$

For log law the ansatz to be taken is:

$$g(s) = Ae^{-B^2s^2}. \quad (6.96)$$

Substituting this hypothesis into the stationary integral (6.95) and performing the corresponding integration yields

$$J = \Gamma\left(\frac{1}{2}\right) \left[ \frac{\sqrt{2}(\omega + a\kappa^2)A^2}{B} - \frac{(4\kappa^2\theta_1 - \kappa\lambda)A^4}{2B} - \frac{\sqrt{2}c(4 \ln A - 3)A^2}{4B} - \frac{\sqrt{2}aA^2B}{2} + 3\theta_1A^4B \right]. \quad (6.97)$$

Then equations (6.11) and (6.12) for log law nonlinearity, after simplification, are respectively given by

$$4\sqrt{2}(\omega + a\kappa^2) - 4(4\kappa^2\theta_1 - \kappa\lambda)A^2 - \sqrt{2}c(4 \ln A - 1) - 2\sqrt{2}aB^2 + 24\theta_1A^2B^2 = 0, \quad (6.98)$$

and

$$4\sqrt{2}(\omega + a\kappa^2) - 2(4\kappa^2\theta_1 - \kappa\lambda)A^2 - \sqrt{2}c(4 \ln A - 3) + 2\sqrt{2}aB^2 - 12\theta_1A^2B^2 = 0. \quad (6.99)$$

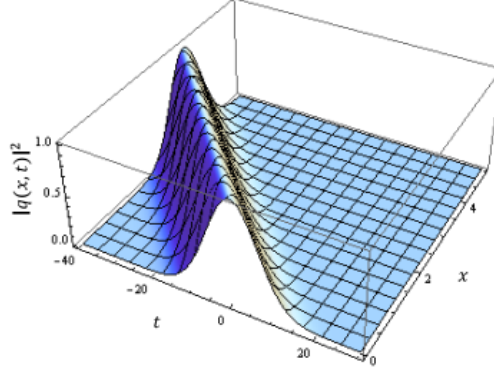


Figure 6.7: *Bright soliton (Gausson) with Log law.*

From the last two identities one can get the relation between the amplitude and the inverse width of the soliton as

$$B = \sqrt{\frac{(4\kappa^2\theta_1 - \kappa\lambda) A^2 + \sqrt{2}c}{18\theta_1 A^2 - 2\sqrt{2}a}}. \quad (6.100)$$

The last relation imposes the inequality

$$\left\{ (4\kappa^2\theta_1 - \kappa\lambda) A^2 + \sqrt{2}c \right\} \left( 18\theta_1 A^2 - 2\sqrt{2}a \right) > 0, \quad (6.101)$$

in order for the soliton to exist. Finally, the Gaussons for metamaterials is given by

$$q(x, t) = A e^{-B^2(x-vt)^2} e^{i(-\kappa x + \omega t + \theta)}, \quad (6.102)$$

where all the parameters are respectively defined with their corresponding domain restrictions.

The figure in **Fig. 6.7** shows a surface plot of a single bright soliton solution in optical metamaterials. Here,  $a = 0.1$ ,  $c = 1$ ,  $\alpha = 0.1$ ,  $\lambda = 1$ ,  $\nu = -0.9$ ,  $\theta_1 = 0.1$ ,  $\theta_2 = 0.2$ ,  $\theta_3 = 0.1$ .

## 6.4 Conclusions

This chapter applied SVP to extract bright and a couple of exotic soliton solutions. There are five nonlinear forms that were studied. For Kerr law nonlinearity, a couple of exotic soliton were obtained in addition to bright soliton. These are analytical solutions that are not exact. The numerical simulations are provided for each of the cases where the intensity of the soliton are plotted. There are domain restrictions, also referred to as constraint conditions for each such soliton that are listed. These guarantee the existence of such soliton studied in this chapter.

The results of this chapter stand on a very strong footing. Later, these research results will be applied to different situations such as optical couplers. DWDM systems and several others. In addition, polynomial law nonlinearity and triple-power law nonlinearity are to be considered in future.

# Chapter 7

## RAMAN SOLITON IN NANOSCALE OPTICAL WAVEGUIDES, WITH METAMATERIALS, HAVING POLYNOMIAL LAW NON-LINEARITY

Raman optical soliton pulses evolve due to a delicate balance between dispersion and non-linearity [21, 68, 76]. Soliton will dissipate in nature while propagating through double negative material(DNG) medium. Loss compensation is a challenge to engineer these types of materials. Dispersion profile of the wavelength structure is critically needed to determine the soliton pulse nature. In particular, Raman soliton self-frequency shift in metamaterials is induced by the stimulated Raman scattering (SRS) effect. Since the SRS effect enables the energy of the short pulse transferred from higher to lower frequency continuously by C. V. Raman and K. S. Krishnan [76]. It is possible that the whole spectrum moves toward the longer wavelength region. The chapter conducts theoretical analysis to illustrate the controllability of the Raman soliton self-frequency shift in non-linear metamaterials by numerical results.

### 7.1 Governing model

The dimensionless form nonlinear *Schrödinger's* equation (NLSE) that governs the propagation of raman soliton through optical metamaterials, with polynomial law nonlinearity, is given by [1, 2, 4, 21, 29, 3, 78, 79, 80]

$$\begin{aligned}
 & i q_t + a q_{xx} + \left( c_1 |q|^2 + c_2 |q|^4 + c_3 |q|^6 \right) q \\
 = & i \alpha q_x + i \lambda \left( |q|^2 q \right)_x + i \nu \left( |q|^2 \right)_x q + \theta_1 \left( |q|^2 q \right)_{xx} + \theta_2 |q|^2 q_{xx} + \theta_3 q^2 q_{xx}^*. \quad (7.1)
 \end{aligned}$$

In this model  $q(x, t)$  represents the complex valued wave function with the independent variables being  $x$  and  $t$  that represent spatial and temporal variables respectively. The first term represents the temporal evolution of nonlinear wave, while the coefficient  $a$  is the group velocity dispersion (GVD). The coefficients of  $c_j$  for  $j = 1, 2, 3$  corresponds to the nonlinear terms. Together, they form polynomial law nonlinearity. It must be noted here that when  $c_2 = c_3 = 0$  and  $c_1 \neq 0$ , the

model (7.1) collapses to Kerr law nonlinearity. However, if  $c_3 = 0$  and  $c_1 \neq 0$  and  $c_2 \neq 0$ , one arrives at parabolic law nonlinearity. Thus, polynomial law stands as an extension version to Kerr and parabolic laws.

On the right hand side of (7.1),  $\alpha$  represents the coefficient of inter-modal dispersion. This arises when the group velocity of light propagating through a metamaterial is dependent on propagation mode in addition to chromatic dispersion. The factors  $\lambda$  and  $\nu$  are accounted for self-steepening for preventing shock-waves, and nonlinear dispersion. Finally, the terms with  $\theta_j$  for  $j = 1, 2, 3$  arise in the context of optical metamaterials where functional variable method and first integral approach lead to bright and singular 1-soliton solution, as well as continuous waves [3]; the ansatz method of integration is employed to extract the 1-soliton solutions and numerical simulations are given to expose the dissipative effects [1]; the simplest equation approach also leads to topological soliton, rational solution and singular periodic solution [2]; the mapping method is applied to obtain soliton solutions with Kerr and Parabolic law [29]; by the aid of collective variables, the numerical simulations of soliton parameter variation are given for specific values of the super-Gaussian pulse parameters [81]; a theoretical investigation on the controllability of the Raman soliton self-frequency shift in the metamaterials [21]; bright 1-soliton solution is derived by the aid of traveling wave hypothesis in Kerr law, parabolic law and log law nonlinearity [60].

This model equation has studied for five forms of nonlinear media by the aid of ansatz method [1, 77], traveling wave hypothesis [60] as well as mapping methods [29] and collective variables approach [81]. This chapter will employ the traveling wave hypothesis to secure solutions to the model (7.1) that is with polynomial law nonlinearity. The starting hypothesis is the traveling wave argument given by [60, 78, 79]

$$q(x, t) = g(s)e^{i\phi}, \quad (7.2)$$

where  $g(s)$  represents the shape of the wave profile, and

$$s = x - vt, \quad (7.3)$$

with  $v$  being the speed of the wave. The phase component  $\phi(x, t)$  is defined as

$$\phi(x, t) = -\kappa x + \omega t + \theta, \quad (7.4)$$

where  $\kappa$  represents the soliton frequency, and  $\omega$  the wave number while  $\theta$  the phase constant. Therefore by substituting the hypothesis (7.2) into (7.1) and decomposing into real and imaginary parts one obtains the real part as:

$$ag'' - (\omega + \alpha\kappa + a\kappa^2)g + (c_1 - \kappa\lambda)g^3 + c_2g^5 + c_3g^7 = 0, \quad (7.5)$$

and the imaginary part as:

$$v + \alpha + 2a\kappa + \{3\lambda + 2\nu - 2\kappa(3\theta_1 + \theta_2 - \theta_3)\}g^2 = 0. \quad (7.6)$$

The notations  $g' = dg/ds$ ,  $g'' = d^2g/ds^2$ , and so on, are introduced in (7.5) for convenience.

From the imaginary part equation (7.6), upon setting the coefficients of linearly independent functions to zero gives

$$v = -\alpha - 2a\kappa, \quad (7.7)$$

and the relation

$$3\lambda + 2\nu = 2\kappa(3\theta_1 + \theta_2 - \theta_3). \quad (7.8)$$

Equation (7.8) serves as the constraint condition between soliton parameters and its coefficients, while (7.7) reveals the soliton velocity in polynomial law medium.

From the real part equation (7.5), multiplying both sides by  $g'$  and integrating after separation of variables yields the implicit solution:

$$\begin{aligned} & \frac{x - vt}{2\sqrt{3a}} g_3 \sqrt{6(\lambda\kappa - c_1)g^2 - 4c_2g^4 - 3c_3g^6 + 12(\omega + \alpha\kappa + a\kappa^2)} \\ = & -\Pi \left( 1 - \frac{g_2}{g_3}; \sin^{-1} \left[ \frac{g_3 - g^2}{g_3 - g_2} \right] \middle| \frac{g_2 - g_3}{g_1 - g_3} \right) \sqrt{\frac{(g^2 - g_1)(g^2 - g_2)(g^2 - g_3)}{g_1 - g_3}}, \end{aligned} \quad (7.9)$$

where incomplete elliptic integral of third kind is defined as

$$\Pi(n; \phi|\alpha) = \int_0^\phi \frac{d\theta}{(\alpha - n \sin^2 \theta) \sqrt{1 - \sin^2 \alpha \sin^2 \theta}}, \quad (7.10)$$

and

$$g_1 = -\frac{1}{9c_3} \left\{ 4c_2 - \frac{2(8c_2^2 - 27c_1c_3 + 27c_3\lambda\kappa)}{R^{\frac{1}{3}}} + R^{\frac{1}{3}} \right\}, \quad (7.11)$$

$$g_2 = -\frac{1}{9c_3} \left\{ 4c_2 - \frac{(1 + i\sqrt{3})(8c_2^2 - 27c_1c_3 + 27c_3\lambda\kappa)}{R^{\frac{1}{3}}} - \frac{(1 - i\sqrt{3})R^{\frac{1}{3}}}{2} \right\}, \quad (7.12)$$

$$g_3 = -\frac{1}{9c_3} \left\{ 4c_2 - \frac{(1 - i\sqrt{3})(8c_2^2 - 27c_1c_3 + 27c_3\lambda\kappa)}{R^{\frac{1}{3}}} - \frac{(1 + i\sqrt{3})R^{\frac{1}{3}}}{2} \right\}, \quad (7.13)$$

with

$$R = 2r + \sqrt{r^2 - 8(8c_2^2 - 27c_1c_3 + 27c_3\lambda\kappa)^3}, \quad (7.14)$$

and

$$r = 2 \{ 32c_2^3 - 162(\lambda\kappa - c_1)c_2c_3 - 729c_2^2(\omega + \alpha\kappa + a\kappa^2) \}, \quad (7.15)$$

Equation (7.14) prompts the constraint condition

$$r^2 > 8(8c_2^2 - 27c_1c_3 + 27c_3\lambda\kappa)^3, \quad (7.16)$$

that must remain valid for the existence of the solution.

From a historic standpoint, it must be noted that such an algorithm has already been applied in the past for the study of soliton propagation through optical fibers [78, 79]. During the second

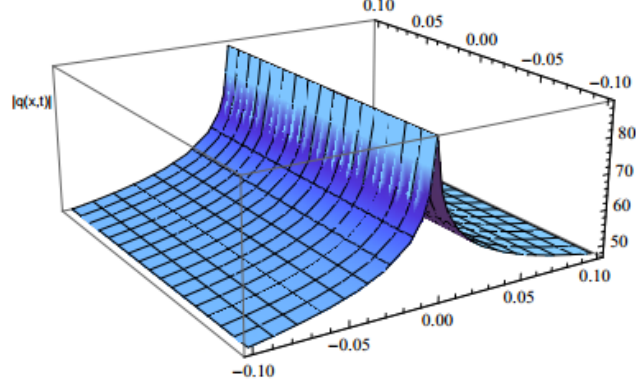


Figure 7.1: Soliton profile with Polynomial law nonlinearity.

round, this analysis was carried out in presence of spatio-temporal dispersion (STD) in addition to GVD [78].

**Fig. 7.1** shows the profile of the soliton solution in formula (7.9) for selected parameter values. In this case,  $a = 1$ ,  $c_1 = 10$ ,  $c_2 = -10,000$ ,  $c_3 = 5$ ,  $\alpha = 100$ ,  $\lambda = -2$ ,  $\nu = -1$ ,  $\omega = 1$ ,  $\kappa = 1$ .

## 7.2 Generalization

In this part, the triple-power law, i.e. the extension of parabolic law nonlinearity that is given by

$$\begin{aligned}
 & i q_t + a q_{xx} + \left( c_4 |q|^{2n} + c_5 |q|^{4n} + c_6 |q|^{6n} \right) q \\
 = & i \alpha q_x + i \lambda \left( |q|^2 q \right)_x + i \nu \left( |q|^2 \right)_x q + \theta_4 \left( |q|^2 q \right)_{xx} + \theta_5 |q|^2 q_{xx} + \theta_6 q^2 q_{xx}^*. \quad (7.17)
 \end{aligned}$$

Therefore, the NLSE (7.17) transforms to

$$x - vt = \sqrt{2a(n+1)(2n+1)(3n+1)} \int \frac{dg}{g\sqrt{Q(g)}}, \quad (7.18)$$

were

$$\begin{aligned}
 Q(g) = & (n+1)(2n+1)(3n+1) \left( 2(\omega + a\kappa + \alpha\kappa^2) + \kappa\lambda g^2 \right) \\
 & - 2(2n+1)(3n+1)c_4 g^{2n} - 2(n+1)(3n+1)c_5 g^{4n} - 2(n+1)(2n+1)c_6 g^{6n}. \quad (7.19)
 \end{aligned}$$

Assume  $\lambda = 0$ , integrating (7.18) leads to

$$\frac{(x - vt)n}{\sqrt{a(n+1)(2n+1)(3n+1)}} \\ \sqrt{(3n+1)((n+1)(2n+1)(\omega + a\kappa + \alpha\kappa^2) + (2n+1)c_4g^{2n} + (n+1)c_5g^{4n}) + (n+1)(2n+1)c_6g^{6n}g_6} \\ = -\Pi\left(1 - \frac{g_5}{g_6}; \sin^{-1}\left[\frac{g_6 - g^{2n}}{g_6 - g_5}\right] \middle| \frac{g_5 - g_6}{g_4 - g_6}\right) \sqrt{\frac{(g^{2n} - g_4)(g^{2n} - g_5)(g^{2n} - g_6)}{g_4 - g_6}}, \quad (7.20)$$

where

$$g_4 = \frac{1}{3(1+3n+2n^2)} \left[ 2(1+4n+3n^2) - \frac{2^{\frac{1}{3}}h_1}{5R} + \frac{R}{5 * 2^{\frac{1}{2}}} \right], \quad (7.21)$$

$$g_5 = \frac{1}{3(1+3n+2n^2)} \left[ 2(1+4n+3n^2) + (1+i\sqrt{3}) \frac{h_1}{5 * 2^{\frac{2}{3}}R} - (1-i\sqrt{3}) \frac{R}{10 * 2^{\frac{1}{2}}} \right], \quad (7.22)$$

$$g_6 = \frac{1}{3(1+3n+2n^2)} \left[ 2(1+4n+3n^2) + (1-i\sqrt{3}) \frac{h_1}{5 * 2^{\frac{2}{3}}R} - (1+i\sqrt{3}) \frac{R}{10 * 2^{\frac{1}{2}}} \right], \quad (7.23)$$

with  $R_1$  being given by

$$R_1 = (r_1 + \sqrt{4h_1^3 + r_1^2})^{\frac{1}{3}}, \quad (7.24)$$

$$r_1 = 4502000 + 675\kappa + 67500\kappa^2 + 54024000n + 8100\kappa n + 810000\kappa^2n + 261114000n^2 + 675\omega + \\ 40500(\kappa + 100\kappa^2)n^2 + 648272000n^3 + 109350(\kappa + 100\kappa^2)n^3 + (868842000 + 172125\kappa)n^4 \\ + 17212500\kappa^2n^4 + 594216000n^5 + 157950(\kappa + 100\kappa^2)n^5 + 162054000n^6 + 78300(\kappa + 100\kappa^2 + \omega)n^6 \\ + 16200(\kappa + 100\kappa^2 + \omega)n^7 + 8100n\omega + 40500n^2\omega + 109350n^3\omega + 172125n^4\omega + 157950n^5\omega, \quad (7.25)$$

$$h_1 = -(150100 + 1200800n + 3452200n^2 + 4202400n^3 + 1800900n^4). \quad (7.26)$$

**Fig. 7.2** shows the profile of the soliton solution in formula(7.20) for selected parameter values. In this case,  $a = 100$ ,  $c_4 = -10000$ ,  $c_5 = -10$ ,  $c_6 = 10$ ,  $\alpha = 100$ ,  $\nu = -1$ ,  $\omega = 1$ ,  $\kappa = 1$  and  $n = 2$ .

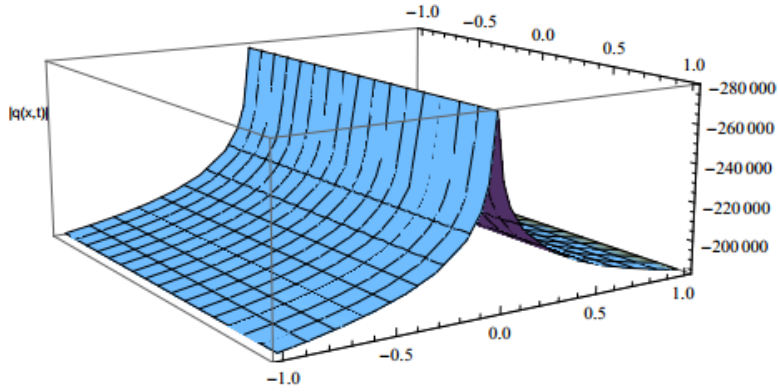


Figure 7.2: *Soliton profile with Polynomial law nonlinearity.*

### 7.3 Conclusions

This paper gives raman soliton solutions in optical metamaterials that is studied with polynomial law and triple law nonlinearity. The analytical results are supplemented with numerical simulation. This paper is an extension to the ones that were studied earlier in optical fibers [78, 79]. The results of this paper are encouraging to conduct further research in this field.

In future, additional perturbation terms such as Raman scattering, saturable amplifiers, higher order dispersions and several others will be included. Additionally, soliton in optical metamaterials will be considered with STD in addition to GVD. There are several other forms of nonlinear media that are yet to be explored. These are saturable law, exponential law, triple power law, threshold law. In particular the triple-power law nonlinearity that is a direct generalization of polynomial law will be studied. Although this law is investigated in optical fibers, the results are unknown at this stage for optical metamaterials. Furthermore, optical metamaterials will be handled in the context of couplers. From a mathematical perspective, the governing NLSE will be analyzed with fractional temporal evolution. This will lead to the attainment of slow-light soliton in optical metamaterials in order to address Internet bottleneck that is a growing concern in this industry. The results of all of these research will be gradually disseminated elsewhere.

## Chapter 8

# EVOLUTIONARY PATTERN FORMATION FOR COMPETING POPULATIONS WITH ASYMMETRIC NON-LOCAL COUPLING UNDER SINUSOIDAL TEMPORAL SEASONAL FORCING

Population models can be used to understand the Honey Bee Population Dynamics [96, 97, 98] and other species at interest and also be used to understand the spread of parasites [99], viruses [100], and disease [101]. For example, explore the impact of different death rates of forager bees on colony growth and development [102], evaluate the effects of artificial feeding on bee colony population dynamics [103], recognize the importance of pollination to our food systems and economics [104]. Additionally, contact and competition among different species within a community matters when it comes to the possibility of parasite disease outbreak [105], evolution of plant viruses [106] and ecology of tumors [107]. A model of competing species is developed in [108], which is based on the diffusive logistic model (Fisher's equation) and extends the scalar model to account for two competing species. In [108] a non-local competition term is used to model competition between species. The nonlinear term uses a convolution of a kernel,  $\phi_{\alpha,\delta}$ , with the population,  $u$ , to capture non-local interactions. The biological phenomenon of the non-local coupling can be attributed to the effect of mobility. If species compete for a sparse resource, then due to mobility the inhibiting effect of depletion of this resource should depend not just on the populations at a point but on some weighted average of the populations [108]. Additionally, the kernel,  $\phi_{\alpha,\delta}$ , used to capture non-local effects is asymmetric. This asymmetry can be used to capture unsymmetrical terrain or other effects. Recently, there has been a growing interest in the development of predictive modeling tools to species dynamics [96, 97, 98, 109, 110, 111, 112, 113]. We add seasonal variations to our model to understand how species respond to larger disturbances such as changes in climate. The seasonal forcing is through a sinusoidal nonlinear perturbation of the competition term.

The scalar model was initially shown in [108, 114] and then in [115, 116, 117, 118, 119, 120]. The kernel function in [108, 114] was symmetric, which was equivalent that the non-local interaction

at any specified point  $x$  weights the population symmetrically about  $x$ . In these cases we can see unstable, nonlinear effects when the interaction range of the kernel,  $\delta$ , is sufficiently large. In this case we see stationary, nonlinear patterns. The patterns were built up by islands of nonzero population separated by dead-zones where the population was exponentially small. Stability analyses in [115, 116, 117] considered the effort of the kernel function in destabilizing this equilibrium. In the unstable cases, nonlinear patterns consisted of islands separated by dead-zones.

Asymmetric non-local interactions, i.e., convolutions with uneven kernel function brought out complex valued Fourier transforms in [117, 118, 119]. In this case instability was still a function of the degree of non-locality,  $\delta$ , but the stability limit fluctuates depending on the degree of asymmetry in the kernel,  $\alpha$ . In these cases the nonlinear patterns are no longer stationary, but more with a velocity depending on  $\alpha$ .

In this paper, we are interested in finding persistence phenomenon in modeling competing species. In our model, we try to account for various factors including non-local competition, asymmetrical behavior, and seasonal effects. The non-local coupling is modeled through convolution integrals, which is attributed to the effect of mobility, i.e., resource should depend not just on the populations at a point but on some weighted average of the populations, due to its inhibiting effect of depletion [108, 120]. The asymmetry is introduced via the convolution integral with non-even kernel functions. This asymmetry can arise in many ways. In tumors it can be found as the result of complex steady-state dynamics of population distribution [121]. Within each tumor, clones can evolve that harbor selectively advantageous mutations (called drivers), neutral mutations (called passengers), and deleterious mutations. The temporal effect is via sinusoidal forcing. This is likely to become increasing important in coming years, as the climate is expected to become more variable [111, 112, 113].

We study the case where the model admits a stable coexistence Limit Cycle solution. We show that this solution can be de-stabilized by the non-local coupling, access stability conditions of this critical point as a function of  $\alpha$ , determine unstable wave number bands with  $\delta$  beyond the stability boundary and compare results with different  $p$ . We consider the nonlinear patterns with

sufficiently non-localization under varying  $p$ . Patterns consist of arrays of islands, regions of non-zero population, separated by either near dead-zones where populations are exponentially small and essentially extinct under perturbation, which is stimulated by both *Matlab* and *CLanguage*. We start with modeling and analysing the spread dynamic of coupled populations, and then focus on the impacts of population interactions on spread behavior to estimate the convolutionary pattern of a relative heterogeneous environment. We have derived the stability conditions, and some nonlinear patterns under varying seasonal forcing.

## 8.1 Governing model

The model consisting of two coupled integro-differential equations was initially introduced in [108] and developed in [114]-[121], with  $u$  and  $v$  denoting competing species. The model is

$$u_{\tilde{t}} = d_1 u_{\tilde{x}\tilde{x}} + a_1 u - u(b_1 u * \tilde{\phi}_{\alpha, \tilde{\delta}} + c_1 v * \tilde{\phi}_{\alpha, \tilde{\delta}}), \quad (8.1a)$$

$$v_{\tilde{t}} = d_2 v_{\tilde{x}\tilde{x}} + a_2 v - v(b_2 v * \tilde{\phi}_{\alpha, \tilde{\delta}} + c_2 u * \tilde{\phi}_{\alpha, \tilde{\delta}}). \quad (8.1b)$$

The parameters of  $d_1$  and  $d_2$  describe the diffusion of the system. The parameters  $a_1$  and  $a_2$  describe the natural linear net rate of change of the populations (linear birth rate minus linear death rate) for  $u$  and  $v$ , respectively. We always assume  $a_1 > 0$ ,  $a_2 > 0$  so that extinction of both species ( $u=v=0$ ) is unstable. We take  $b_1$ ,  $b_2$ ,  $c_1$  and  $c_2$  as positive, so that the quadratic terms in fact correspond to a reduction of the natural growth rate (or enhanced death rate) of the populations due to intra species ( $b_1 u \tilde{\phi}_{\alpha, \tilde{\delta}} * u$ ,  $b_2 v \tilde{\phi}_{\alpha, \tilde{\delta}} * v$ ) and inter species ( $c_1 u \tilde{\phi}_{\alpha, \tilde{\delta}} * v$ ,  $c_2 v \tilde{\phi}_{\alpha, \tilde{\delta}} * u$ ) competition, or overpopulation. Therefore, we take the standard assumptions of logistic population evolution-linear growth and quadratic decay. We use  $u \cdot \tilde{\phi}_{\alpha, \tilde{\delta}} * u$  in place of pure quadratic decay to represent the computation over a range rather than at a local point. The parameters  $\tilde{\delta}$  and  $\alpha$  in the kernel represent range of competition,  $\tilde{\delta}$ , and asymmetry,  $\alpha$ , respectively.

We account for the temporal seasonal forcing factor based on previous research. In our model, we are interested in finding persistence phenomenon in modeling competing species by accounting for various factors including non-local competition, asymmetrical behavior and seasonal effects. This

is likely to become increasingly important in coming years, as the climate is expected to become more variable [111, 112, 113]. We introduce seasonal variances through the term  $(1 + p \sin(ft))$ , where  $p$  is the magnitude of seasonal effects and  $f$  is the frequency factor,

$$u_{\tilde{t}} = d_1 u_{\tilde{x}\tilde{x}} + a_1 u - (1 + p \sin(f\tilde{t}))u(b_1 u * \tilde{\phi}_{\alpha, \tilde{\delta}} + c_1 v * \tilde{\phi}_{\alpha, \tilde{\delta}}), \quad (8.2a)$$

$$v_{\tilde{t}} = d_2 v_{\tilde{x}\tilde{x}} + a_2 v - (1 + p \sin(f\tilde{t}))v(b_2 v * \tilde{\phi}_{\alpha, \tilde{\delta}} + c_2 u * \tilde{\phi}_{\alpha, \tilde{\delta}}). \quad (8.2b)$$

Here  $u$  and  $v$  are the population densities for the two competing species,  $\tilde{t}$  and  $\tilde{x}$  denote time and space,  $u_{\tilde{t}}$  and  $u_{\tilde{x}\tilde{x}}$  denote partial derivatives and  $*$  denotes spatial convolution, i.e.,

$$\tilde{\phi}_{\alpha, \tilde{\delta}} * \omega(\tilde{x}, \tilde{t}) = \int_{-\infty}^{\infty} \tilde{\phi}_{\alpha, \tilde{\delta}}(\tilde{y}) \omega(\tilde{x} - \tilde{y}, \tilde{t}) d\tilde{y}, \quad (8.3)$$

where  $\tilde{\phi}_{\alpha, \tilde{\delta}}$  is a specified even, nonnegative kernel function such that

$$\int_{-\infty}^{\infty} \tilde{\phi}_{\alpha, \tilde{\delta}}(\tilde{y}) d\tilde{y} = 1, \quad (8.4)$$

, where  $\tilde{\delta}$  represents the spatial extend of the kernel function, with  $\tilde{\delta} \rightarrow 0$  corresponding to the local pattern;  $\alpha$  denotes the degree of asymmetry, with  $\alpha \rightarrow 0$  corresponding to symmetric non-local coupling. So that  $\tilde{\phi}_{\alpha, \tilde{\delta}}$  behaves like a  $\delta$ -function.

We non-dimensionalize by setting

$$t = a_1 \tilde{t}; U = \frac{b_1}{a_1} u; V = \frac{b_2}{a_1} v; U_t = \frac{b_1}{a_1^2} u_t; V_t = \frac{b_2}{a_1^2} v_t; f = \frac{\omega}{a_1}; h_1 = \frac{c_1}{b_2}; h_2 = \frac{c_2}{b_1}; \zeta = \frac{a_2}{a_1}; d = \frac{d_2}{d_1}, \quad (8.5)$$

and assume the non-dimensional kernel function

$$\phi_{\alpha, \delta} = \tilde{\phi}_{\alpha, \tilde{\delta}}. \quad (8.6)$$

From equations (8.3)-(8.6), we get

$$\phi_{\alpha,\delta} * \omega(x, t) = \int_{-\infty}^{\infty} \phi_{\alpha,\delta}(y)\omega(x - y, t)dy, \quad (8.7)$$

and

$$\int_{-\infty}^{+\infty} \phi_{\alpha,\delta}(y)dy = 1. \quad (8.8)$$

The parameter  $\delta$  is a measure of the spatial extent of the kernel function relative to the reference length. We will always assume that  $\phi_{\alpha,\delta}$  is exponentially small for large  $y$ .

From the system (8.2) and the non-dimensionalized parameter set (8.5) and (8.6), we have

$$U_t = U_{xx} + U - (1 + p \sin(ft))U(U * \phi_{\alpha,\delta} + h_1V * \phi_{\alpha,\delta}), \quad (8.9a)$$

$$V_t = dV_{xx} + \zeta V - (1 + p \sin(ft))V(V * \phi_{\alpha,\delta} + h_2U * \phi_{\alpha,\delta}), \quad (8.9b)$$

where uppercase letter  $U$  and  $V$  denote non-dimensional quantities. Therefore, for any set of dimensional diffusivities and kinetic parameters, the dimensional model (8.2) is equivalent to the system (8.9).

In view of (8.9), critical points, i.e., spatially uniform stationary solutions  $U_0$  and  $V_0$  satisfy the algebraic system of equations

$$U_{0t} = U_0 - (1 + p \sin(ft))U_0(U_0 + h_1V_0), \quad (8.10a)$$

$$V_{0t} = \zeta V_0 - (1 + p \sin(ft))V_0(V_0 + h_2U_0). \quad (8.10b)$$

By (8.10) and (8.9), the solution of  $U_0 = V_0 = 0$  corresponds to extinction of both species, which is unstable.

We consider the coexistence critical point, where not both  $U_0$  and  $V_0$  are zero. We are trying to examine solutions in limit cycle (L.C.) with temporal forcing caused by  $1 + p \sin(ft)$ . We can't have a steady state solution, but we examine the numerical solution approaches a limit cycle, in which solutions are uniform in space and change periodically in temporal space. We get the L.C.

solution by using the perturbation method. Assume

$$U_0 = U^{(0)} + pU^{(1)} + p^2U^{(2)} + \dots, \quad (8.11a)$$

$$V_0 = V^{(0)} + pV^{(1)} + p^2V^{(2)} + \dots \quad (8.11b)$$

Substitute (8.11) into (8.10), we get

$$U_t^{(0)} + pU_t^{(1)} + p^2U_t^{(2)} + \dots = (U^0 + pU^{(1)} + p^2U^{(2)} + \dots) - (1 + p \sin(ft))*$$

$$[U^{(0)} + pU^{(1)} + p^2U^{(2)} + \dots + h_1V^{(0)} + h_1pV^{(1)} + h_1p^2V^{(2)} + \dots](U^{(0)} + pU^{(1)} + p^2U^{(2)} + \dots), \quad (8.12)$$

$$V_t^{(0)} + pV_t^{(1)} + p^2V_t^{(2)} + \dots = \zeta(V^0 + pV^1 + p^2V^2 + \dots) - (1 + p \sin(ft))*$$

$$[V^{(0)} + pV^{(1)} + p^2V^{(2)} + \dots + h_2U^{(0)} + h_2pU^{(1)} + h_2p^2U^{(2)} + \dots](V^{(0)} + pV^{(1)} + p^2V^{(2)} + \dots). \quad (8.13)$$

Thus from (8.12) and (8.13), the coefficient of  $O(p^0)$ ,

$$U_t^{(0)} = U^{(0)} - U^{(0)2} - h_1V^{(0)}U^{(0)}, \quad (8.14a)$$

$$V_t^{(0)} = \zeta V^{(0)} - V^{(0)2} - h_2V^{(0)}U^{(0)}. \quad (8.14b)$$

Then

$$U^{(0)} = \frac{1 - h_1\zeta}{1 - h_1h_2}, \quad (8.15a)$$

$$V^{(0)} = \frac{\zeta - h_2}{1 - h_1h_2}. \quad (8.15b)$$

Also from (8.12) and (8.13), the coefficient of  $O(p^1)$ ,

$$U_t^{(1)} + U^{(0)}U^{(1)} + h_1U^{(0)}V^{(1)} = -U^{(0)} \sin(ft), \quad (8.16a)$$

$$V_t^{(1)} + h_2V^{(0)}U^{(1)} + V^{(0)}V^{(1)} = -\zeta V^{(0)} \sin(ft). \quad (8.16b)$$

Suppose

$$U^{(1)} = A \sin(ft) + B \cos(ft), \quad (8.17a)$$

$$V^{(1)} = C \sin(ft) + D \cos(ft), \quad (8.17b)$$

through (8.16) and (8.17), we get

$$\begin{pmatrix} A \\ B \\ C \\ D \end{pmatrix} = \begin{pmatrix} f & U^{(0)} & 0 & h_1 U^{(0)} \\ U^{(0)} & -f & h_1 U^{(0)} & 0 \\ 0 & h_2 V^{(0)} & f & V^{(0)} \\ h_2 V^{(0)} & 0 & V^{(0)} & -f \end{pmatrix}^{-1} \begin{pmatrix} 0 \\ -U^{(0)} \\ 0 \\ -\zeta V^{(0)} \end{pmatrix}. \quad (8.18)$$

Then

$$\begin{pmatrix} A \\ B \\ C \\ D \end{pmatrix} = -\frac{1}{T} \begin{pmatrix} [f^2 + V^{(0)2} - h_1 h_2 V^{(0)2}] U^{(0)2} + \zeta [f^2 + (h_1 h_2 - 1) U^{(0)} V^{(0)}] h_1 U^{(0)} V^{(0)} \\ -[f^2 + V^{(0)2} + h_1 h_2 U^{(0)} V^{(0)}] f U^{(0)} + \zeta [U^{(0)} + V^{(0)}] h_1 U^{(0)} V^{(0)} f \\ [f^2 + (h_1 h_2 - 1) U^{(0)} V^{(0)}] h_2 U^{(0)} V^{(0)} + \zeta [f^2 + U^{(0)2} - h_1 h_2 U^{(0)2}] V^{(0)2} \\ [U^{(0)} + V^{(0)}] h_2 U^{(0)} V^{(0)} f - \zeta [f^2 + U^{(0)2} + h_1 h_2 U^{(0)} V^{(0)}] f V^{(0)} \end{pmatrix},$$

where

$$T = f^4 + 2f^2 h_1 h_2 U^{(0)} V^{(0)} + f^2 (U^{(0)2} + V^{(0)2}) + (h_1 h_2 + 1)^2 (U^{(0)} V^{(0)})^2.$$

Therefore, from (8.11)-(8.18), the L.C. solution

$$U_0 = U^{(0)} + pU^{(1)}, \quad (8.19a)$$

$$V_0 = V^{(0)} + pV^{(1)}, \quad (8.19b)$$

where expressions of  $U^{(0)}$ ,  $V^{(0)}$ ,  $U^{(1)}$  and  $V^{(1)}$  are found in (8.15), (8.17) and (8.18).

We will consider the following asymmetric Gaussian kernel function

$$\phi_{\alpha,\delta}(y) = \frac{1}{\delta\sqrt{\pi}} \exp\left(-\left(\frac{y - \delta\alpha}{\delta}\right)^2\right). \quad (8.20)$$

The equation (8.20) in (8.2) describes a non-local coupling which is an asymmetric weighted average. In addition, for any given spatial location  $x$ , (8.20) implies that the primary contribution to the integral terms in (8.2) does not come from the solution at the given point  $x$ , but rather at the displaced point  $x - \delta\alpha$ . Therefore, (8.20) de-emphasizes the local, self-regulating properties of properties of (8.2) in controlling the exponential growth in population due to the positive linear net birth rates in favor of a long-range control at the displace point  $x - \delta\alpha$ .

## 8.2 Stability analysis

In this section, we perform a linear analysis to determine stability boundaries. We consider the following two parameter sets for the asymmetric kernel function (8.20). It is already known that the equilibrium solution  $(U_0, V_0)$  is stable for all  $\delta$  with the symmetric Gaussian Kernel [120, 121]. The de-stabilization has been found for Gaussian is due solely to the asymmetry ( $\alpha > 0$ ) [121]. Rather than at a fixed time we will study the stability situation under the sinusoidal temporal perturbation dynamics.

Assuming

$$\begin{pmatrix} U \\ V \end{pmatrix} = \begin{pmatrix} U_0 + \varepsilon \tilde{U} e^{\lambda t} \\ V_0 + \varepsilon \tilde{V} e^{\lambda t} \end{pmatrix}, \quad (8.21)$$

substituting into (8.9), replacing  $\phi_{\alpha,\delta}$  by  $\phi$  and keeping only first order terms in  $\varepsilon$  leads to

$$\begin{aligned} (\lambda - 1 + (U^{(0)}\hat{\phi} + h_1V^{(0)}\hat{\phi})(1 + p \sin(ft)))\tilde{U} &= \tilde{U}_{xx} - (1 + p \sin(ft))U_0(\tilde{U} * \phi + h_1\tilde{V} * \phi), \\ (\lambda - \zeta + (V^{(0)}\hat{\phi} + h_2U^{(0)}\hat{\phi})(1 + p \sin(ft)))\tilde{V} &= d\tilde{V}_{xx} - (1 + p \sin(ft))V_0(\tilde{V} * \phi + h_2\tilde{U} * \phi). \end{aligned} \quad (8.22)$$

Next take Fourier transform of (8.22),

$$\hat{U} = \int_{-\infty}^{\infty} \tilde{U} e^{ikx} dx, \hat{V} = \int_{-\infty}^{\infty} \tilde{V} e^{ikx} dx, \hat{\phi} = \int_{-\infty}^{\infty} \phi e^{ikx} dx. \quad (8.23)$$

and let  $\beta = k\delta$  and  $\chi = \frac{1}{\delta^2}$ , where  $k$  is the Fourier scaling number.

Write the Fourier transform of the kernel as

$$\hat{\phi} = \phi_R + i\phi_I, \quad (8.24)$$

where  $\phi_R$  and  $\phi_I$  are the real and imaginary parts of  $\hat{\phi}$ , respectively.

Take Fourier transform in  $x$  of (8.22) to obtain,

$$\begin{aligned} (\lambda + p \sin(ft))\hat{U} &= -(\chi\beta^2)\hat{U} - (1 + p \sin(ft))U_0((\phi_R + i\phi_I)\hat{U} + h_1(\phi_R + i\phi_I)\hat{V}), \\ (\lambda + \zeta p \sin(ft))\hat{V} &= -(\chi\beta^2)d\hat{V} - (1 + p \sin(ft))V_0((\phi_R + i\phi_I)\hat{V} + h_2(\phi_R + i\phi_I)\hat{U}). \end{aligned} \quad (8.25)$$

When  $p = 0$ , it is the same as in[121]. However we are more interested in the behavior for nonzero  $p$ . We note that if  $O(\zeta - 1) \approx O(p)$ , then we can define (8.25) to be

$$\begin{aligned} (\lambda + p \sin(ft))\hat{U} &= -(\chi\beta^2)\hat{U} - (1 + p \sin(ft))U_0((\phi_R + i\phi_I)\hat{U} + h_1(\phi_R + i\phi_I)\hat{V}), \\ (\lambda + p \sin(ft))\hat{V} &= -(\chi\beta^2)d\hat{V} - (1 + p \sin(ft))V_0((\phi_R + i\phi_I)\hat{V} + h_2(\phi_R + i\phi_I)\hat{U}). \end{aligned} \quad (8.26)$$

So, the matrix form of (8.26) is

$$\tilde{\lambda}I \begin{pmatrix} \hat{U} \\ \hat{V} \end{pmatrix} = M \begin{pmatrix} \hat{U} \\ \hat{V} \end{pmatrix}, \quad (8.27)$$

where

$$M = \begin{pmatrix} -((\chi\beta^2)^2) - (1 + p \sin(ft))U_0(\phi_R + i\phi_I) & -h_1(1 + p \sin(ft))U_0(\phi_R + i\phi_I) \\ -h_2(1 + p \sin(ft))V_0(\phi_R + i\phi_I) & -d(\chi\beta^2) - (1 + p \sin(ft))V_0(\phi_R + i\phi_I) \end{pmatrix}.$$

and  $\tilde{\lambda} = \lambda + p \sin(ft)$ . Linear stability requires that the eigenvalues of  $M$  be either in the left half plane or on the imaginary axis conditions, i.e.,  $\text{trace}(M) \leq 0$  and  $\text{det}(M) \geq 0$ .

Therefore,

$$\begin{aligned} & -(1+d)(\chi\beta^2) - (1+p\sin(ft))(U_0+V_0)(\phi_R+i\phi_I) \leq 0, \\ & \text{det}[M - \tilde{\lambda}I] = -(1+p\sin(ft))^2 h_1 h_2 U_0 V_0 (\phi_R+i\phi_I)^2 \\ & (\tilde{\lambda} + (\chi\beta^2) + (1+p\sin(ft))U_0(\phi_R+i\phi_I))(\tilde{\lambda} + (\chi\beta^2)d + (1+p\sin(ft))V_0(\phi_R+i\phi_I)) \geq 0. \end{aligned} \quad (8.28)$$

Assume  $\tilde{\lambda} = i\omega(t)$ , where  $\omega(t)$  is real, we have

$$\begin{aligned} & -\omega^2 + i\omega(1+p\sin(ft))(U_0+V_0)(\phi_R+i\phi_I) + (dU_0+V_0)\chi\beta^2(1+p\sin(ft))(\phi_R+i\phi_I) + \\ & i\omega\chi\beta^2(1+d) + (\chi\beta^2)^2 d + (1+p\sin(ft))^2(1-h_1h_2)U_0V_0(\phi_R^2 - \phi_I^2 + 2i\phi_R\phi_I) \geq 0, \end{aligned}$$

From the imaginary part, it follows

$$\omega = -\frac{\chi\beta^2(1+p\sin(ft))(dU_0+V_0) + 2(1+p\sin(ft))^2(1-h_1h_2)U_0V_0\phi_R}{\chi\beta^2(1+d) + (1+p\sin(ft))(U_0+V_0)\phi_R} \phi_I, \quad (8.29)$$

By the real part, it has

$$\begin{aligned} & (\chi\beta^2)^4 s^2 d + (\chi\beta^2)^3 (1+p\sin(ft))(2d\theta + s\zeta)s\phi_R + \\ & (\chi\beta^2)^2 (1+p\sin(ft))^2 ((s\zeta\theta - \zeta^2 - s^2\sigma)\phi_I^2 + (d\theta^2 + 2s\zeta\theta + s^2\sigma)\phi_R^2) \\ & (\chi\beta^2)(1+p\sin(ft))^3 ((2s\sigma + \zeta\theta)\theta\phi_R^2 + (\theta^2 - 4\sigma)\zeta\phi_I^2)\phi_R \\ & (1+p\sin(ft))^4 (\theta^2 - 4\sigma)\phi_R^2\phi_I^2\sigma + (1+p\sin(ft))^4 \sigma\theta^2\phi_R^4 \geq 0, \end{aligned} \quad (8.30)$$

where

$$\theta = U_0 + V_0, \quad \zeta = dU_0 + V_0, \quad D = 1 - h_1 h_2, \quad \sigma = U_0 V_0 D, \quad s = 1 + D.$$

Next, we consider both species have the same diffusivity, i.e.,  $d = 1$ . We define  $\kappa = \frac{\sigma}{\theta^2}, \phi = \frac{\phi_I}{\phi_R}$ , and  $Z = \frac{2\beta^2}{\theta\phi_R}\chi$  and find that  $s = 2$  and  $\zeta = 0$ . We have  $0 < \kappa < \frac{1}{4}$  due to  $D > 0$ .

We can then rewrite (8.30) as

$$\begin{aligned} Z^4 + 4Z^3(1 + p \sin(ft)) + Z^2(1 + p \sin(ft))^2((1 - 4\kappa)\phi^2 + (5 + 4\kappa)) + 4(1 + p \sin(ft))^4\kappa \\ + 2Z(1 + p \sin(ft))^3((4\kappa + 1) + (1 - 4\kappa)\phi^2) + 4(1 + p \sin(ft))^4(1 - 4\kappa)\kappa\phi^2 \geq 0. \end{aligned} \quad (8.31)$$

If we assume  $\kappa_0 = (1 - 4\kappa)(1 + p \sin(ft))^2$ , so that  $0 < \kappa_0 < 1$ , and  $U = Z + (1 + p \sin(ft))$ , (8.31) can be rewritten as

$$(U^2 + \kappa_0\phi^2)(U^2 - \kappa_0) \geq 0. \quad (8.32)$$

By (8.32), we have

$$\chi \geq f(\beta), \quad (8.33)$$

where  $f(\beta) = -\frac{\theta}{2}(1 + p \sin(ft) \mp \sqrt{1 - 4\frac{\sigma}{\theta^2}}(1 + p \sin(ft)))\frac{\phi_R}{\beta^2}$ , and  $\phi_R < 0$  is necessary but not sufficient for instability, which is in accord with paper [121] when  $p = 0$ . We note that for more general case when  $p$  is nonzero, we actually have  $\tilde{\lambda} < -p$ . This is because  $\tilde{\lambda} = \lambda + p \sin(ft)$ , thus  $\tilde{\lambda}_{max} = -p$ .

We examine the stable boundary by using the following two different sets of parameters:

$$d_1 = 1, d_2 = 1, \tilde{a}_1 = 49, \tilde{a}_2 = 1, \tilde{b}_1 = 25, \tilde{b}_2 = 3, \tilde{c}_1 = 10, \tilde{c}_2 = 4. \quad (8.34)$$

$$d_1 = 1, d_2 = 4, \tilde{a}_1 = 49, \tilde{a}_2 = 1, \tilde{b}_1 = 25, \tilde{b}_2 = 3, \tilde{c}_1 = 10, \tilde{c}_2 = 4. \quad (8.35)$$

## ASYMMETRIC GAUSSIAN

Upon Fourier transforming (8.20) and using the definition of  $\beta$  we have

$$\hat{\phi} = e^{-\frac{\beta^2}{4}} (\cos(\alpha\beta) + i \sin(\alpha\beta)),$$

so that

$$\phi_R = e^{-\frac{\beta^2}{4}} \cos(\alpha\beta), \phi_I = e^{-\frac{\beta^2}{4}} \sin(\alpha\beta). \quad (8.36)$$

Use the explicit Fourier transform of (8.20) to rewrite (8.30) as

$$\begin{aligned}
& (\chi\beta^2 e^{\frac{\beta^2}{4}})^4 s^2 d + (\chi\beta^2 e^{\frac{\beta^2}{4}})^3 (1 + p \sin(ft))(2d\theta + s\zeta)s \cos(\alpha\beta) + \\
& (\chi\beta^2 e^{\frac{\beta^2}{4}})^2 (1 + p \sin(ft))^2 ((s\theta\zeta - \zeta^2 - s^2\sigma) \sin^2(\alpha\beta) + (d\theta^2 + 2s\zeta\sigma + s^2\sigma) \cos^2(\alpha\beta)) + \\
& (\chi\beta^2 e^{\frac{\beta^2}{4}}) (1 + p \sin(ft))^3 ((2s\sigma + \zeta\theta)\theta \cos^2(\alpha\beta) + (\theta^2 - 4\sigma)\zeta \sin^2(\alpha\beta)) \cos(\alpha\beta) + \\
& + (1 + p \sin(ft))^4 ((\theta^2 - 4\sigma) \sin^2(\alpha\beta) + \theta^2 \cos^2(\alpha\beta)) \sigma \cos^2(\alpha\beta) = 0,
\end{aligned} \tag{8.37}$$

$$\frac{d\tilde{\lambda}}{d\delta} = \frac{2}{\delta} \chi\beta^2 \frac{2(\chi\beta^2)d + (dU_0 + V_0)(1 + p \sin(ft))(\phi_R + i\phi_I) + (1 + d)\lambda}{(\chi\beta^2)(1 + d) + (dU_0 + V_0)(1 + p \sin(ft))(\phi_R + i\phi_I) + 2\lambda}, \tag{8.38}$$

If  $d = 1$ , (8.38) reduces to

$$\frac{d\tilde{\lambda}}{d\delta} = \frac{2}{\delta} \chi\beta^2. \tag{8.39}$$

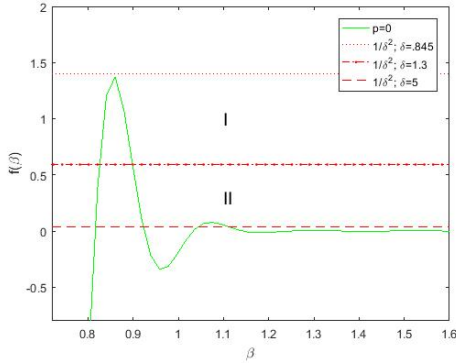
As  $\tilde{\lambda}$  is monotonically increasing, both eigenvalues cross the real axis once when  $d = 1$ . There is a single stability boundary in  $\delta$ .

Using the parameter set (8.34) and under  $p = 0$ , the unstable regions are visualized in **Fig. 8.1a**, where we plot  $f(\beta)$  against  $\beta$  and in **Fig. 8.1b**,  $\delta(\alpha)$  is shown for asymmetric Gaussian kernel function. The seasonal forcing doesn't play an obvious roll in the stability analysis process.

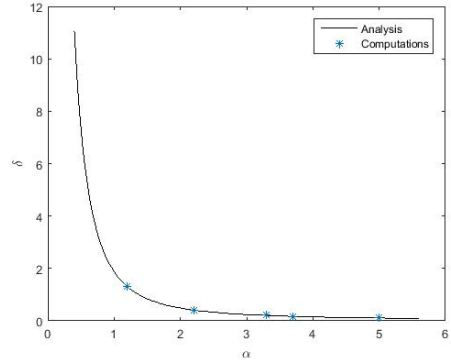
### 8.3 Computational Analysis

We solve (8.2) using a pseudo-spectral predictor-corrector method. Periodicity is assumed on the interval  $-L \leq x \leq L$  and  $L = 1500$ . The unknowns are updated in Fourier space where the spatial derivatives and convolutions are computed under sinusoidal temporal seasonal forcing. Nonlinear terms are computed in physical space and then transformed to Fourier space for the solution update with seasonal forcing. We integrate the solutions in time until steady state conditions or consistent solutions are obtained.

In our computations, we concentrate on the asymmetric Gaussian (8.20) with temporal



(a)  $f(\beta)$  and for asymmetric Gaussian function with  $p = 0$ .  $1/\delta^2$  for  $\delta = .845$ ,  $1.3$  and  $5$ . Parameters are give in (8.34). If  $\delta = .845$ , coexistence critical points  $(U_0, V_0)$  is stable. If  $\delta = 1.3$ , coexistence critical points  $(U_0, V_0)$  is unstable in the first region. If  $\delta = 5$ , coexistence critical points  $(U_0, V_0)$  is unstable in the first and second region.



(b)  $\delta(\alpha)$  for asymmetric Gaussian function with  $p = 0$ . Parameters are given in (8.34).

Figure 8.1:  $f(\beta)$  and  $\delta$

seasonal forcing. We mainly depict results for fully nonlinear patterns away from the stability boundary. We also capture and compare the nonlinear patterns near stability boundary under different sinusoidal disturbance via  $(1+p \sin(ft))$  through varying values of  $p$ . Different seasonal forcing can push the long-time behavior to different steady state. The amplitude declines and the width becomes narrower of the islands as the amplitude( $p$ ) of seasonal forcing increases. When  $\delta$  is far from the stability boundary, the semi-extinction, where the population is nonzero and above the truncation level of the calculations occurs in the nonlinear regime. Different sinusoidal patterns for both  $U$  and  $V$  are found and compared near the stability boundary under varying temporal seasonal forcing(different  $p$ ), in which the wave pattern is in accordance with [117] when  $p = 0$ .

We use the parameter sets (8.34) or (8.35) and  $L = 1500$  to find the following nonlinear patterns. The variables in our calculations are  $\delta$ ,  $\alpha$ ,  $p$  and initial conditions. The results in [121] for asymmetric non-local coupling indicate that there are generally many stable

patterns. In [121] it is shown that nonlinear patterns for asymmetric coupling consisted of stationary stationary arrays of islands, where the populations are nonzero, separated by dead-zones, where the populations are exponentially small and can be considered essentially extinct(true dead-zones). The island/dead-zone patterns propagate. Additionally, for some patterns the islands of  $V$  are separated by zones in which the population is nonzero and above the truncation level of the calculations(near-dead-zones or semi-extinction). It is also the similar case with temporal seasonal forcing here. For initial conditions, we perturb out limit cycle,  $(U_0, V_0)$  with a sin wave of mode  $m$  and consider initial conditions of the form

$$U(x, 0) = U_0 + 0.01 \sin(mx \frac{\pi}{L}), \quad (8.40a)$$

$$V(x, 0) = V_0 + 0.01 \sin(mx \frac{\pi}{L}), \quad (8.40b)$$

We present results for 5 different values of  $p$ ,  $p = 0, 0.1, 0.2, 0.3$  and  $0.5$ . In all cases, there are two different patterns that we find: (i) **traveling waves**, (ii) **colony formation(*type I*)**, (iii) **Adjustment of wave frequency**.

In the following table, we tabulate solutions for Travelling wave solutions and colony formation. S.E denotes if the wave extinct or not. It is not necessary that the same steady state pattern results from the same initial conditions.

Solutions for L=1500 with $i = 0, 1, 2, 3$ and $5$		
Nature of solution	I.C.	S.E.
$p.id100TWa$	m=5	Y
$p.id100TWb$	m=5	Y
$p.id150TWPDB$	m=5	N
$p.id100CIb$	m=5	Y
$p.id150CIIb$	m=5	N

Our notation for each pattern is as follows:

- Each pattern identifier begins with  $p$  and a number which indicates  $p$ . For example,  $p.35$  indicates  $p = 0.35$ .
- There is then the  $d$  which indicates  $\delta$ . For example,  $d100$  indicates  $\delta = 100$ .
- There then follows either  $TW$  and  $C$  indicating that the pattern is either a traveling wave or colony formation.  $CI$  indicates **colony formation(*type I*)** and  $CII$  indicates **colony formation(*type II*)** which is **Adjustment of wave frequency**.
- We note that there can be two patterns of the same type depending on whether (8.34) or (8.35) is employed. When this occurs, we distinguish the two parameters by appending an  $a$  or  $b$  to the end of the pattern for (8.34) and (8.35), respectively.
- We employ lowercase letters  $a$  or  $b$  to identify convention for  $\alpha = 1$ , and uppercase letters  $A$  or  $B$  to indicate  $\alpha = 0.75$ .

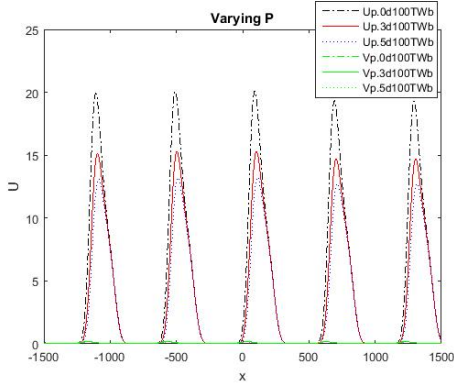
We list properties of these islands solutions,

- 1: The island is distributed around their midpoint. We solve the problem using a Fourier spectral method. The spatial derivatives and convolutions are computed in Fourier space. Nonlinear terms are computed in physical space and then transform to Fourier for the solution update. We assume periodicity on the interval  $-L \leq x \leq L$ , and  $L = 1500$ . We focus on asymmetric Gaussian (8.20). Furthermore, we show results for fully nonlinear patterns, away from the stability boundary with varying seasonal forcing. When  $p = 0$ , our results are similar in [121]. Besides, all of our results indicate that the transition at the stability boundary (Their structure is similar to a Trigonometry function curve), which is in accord with [121].
- 2: The amplitude and extent of the islands is slightly different for varying  $p$ . The larger the  $p$ , the smaller the amplitude and the narrower the extent. For these parameters, the tail of the island includes a small region where species with small  $p$  is essentially extinct.
- 3: The islands are surrounded by dead-zone where the populations exhibit semi-extinction. For example, in the dead-zone, say at  $x = 1050$  in **Fig. 8.2a**,  $U$  and  $V$  are of the order of

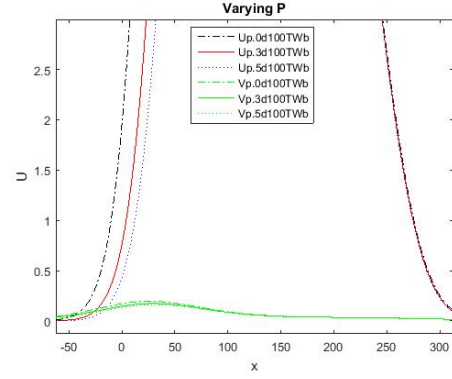
$10^{-4}$ .

Thus, within each dead-zone both species are essentially extinct. It is reasonable for  $V$  to be the more vulnerable species. Since the relative linear net growth rate  $\zeta$  for  $V$  in (8.35), is less than the unity in (8.34). The enhanced diffusivity for  $V$  in (8.35) can inhibit extinction for  $V$ , while some patterns found with (8.35) allow for the survival of  $V$ . The enhanced diffusion for  $V$ (convolution integral) may be small due to the interspecies competition be less effective in pushing  $V$  to extinct since  $V$  spreads more and competition may be small due to narrowness of the  $U$ -island. Under sinusoidal temporal seasonal forcing, i.e.,  $p$  is nonzero. We found patterns consisting of arrays with one larger and one smaller repeating format of islands. The larger of the temporal seasonal forcing, the smaller of the amplitude and the narrower of the extent. It is not unreasonable for the species. The enhanced temporal forcing weakens the enhancement of the amplitude and degree of extension. It is more reasonable because the amount of species varies more under isometric environment and thereby interspecies competition may be less effective due to seasonal forcing.

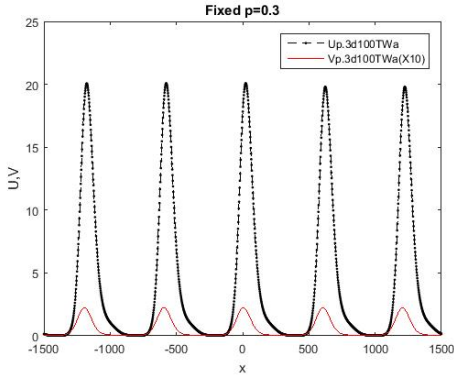
First, we illustrate traveling wave solutions. We consider a sample population. In **Fig. 8.2a**, the solution is characterized by 5 identical islands of nonzero population, separated by dead-zones where populations are essentially zero. As  $p$  is varied, the only difference is in the amplitude and width of islands in the computational domain. In order to clarify the structure of the islands, we amplify the **Fig. 8.2a** to get the **Fig. 8.2b**, where the solution is over just one island. As  $p$  increases, the amplitude is smaller and width becomes narrower. In **Fig. 8.2c**, we plot  $U$  and  $V$  under temporal seasonal forcing with  $p = 0.3$  at a fixed point in time.  $V$  for the  $Vp.3d100TWa$  solution is essentially zero. Additionally, we have scaled  $V$  for the  $Vp.3d100TWa$  solution by a factor of 10 in order to show both species in the same figure. It is the pattern that is constructed by 5 arrays of islands. We note that the islands of both species are asymmetric about their midpoint. We believe this is due to the isometric periodic conditions. We next illustrate the  $Up.3d150CIb$  solution. In **Fig. 8.3a**, we plot a



(a)  $U$  and  $V$  for  $Up.id100TWb$  and  $Vp.id100TWb$  solutions at a fixed time,  $i = 0, 3, \text{ and } 5$ .



(b) Amplified  $U$  and  $V$  for  $Up.id100TWb$  and  $Vp.id100TWb$  solutions at a fixed time,  $i = 0, 3, \text{ and } 5$ .



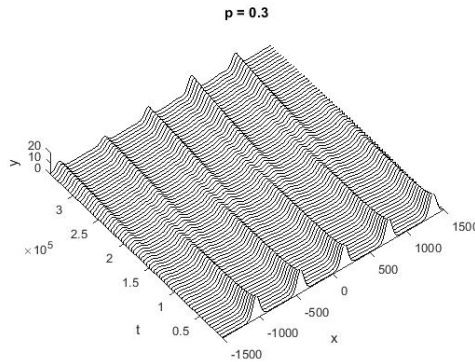
(c) With solid  $p = 0.3$ ,  $U$  and  $V$  for  $Up.3d100TWa$  and  $Vp.3d100TWa$  solutions at a fixed time.

Figure 8.2:  $Ud100TWa$  and  $Vd100TWa$  solutions at a fixed time.

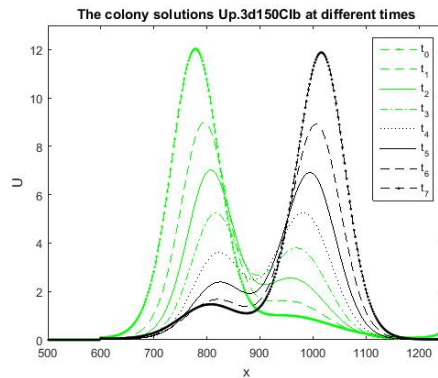
space-time surface of  $U$  as a function of  $t$  and  $x$ . As time evolves, islands propagate to the left, but there is also a counter propagating wave where the pattern jumps, the propagating island vanishes and a slightly displaced colony forms which continues the propagation. We term this behavior **Colony formation(type I)**.

In order to describe the process of **Colony formation(type I)**, we consider the  $Up.3d150CIb$  solution from  $x = 500$  to  $x = 1000$  in eight (uniformly spaced) values of  $t$ . From  $t_0$  to  $t_1$ , there is a small decrease in the amplitude of the original island. At  $t_2$ , there is incipient

colony formation as the parent island decreases in the amplitude. From  $t_3$  to  $t_4$ , the subsequent colony growth is at the expense of the original island. Finally, the colony pattern forms as the parent island is no longer visible ( $t_5 - t_7$ ) giving the appearance of jumps in the visualization in **Fig. 8.3b**. Still, the formed colony pattern is constructed by arrays of islands which are surrounded by dead-zones. We call this is **Colony formation(*type I*)**.



(a) *Surface plot of  $U(x, t)$  for  $Up.3d150CIb$  solution.*

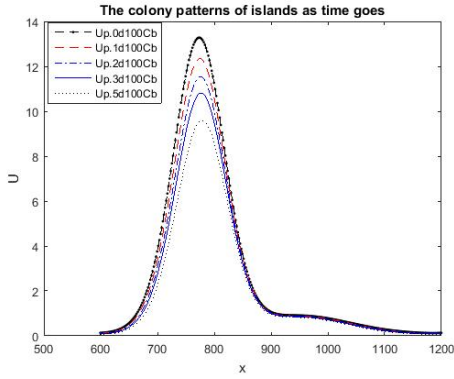


(b)  *$U(x, t)$  for  $Up.3d150CIb$  solution at times  $t_0 - t_7$ .*

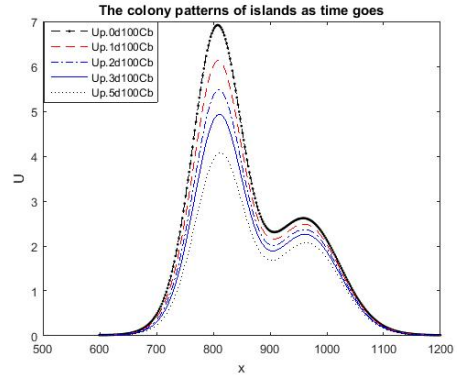
Figure 8.3:  *$Up.3d150CIb$  solution when time goes.*

In the series **Figs. 8.4**, we study the process of **Colony formation(*type I*)** for varying  $p$ .

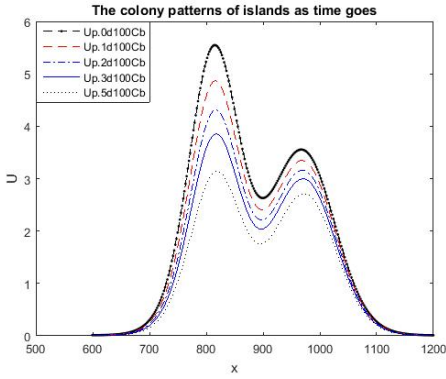
The larger amplitude of the seasonal forcing, the smaller of the amplitude of the island,



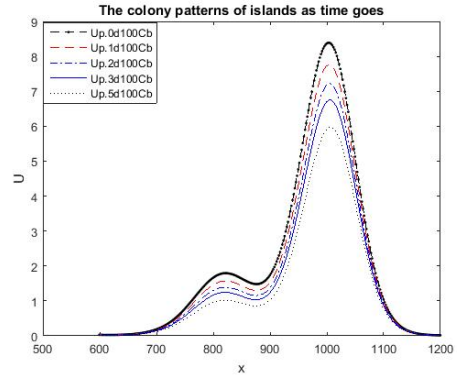
(a)  $U$  for  $Up.id100CIb$  solution where  $i = 0, 1, 2, 3$  and  $5$  at time  $t_0$ .



(b)  $U$  for  $Up.id100CIb$  solution where  $i = 0, 1, 2, 3$  and  $5$  at time  $t_1$ .



(c)  $U$  for  $Up.id100CIb$  solution where  $i = 0, 1, 2, 3$  and  $5$  at time  $t_2$ .



(d)  $U$  for  $Up.id100CIb$  solution where  $i = 0, 1, 2, 3$  and  $5$  at time  $t_3$ .

Figure 8.4:  $Ud150CIb$  solutions when time goes.

which is in accord with the conclusion in Traveling waves in **Figs. 8.2**.

Next, we analyze the process of colony formation for  $Vp.3d100CIIB$  solution. In **Fig. 8.5**, we show a space-time surface plot for  $V$  indicating the uniform propagation speed and the splitting of the amplitude of adjacent islands.

This can be further illustrated in **Fig. 8.6**, where line plots of  $U$  at various times encompass colony formation for the islands from  $x = -1500$  to  $x = 1500$ . From  $t_1$  to  $t_2$ , there is a small decrease in the amplitude of the parent island. At  $t_3$ , there is incipient colony formation as the parent island decreases in the amplitude. From  $t_4$  to  $t_5$ , the subsequent

colony growth is at the expense of the original island. At  $t_6$ , the traveling shaped pattern forms as the inter-media wave. Finally, the colony pattern forms as the parent island is no longer visible ( $t_7 - t_8$ ) giving the appearance of jumps in the visualization in **Fig. 8.6**. The formed colony pattern is constructed by arrays of islands which are travelling wave shaped and not semi-extinction. We call this as **Adjustment of wave frequency**.

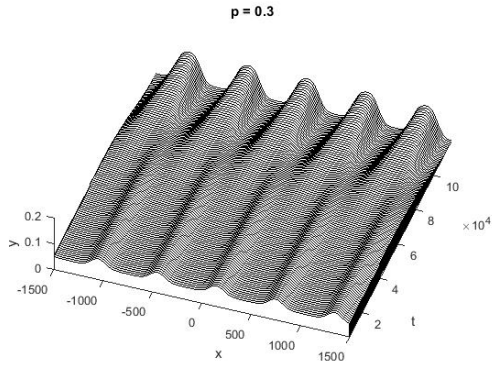


Figure 8.5:  $Vp.3d100CIIB$  solution when time goes.

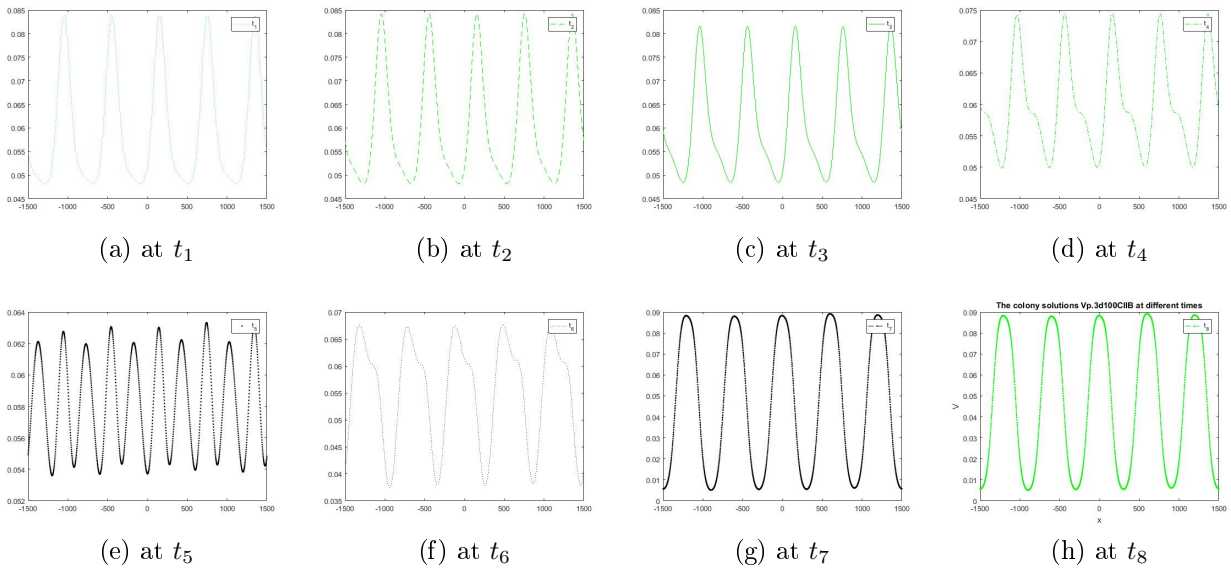


Figure 8.6:  $Vp.3d100CIIB$  when time goes.

## 8.4 Conclusions

We have focused on a system of competing populations with non-local interactions under sinusoidal temporal seasonal forcing. The system is a two-species extension of the Fisher equation with the non-locality due to convolution integrals against specified kernel functions and seasonal forcing by sinusoidal type functions. While previous studies have disregarded seasonal variation and have concentrated on depicting competing species at static structures, we considered the effect of asymmetry in the non-local interaction with seasonal forcing. We introduced three parameters (i)  $\delta$ , describing the extent of the non-local interaction, with  $\delta = 0$  corresponding to local interaction, (ii)  $\alpha$ , describing the degree of asymmetry, with  $\alpha = 0$  corresponding to symmetric non-local interaction, and (iii)  $p$ , describing the seasonal forcing, with  $p = 0$  corresponding to static structure and devoid of any dynamics.

We considered the case where the coexistence limit cycle solution,  $(U_0, V_0)$  is stable for local interactions and is de-stabilized as the non-locality ( $\delta$ ) is increased with sinusoidal seasonal forcing which is in accordance with previous studies [120, 121]. We further considered asymmetric Gaussian kernel function. We performed a linear stability analysis of  $(U_0, V_0)$  and determined stability boundary as a function of  $\alpha$  and  $p$ . As  $\delta$  is increased beyond the stability boundary, we found transition of **traveling waves**. We also found in most cases in island/dead-zone structure, but with a modulation in the amplitude and width of the islands with seasonal forcing (by  $p$ ). The larger of the  $p$  value, the lower of the amplitude and the narrower of the width.

In addition, we found patterns of colony formation, where an island generates a nearby colony which subsequently grows as the parent island declines, until the parent island has vanished and propagation continues with the colony with seasonal forcing. This stabilizes the adjacent dead-zone, leading to development of a small colony which then in turn serves to further deplete the parent island. We find two colony patterns: (i) **colony formation (type I)**; the formed colony pattern is constructed by arrays of islands which are surrounded by dead-

zones, (ii) **Adjustment of wave frequency**; the formed colony pattern is constructed by arrays of islands which are travelling wave shaped and not semi-extinction. We showed evolutionary colony patterns under varying seasonal forcing with sufficient non-localization. The larger amplitude of the seasonal forcing, the smaller of the amplitude of the island.

Understanding and quantifying seasonal forcing such as climatic conditions or patterns of human aggregation contribute to our fundamental understanding of epidemic dynamics; how micro-environmental changes can alter the fitness effects of mutations, which increase the rate of other genetic changes in a heterogeneous tissue containing not only cancer cells, but also stromal and immune cells. This paper is an extension to the ones that were studied earlier in population pattern formation [120, 121]. Future studies will have to take the temporal dynamics of tumors cells population into account to allow for a systems view on cancer progression.

## Chapter 9

# CONCLUSIONS

### 9.1 Part I: Optical Soliton Propagation in Metamaterials

The dynamics of soliton propagation through these optical metamaterials is governed by the nonlinear *Schrödinger's* equation(NLSE) with a few perturbation terms.

In the second chapter, we study soliton in optical metamaterials by the aid of collective variables. As an assumption, super-Gaussian soliton are selected to keep these pulses on a generalized setting. The numerical simulations of soliton parameter variation are given for specific values of the Super-Gaussian pulse parameters.

The dynamics of soliton parameters are studied numerically in this chapter by the aid of CV approach. Super-Gaussian soliton are considered. The two cases where  $m = 2$  and  $m = 4$  are studied numerically. This chapter stands on a strong foundation for further future work. While this chapter addresses Kerr law nonlinearity, later parabolic law nonlinearity will be studied. The results of those researches will be available soon.

In the third chapter, we recover bright 1-soliton solution, in optical metamaterials, by the aid of travelling wave hypothesis. This integration scheme is not applicable to retrieve bright soliton solutions for power law and dual-power law media. Also, it must be noted that there are soliton solutions that are reported earlier by this same integration scheme, namely traveling wave hypothesis applicable to five forms of nonlinearity that includes powers law and dual-power law [5, 6, 7]. However, for optical metamaterials, the situation is a little different. The governing equations have parameters that obey constraint relations, as discussed in Section-3, and thus prevent integrability by traveling wave hypothesis for power law and dual-power law.

Another disadvantage of this scheme is that one can retrieve only bright 1-soliton solutions and not dark or singular optical soliton. Later, the focus will be on the application of additional integration techniques to retrieve dark and singular soliton along with bright-dark combo optical soliton. The results of those research will be applied soon. Additionally, soliton perturbation theory

as well as quasi-stationary soliton solutions will be obtained. Finally, the quasi-particle theory, for suppression of intra-channel collision, will also be developed and reported.

In the fourth chapter, we retrieve soliton solutions to the NLSE in optical metamaterials with Kerr and parabolic law nonlinearity. The mapping method is applied to obtain these solutions. The results of this chapter came with certain constraints that must hold for these soliton to exist. These soliton solutions are recovered after a limiting process applied to doubly periodic functions when the modulus of ellipticity approached unity. This approach is therefore a very unique method to derive soliton solutions.

Later the results will be extended to the case when several perturbation terms will be considered. Better yet, soliton perturbation theory will be applied to give the adiabatic variation of these soliton parameters. Several other integration tools will be adopted to obtain soliton and other solutions. The results of those researches are awaited at this time.

In the fifth chapter, we obtain soliton solutions in optical metamaterials with five forms of nonlinear media. For Kerr law nonlinearity, there are three forms of soliton that are already reported earlier; therefore this paper derived only singular soliton (Type-II). For the remaining laws all soliton solutions and their derivations are comprehensively reported in this chapter. These solutions come with respective integrability criteria that are listed as constraint conditions. These solutions will be immensely useful in the literature of optical metamaterials.

These soliton solutions will be a great asset in all future investigations in this area of nonlinear optics. In the presence of perturbation terms these soliton will dictate the adiabatic parameter dynamics and other such features that will be obtained. The quasi-particle theory of optical soliton interaction will be reported. Later bifurcation analysis of soliton in optical metamaterials will be carried out. Other integration schemes will be applied to these models and those will reveal additional solutions, such as plane waves and periodic singular solutions. The semi-inverse variational principle will extract exotic soliton such as cosh-Gaussian pulses and bright-dark combo optical soliton. All of these are currently under investigation. The results of those research will be reported gradually and sequentially. Finally, the study will be extended to DWDM systems so that efficient

soliton transmission can be conducted in parallel, thus improving performance enhancement. These just form a tip of the iceberg.

In the sixth chapter, we apply SVP to extract bright and a couple of exotic soliton solutions. There are five nonlinear forms that were studied. For Kerr law nonlinearity, a couple of exotic soliton were obtained in addition to bright soliton. These are analytical solutions that are not exact. The numerical simulations are provided for each of the cases where the intensity of the soliton are plotted. There are domain restrictions, also referred to as constraint conditions for each such soliton that are listed. These guarantee the existence of such soliton studied in this chapter.

The results of this chapter stand on a very strong footing. Later, these research results will be applied to different situations such as optical couplers. DWDM systems and several others. In addition, polynomial law nonlinearity and triple-power law nonlinearity are to be considered in future.

In the seventh chapter, we give raman soliton solutions in optical metamaterials that is studied with polynomial law and triple law nonlinearity. The analytical results are supplemented with numerical simulation. This paper is an extension to the ones that were studied earlier in optical fibers [78, 79]. The results of this paper are encouraging to conduct further research in this field.

In future, additional perturbation terms such as Raman scattering, saturable amplifiers, higher order dispersions and several others will be included. Additionally, soliton in optical metamaterials will be considered with STD in addition to GVD. There are several other forms of nonlinear media that are yet to be explored. These are saturable law, exponential law, triple power law, threshold law. In particular the triple-power law nonlinearity that is a direct generalization of polynomial law will be studied. Although this law is investigated in optical fibers, the results are unknown at this stage for optical metamaterials. Furthermore, optical metamaterials will be handled in the context of couplers. From a mathematical perspective, the governing NLSE will be analyzed with fractional temporal evolution. This will lead to the attainment of slow-light soliton in optical metamaterials in order to address Internet bottleneck that is a growing concern in this industry. The results of all of these research will be gradually disseminated elsewhere.

## 9.2 Part II: Evolutionary Pattern Formation for Competing Populations under Seasonal Forcing

In this project, we are interested in finding persistence phenomenon in modeling competing species. In our model, we have considered the effect of asymmetry in the non-local interaction with seasonal forcing. We introduced three parameters (i)  $\delta$ , describing the extent of the non-local interaction, with  $\delta = 0$  corresponding to local interaction, (ii)  $\alpha$ , describing the degree of asymmetry, with  $\alpha = 0$  corresponding to symmetric non-local interaction, and (iii)  $p$ , describing the seasonal forcing, with  $p = 0$  corresponding to static structure and devoid of any dynamics.

We considered the case where the coexistence limit cycle solution,  $(U_0, V_0)$  is stable for local interactions and is de-stabilized as the non-locality ( $\delta$ ) is increased with sinusoidal seasonal forcing which is in accordance with previous studies [120, 121]. We further considered asymmetric Gaussian kernel function. We performed a linear stability analysis of  $(U_0, V_0)$  and determined stability boundary as a function of  $\alpha$  and  $p$ . As  $\delta$  is increased beyond the stability boundary, we found transition of **traveling waves**. We also found in most cases in island/dead-zone structure, but with a modulation in the amplitude and width of the islands with seasonal forcing (by  $p$ ). The larger of the  $p$  value, the lower of the amplitude and the narrower of the width.

In addition, we found patterns of colony formation, where an island generates a nearby colony which subsequently grows as the parent island declines, until the parent island has vanished and propagation continues with the colony with seasonal forcing. This stabilizes the adjacent dead-zone, leading to development of a small colony which then in turn serves to further deplete the parent island. We find two colony patterns: (i) **colony formation (type I)**; the formed colony pattern is constructed by arrays of islands which are surrounded by dead-zones, (ii) **Adjustment of wave frequency**; the formed colony pattern is constructed by arrays of islands which are travelling wave shaped and not semi-extinction. We showed evolutionary colony patterns under varying seasonal forcing with sufficient non-localization. The larger amplitude of the seasonal forcing, the smaller of the amplitude of the island.

Understanding and quantifying seasonal forcing such as climatic conditions or patterns of

human aggregation contribute to our fundamental understanding of epidemic dynamics; how micro-environmental changes can alter the fitness effects of mutations, which increase the rate of other genetic changes in a heterogeneous tissue containing not only cancer cells, but also stromal and immune cells. This chapter is an extension to the ones that were studied earlier in population pattern formation [120, 121]. Future studies will have to take the temporal dynamics of tumors cells population into account to allow for a systems view on cancer progression.

## BIBLIOGRAPHY

- [1] A. Biswas, K.R. Khan M.F. Mahmood, M. Belic, Bright and dark solitons in optical metamaterials, *Optik* 125(13)(2014) 3299-3302.
- [2] A. Biswas, M. Mirzazadeh, M. Savescu, D. Milovic, K. R. Khan, M. F. Mahmood & M. Belic. "Singular solitons in optical metamaterials by ansatz method and simplest equation approach". *Journal of Modern Optics*. Volume 61, Issue 19, 1550-1555. (2014).
- [3] A. Biswas, M. Mirzazadeh, M. Eslami, D. Milovic, M. Belic, Solitons in optical metamaterials by functional variable method and first integral approach, *Frequenz* 68(11-12)(2014) 525-530.
- [4] G. Ebadi, A. Mohavir, J.V. Guzman, K.R. Khan, M.F. Mahmood, L. Moraru, A. Biswas, M. Belic, Solitons in optical metamaterials by F-expansion scheme, *Optoelectron, Adv. Mater.-Rapid Commun* 8(9-10)(2014) 828-834.
- [5] A. Biswas, M. Fessak, S. Johnson, S. Beatrice, D. Milovic, Z. Jovanoski, R. Kohl & F. Majid. "Optical soliton perturbation in non-Kerr law media: Traveling wave solution". *Optics and Laser Technology*, Volume 44, Issue 1, 1775-1780. (2012).
- [6] M. Savescu, K. R. Khan, P. Naruka, H. Jafari, L. Moraru & A. Biswas. "Optical solitons in photonic nano-waveguides with an improved nonlinear Schrödinger's equation". *Journal of Computational and Theoretical Nanoscience*. Volume 10, Number 5, 1182-1191. (2013).
- [7] M. Savescu, K. R. Khan, R. Kohl, L. Moraru, A. Yildirim & A. Biswas. "Optical soliton perturbation with improved nonlinear Schrödinger's equation in nanofibers". *Journal of Nanoelectronics and Optoelectronics*. Volume 8, Number 2, 208-220. (2013).
- [8] Z. Jovanoski, D. R. Rowland. "Variational analysis of solitary waves in a homogeneous cubic-quintic nonlinear medium". *Journal of Modern Optics*. 48(7) (2001) 1179-1193.
- [9] M. Saha, A. K. Sarma. "Modulation instability in nonlinear metamaterials induced by cubic-quintic nonlinearities and higher order dispersive effects". *Optics Communications*. 291 (2013) 321-325.
- [10] E. V. Krishnan, Y. Peng. "Two classes of new exact solutions to  $(2+1)$ -dimensional breaking soliton equation". *Journal of the Physical Society of Japan*. 44(5) (2005) 896-897.
- [11] E. V. Krishnan, A. Biswas. "Solutions to the Zakharov-Kuznetsov equation with higher order nonlinearity by mapping and ansatz methods". *Physics of Wave Phenomena*. 18(4) (2010) 256-261.

- [12] Y. Peng. "Exact periodic wave solutions to a new Hamiltonian amplitude equation". *Journal of the Physical Society of Japan*. 72(6) (2003) 1356-1359.
- [13] Y. Peng. "Exact Solutions and Localized Structures for a (3+1)-Dimensional Burgers Equation". *Acta Physica Polonica A* . 122(1) (2012) 20-24.
- [14] D.F. Lawden. "Elliptic Functions and Applications". *Springer Verlag*. New York, NY. USA.(1989).
- [15] A.H. Arnous, M. Mirzazadeh, S. Moshokoa, S. Medhekar, A. Biswas, M. Belic. "Solitons in optical metamaterials with trial solutons approach and Bäcklund transform of Raccati equation", *J. Comput, Theor. Nanosci.* 12(12)(2015) 5940-5948.
- [16] M.A. Baqir, P.K. Choudhury. "Waves in coaxial optical fiber under DB boundaries", *Optik*. 125(2014)2950-2953.
- [17] M.A. Baqir, P.K. Choudhury. "Investigation of uniaxial isotropic chiral metamaterial waveguide with perfect electromagnetic conductor loading", *Optik*. 126(2015)1228-1232.
- [18] A. Biswas, S. Konar. "Introduction to Non-Kerr Law Optical solitons", *CRC Press, Boca Raton, FL, USA*, 2006.
- [19] H. Erfaninia, A. Rostami. "Group velocity reduction in multilayer metamaterial waveguide ", *Optik*. 124(2013)1230-1233.
- [20] V.G. Vaselago. "Electrodynamics of media with simultaneous negative electric permittivity and magnetic permeability", *Sov. Phys. Usp.* 10(1967)509-514.
- [21] Y. Xiang, X. Dai, S. Wen, J. Guo & D. Fan. "Controllable Raman soliton self-frequency shift in nonlinear metamaterials". *Phys. rew.* A 84 (2011) 033815.
- [22] J. Liu, K. Zhang, X. Liu, Z. Zhang, Z. Jin, X. He & G. Ma. "Switchable metamaterials for enhancing and localizing electromagnetic field at terahertz band". *Optics Express* 25(13) (2017) 13944-13952.
- [23] V.M. Shalaev, Optical negative-index metamaterials, *Nat. Photonics* 1 (2007) 41-48.
- [24] K.R.Khan, K. Mnaymneh, H. Awad, I. Hasan, T. Hall, Optical wave propagation in photonic crystal metamaterials, *Appl. Phys. A* 117(2)(2014) 629-634.
- [25] S. Wen, Y. Xiang, W. Su, Y. Hu, X. Fu, D. Fan, Role of anomalous self-steepening effect in modulation instability in negative-index material, *Opt. Express* 14(2006) 1568.
- [26] S. Wen, W. Wang, W. Su, Y. Xiang, X. Fu, D. Fan, Modulation instability in nonlinear negative-index material, *Phys. Rev E* 73(2006) 036617.

- [27] K.R. Khan, M. Mahmood, A. Biswas, Coherent super-continuum generation in PCF at visible and near infrared wavelengths, *IEEE J. Sel. Top. Quantum Electron.* 20(5)(2014) 7400309.
- [28] A. Biswas, M. Mirzazadeh, D. Milovic, K.R. Khan, M.F. Mahmood, M. Belic, Singular and topological solitons in optical metamaterials by Kudryashov's method and G'/G-expansion scheme, *J. Comput. Theor. Nanosci.* 12(12)(2015) 5630-5635.
- [29] E.V. Krishnan, M. Al Gabshi, Q. Zhou, K.R. Khan, M.F. Mahmood, Y. Xu, A. Biswas, M. Belic, Solitons in optical metamaterials by mapping method, *J. Optoelectron. Adv. Mater.* 17(3-4)(2015) 511-516.
- [30] Y. Xu, J. Vega-Guzman, D. Milovic, M. Mirzazadeh, M. Eslami, M.F. Mahmood, A. Biswas, M. Belic, Bright and exotic solitons in optical metamaterials by semi-inverse variational principle *J. of Nonlinear Optical & Materials.* 24(4)(2015)1550042(19 pages).
- [31] A. Biswas, M. Mirzazadeh, M. Eslami, D. Milovic and M. Belic, Solitons in optical metamaterials by functional variable method and first integral approach *Frequenz.* 68(11-12)(2014)525-530.
- [32] S. I. Fewo and T. C. Kofane, A collective variable approach for optical solitons in cubic-quintic complex Ginzburg-Landau equation with third order dispersion *Optics Communications.* 281(10)(2008)2893-2906.
- [33] P. Green, D. Milovic, D. Lott and A. Biswas, Dynamics of Gaussian optical solitons by collective variable method *Applied Mathematics and Information Sciences.* 2(3)(2008)259-273.
- [34] A. B. Moubissi, K. Nakkeeran, P. T. Dinda and T. C. Dinda and T. C. Kofane, Non-lagrangian collective variable approach for optical soliton in fibers *Journal of Physics A.* 34(2001)129-136.
- [35] S. Shwetanshumala and A. Biswas, Femtosecond pulse propagation in optical fibers under higher order effects: A collective variables approach *International Journal of Theoretical Physics.* 47(6)(2008)1699-1708.
- [36] S. Shwetanshumala, Temporal solitons in nonlinear media modeled by modified complex Ginzburg-landau equation under collective variables approach *International Journal of Theoretical Physics.* 48(4)(2008)1122-1131.
- [37] Y. Xu, Q. Zhou, A. H. Bhrawy, K. R. Khan, M. F. Mahmood, K. R. Khan and M. Belic, Bright solitons in optical metamaterials by traveling wave hypothesis *Optoelectronics and Advanced Materials-Rapid Communications.* 9(3-4)(2015)384-387.
- [38] S. Atif, D. Milovic, E. Zerrad & A. Biswas. "Solitons in relativistic plasmas by He's variational principle". *Applied Physics Research.* 2(2), 11-16. (2010).

- [39] A. H. Bhrawy, A. A. Alshaery, E. M. Hilal, K. R. Khan, M. F. Mahmood & A. Biswas. "Optical soliton perturbation with spatio-temporal dispersion in parabolic and dual-power law media by semi-inverse variational principle". *Optik*. Volume 125, 4945-4950. (2014).
- [40] A. Biswas. "Temporal 1-soliton solution of the complex Ginzburg-Landau equation with power law nonlinearity". *Progress in Electromagnetics Research*. Volume 96, Page 1-7. (2009).
- [41] A. Biswas, D. Milovic & E. Zerrad. "Optical soliton perturbation with log law nonlinearity by He's semi-inverse variational principle". *Optics and Photonics Letters*. Volume 3, Number 1, 1-5. (2010).
- [42] A. Biswas & D. Wheeler. "Optical solitons with bandwidth limited amplification in a non-Kerr law media". *Optica Applicata*. Volume 40, Number 4, 801-809. (2010).
- [43] A. Biswas, D. Milovic & D. Milic. "Solitons in  $\alpha$ -helix proteins by He's variational principle". *International Journal of Biomathematics*. Volume 4, Number 4, 423-429. (2011).
- [44] A. Biswas & D. Milovic. "Chiral solitons with Bohm potential by He's variational principle". *Physics of Atomic Nuclei*. Volume 74, Number 5, 781-783. (2011).
- [45] A. Biswas, D. Milovic & R. Kohl. "Optical soliton perturbation in a log law medium with full nonlinearity by He's semi-inverse variational principle". *Inverse Problems in Science and Engineering*. Volume 20, Number 2, 227-232. (2012).
- [46] A. Biswas, S. Johnson, M. Fessak, B. Siercke, E. Zerrad & S. Konar. "Dispersive optical solitons by semi-inverse variational principle". *Journal of Modern Optics*. Volume 59, Number 3, 213-217. (2012).
- [47] A. Biswas. "Soliton solutions of the perturbed resonant nonlinear Schrödinger's equation with full nonlinearity by semi-inverse variational principle". *Quantum Physics Letters*. Volume 1, Number 2, 79-89. (2012).
- [48] A. Biswas, D. Milovic, M. Savescu, M.F. Mahmood, K.R. Khan & R. Kohl. "Optical soliton perturbation in nano fibers with improved nonlinear Schrödinger equation by semi-inverse variational principle". *Journal of Nonlinear Optical Physics & Materials*, Volume 21, Issue 4, 1250054. (2012).
- [49] A. Biswas, K. Khan, M. F. Mahmood, M. Belic. "Bright and dark solitons in optical metamaterials". *Optik*. Volume 125, Issue 13, 3299-3302. (2014).
- [50] A. Biswas, J. Vega-Guzman, A. A. Alshaery, E. M. Hilal, A. H. Bhrawy, M. A. Banaja, S. A. Alkhateeb & M. F. Mahmood. "Bright and exotic optical solitons with LPD model by semi-inverse variational principle". Submitted.

- [51] G. Ebadi, A. Mojaver, J. Vega-Guzman, K. R. Khan, M. F. Mahmood, L. Moraru, A. Biswas & M. Belic. "Solitons in optical metamaterials by  $F$ -expansion scheme". *Optoelectronics and Advanced Materials - Rapid Communications*. Volume 8, Numbers 9-10. 828-832. (2014).
- [52] P. D. Green, D. Milovic, D. A. Lott & A. Biswas. "Optical solitons with higher order dispersion by semi-inverse variational principle". *Progress in Electromagnetic Research*. Volume 102, 337-350. (2010).
- [53] R. Kohl, D. Milovic, E. Zerrad & A. Biswas. "Optical solitons by He's variational principle in non-Kerr law media". *Journal of Infrared Millimeter and Terahertz Waves*, Volume 30, Number 5, 526-537. (2009).
- [54] E. V. Krishnan, M. Al Gabshi, Q. Zhou, K. R. Khan, M. F. Mahmood, Y. Xu, A. Biswas & M. Belic. "Solitons in optical metamaterials by mapping method". *Journal of Optoelectronics and Advanced Materials*. Volume 17, Numbers 3-4, 511-516. (2015).
- [55] T. Ozis & A. Yildirim. "Application of He's semi-inverse method to the nonlinear Schrödinger equation". *Computers and Mathematics with Applications*. Volume 54, Issues 7-8, 1039-1042. (2007).
- [56] S. Shwetanshumala. "Temporal solitons of modified complex Ginzburg-Landau Equation". *Progress in Electromagnetic Research Letters*. Volume 3, 17-24. (2008).
- [57] E. Topkara, D. Milovic, A. K. Sarma, F. Majid & A. Biswas. "A study of optical solitons with Kerr and power law nonlinearities by He's variational principle". *Journal of the European Optical Society*. Volume 4, 09050. (2009).
- [58] M. Veljkovic, Y. Xu, D. Milovic, M. F. Mahmood, A. Biswas & M. R. Belic. "Super-Gaussian solitons in optical metamaterials using collective variables". To appear in *Journal of Computational and Theoretical Nanoscience*.
- [59] Y. Xu, Z. Jovanoski, A. Bouasla, H. Triki, L. Moraru & A. Biswas. "Optical solitons in multi-dimensions with spatio-temporal dispersion and non-Kerr law nonlinearity". *Journal of Nonlinear Optical Physics and Materials*. Volume 22, Number 3. 1350035. (2013).
- [60] Y. Xu, Q. Zhou, A. Bhrawy, K. R. Khan, M. F. Mahmood, A. Biswas & M. Belic. "Bright solitons in optical metamaterials by traveling wave hypothesis". *Optoelectronics and Advanced Materials - Rapid Communications*. Volume 9, Numbers 3-4, 384-387. (2015).
- [61] M. Younis & S. T. R. Rizvi. "Optical solitons for ultrashort pulses in nano fibers". *Journal of Nanoelectronics and Optoelectronics*. Volume 10, Issue 2, 179-182. (2015).

- [62] Q. Zhou, D. Yao & F. Chen. "Analytical study of optical solitons in media with Kerr and parabolic law nonlinearities". *Journal of Modern Optics*. Volume 60, Issue 19, 1652-1657. (2013).
- [63] Q. Zhou, D. Yao, F. Chen & W. Li. "Optical solitons in gas-filled, hollow-core photonic crystal fibers with inter-modal dispersion and self-steepening". *Journal of Modern Optics*. Volume 60, Issue 10, 854-859. (2013).
- [64] Q. Zhou. "Analytical solutions and modulational instability analysis to the perturbed nonlinear Schrödinger equation". *Journal of Modern Optics*. Volume 61, Issue 6, 500-503. (2014).
- [65] Q. Zhou. "Analytic study on solitons in the nonlinear fibers with time-modulated parabolic law nonlinearity and Raman effect". *Optik*. Volume 125, Issue 13, 3142-3144. (2014).
- [66] Q. Zhou, Q. Zhu, Y. Liu, A. Biswas, A. H. Bhrawy, K. R. Khan, M. F. Mahmood & M. R. Belic. "Solitons in optical metamaterials with parabolic law nonlinearity and spatio-temporal dispersion". *Journal of Optoelectronics and Advanced Materials*. Volume 16, Numbers 11-12, 1221-1225. (2014).
- [67] C. Duque, N. Portas-Montenegro, S. Cavalcanti & L. Oliveria, Photonic band structure evolution of a honeycomb lattice in presence of external magnetic fields, *Journal of Applied Physics* 3. 034303. 105-109(2009).
- [68] K. Khan, M.F. Mahmood, A. Biswas & M. Belic, Nonlinear pulse propagation in optical metamaterial, *Journal of Computational and Theoretical Nanoscience*. 12(11)(2015) 4837-4841.
- [69] A. D. Boardman, Y. G. Rapoport, N. King & V. Malnev, Creating stable gain in active metamaterials, *Journal of the Optical Society of America B*. 24(2007) 419-430.
- [70] A. D. Boardman & P. Egan, Novel nonlinear surface and guided TE waves in asymmetric LHM waveguides, *Journal of Optics A: Pure and Applied Optics*. 11(11)(2009) 114032. 1-10
- [71] A. D. Boardman, R. C. Mitchell-Thomas, N. King & Y. G. Rapoport, Bright spatial solitons in metamaterials *Optics Communications*. 283(2010) 1585-1597.
- [72] A. D. Boardman, O. Hess, R. C. Mitchell-Thomas, Y. G. Rapoport & L. Velasco, Temporal solitons in magneto-optic and metamaterial waveguides *Photonics and Nanostructures-Fundamentals and Applications*. 8(2010) 228-243.
- [73] A. D. Boardman, V. V. Giamalsky, Y. S. Kivshar, S. V. Koshevaya, M. Lapine, N. M. Litchinitser, N. V. Malnev, M. Noginov, Y. G. Rapoport & V. M. Shalaev, Active and tunable metamaterials, *Laser and Photonics Reviews*. 5(2)(2011) 287-307.

- [74] W. Bogaerts, R. Baets, P. Dumon, V. Wiaux, S. Beckx, D. Taillaert, B. Luyssaert, J. Van Campenhout, P. Bienstman & D. Van Thourhout. Nanophotonic waveguides in solicom-on-insulator fabrication with CMOS technology, *Journal of Lightwave Technology*. 23(1)(2005) 401-412.
- [75] J. Cardenas, C. B. Potras, J. T. Robinson, K. Preston, L. Chen & M. Lipson. Low loss etchless silicon photonic waveguides, *Optics Express*. 17(6)(2009) 4752-4757.
- [76] C. V. Raman(1928). A new radiation, *Indian J. Phys.*. 2: 387-398. Retrieved by 14 April 2013.
- [77] S. Wen, Y. Xiang, W. Su, Y. Hu, X. Fu & D. Fan. Role of anomalous self-steepening effect in modulation instability in negative-index material, *Optics Express*. 14(2006)1568-1575.
- [78] A. H. Bhrawy, A. A. Alshaery, E. M. hilal, D. Milovic, L. Moraru, M. Savescu & A. Biswas. Optical solitons with polynomial and triple power law nonlinearities and spatio-temporal dispersion, *Proceedings of the Romanian Academy, Series A*. 15(3)(2014)235-240.
- [79] A. Biswas & D. Milovic. Traveling wave solutions of the nonlinear Schrödinger's equation in non-Kerr law media, *Communications in Nonlinear Science and Numerical Simulation*. 14(5)(2009)1993-1998.
- [80] Y. Xu, M. Savescu, K. R. Khan, M. F. Mahmood, A. Biswas & M. Belic. Soliton propagation through nanoscale waveguides in optical metamaterials, *Optics and Laser Technology*. 7(2016)177-186.
- [81] Y. Xu, J. Bega-Guzman, D. Milovic, M. Mirzazadeh, M. Eslami, M. Mahmood, A. Biswas, and M. Belic. Bright and exotic solitons in optical metamaterials by semi-inverse variatioanal principle, *Journal of Nonlinear Optical Phsics & Material*. 24(4)(2015)177-186.
- [82] R. Gauthier, K. Mnaymneh, S. Newman, K. Medri and C. Raup. Hexagonal array photonic crystal with photonic quasi-crystal with photonic quasi-crystal defect inclusion, *Optical Materials*. 31(2008)51-57.
- [83] E. Istrate and E. H. Sargent. Photonic crystal heterostructures and interfaces, *Review of Modern Physics*. 78(2006)455.
- [84] J. D. Joannopoulos, S. G. Johnson, R. D. Meade and J. N. Winn. Photonic Crystals, *Molding the Flow of Light*. 2nd Edition, Princeton University Press, NJ.(2008).
- [85] K. Khan, K. Mnaymneh, H, Awad, I. Hasan and T. Hall. Optical waves in photonic crystal metamaterials, *Journal of Applied Physics*. 117(2)(2014)629-634.

- [86] K. Khan, K. Mnaymneh, H. Awad, I. Hasan and T. Hall. Slow light propagation in tunable nanoscale photonic crystal cavity filled with nematic liquid crystals, *Optical Engineering*. 53(10)(2014)102705, 1-7.
- [87] J. B. Pendry. Negative refraction makes a perfect lens, *Physical Review Letters*. 85(18)(2000)3966-3969.
- [88] M. Saha and A. K. Sarma. Modulational instability in nonlinear metamaterials induced by cubic-quintic nonlinearities and higher order dispersive effects, *Optics Communications*. 291(2013)321-325.
- [89] D. Taillaert, H. Chong, P. Borel L. Frandsen, R. M. de La Rue and R. Baets. A compact two-dimensional grating couple used as a polarization splitter, *IEEE Photonic Technology Letters*. 15(9)(2003)1249-1251.
- [90] S. Wen, W. Wang, W. Su, Y. Xiang, X. Fu and D. Fan. Modulation instability in nonlinear negative-index material, *Physical review E*. 73(2006)036617.
- [91] Y. Xu, Q. Zhou, A. Bhrawy, K. R. Khan, M. F. Mahmood, A. Biswas and M. Belic. Bright solitons in optical metamaterials by traveling wave hypothesis, *Optoelectronics and Advanced Materials Rapid Communications*. 9(3-4)(2015)384-387.
- [92] Y. Xu, M. Savescu, K. R. Khan, M. F. Mahmood, A. Biswas and M. Belic. Soliton propagation through nanoscale waveguides in optical metamaterials, *Optics and Laser Technology*. 77(2016)177-186.
- [93] M. Younis and S. T. R. Rizvi. Optical solitons for ultrashort pulses in nano fibers, *Journal of Nanoelectronics and Optoelectronics*. 10(2)(2015)179-182.
- [94] Y. Zheng, Y. Fu, X. Chen, W. T. Lu and H. Agren. Surface polaritons in two-dimensional left-handed photonic crystals, *Physical Review E*. 73(2006)066625.
- [95] Q. Zhou, D. Yao, F. Chen and W. Li. Optical solitons in gas-filled, hollow-core photonic crystal fibers with inter-modal dispersion and self-steepening, *Journal of Modern Optics*. 60(10)(2013)854-859.
- [96] David S. Khoury, Mary R. Myerscough, and Andrew B. Barron. A Quantitative Model of Honey Bee Colony Population Dynamics, *PLoS ONE*, **6(4)**, 2011. doi.org/10.1371/journal.pone.0018491
- [97] Matt I. Betti, Lindi M. Wahl, Mair Zamir. Effects of Infection on Honey Bee Population Dynamics: A Model, *PLoS ONE*, **9(10)**, 2014. doi.org/10.1371/journal.pone.0110237
- [98] David J. Torres, Ulises M. Ricoy, Shanae Roybal. Modeling Honey Bee Populations, *PLoS ONE*, **10(7)**, 2015. doi.org/10.1371/journal.pone.0130966

- [99] Fabio Augusto Milner, Curtis Allan Patton. A diffusion model for host–parasite interaction, *Journal of Computational and Applied Mathematics*, **154(2)**, 273302, 2003.
- [100] Y. Sidorenko, J. Schulze-Horsel, A. Voigt, U. Reichl, and A. Kienle. Stochastic population balance modeling of influenza virus replication in vaccine production processes, *Chemical Engineering Science*, **63(1)**, 157169, 2008.
- [101] Steven Riley. Large-Scale Spatial-Transmission Models of Infectious Disease, *Science*, **316(5829)**, 1298-301, 2007.
- [102] Clint J. Perry, Eirik Sovik, Mary R. Myerscough and Andrew B. Barron. Rapid behavioral maturation accelerates failure of stressed honey bee colonies, *PNAS*, **112(11)**, 3427-3432, 2013. doi: 10.1073/pnas.1422089112
- [103] David S. Khoury, Andrew B. Barron, and Mary R. Myerscough. Modelling Food and Population Dynamics in Honey Bee Colonies, *PLoS ONE*, **8(5)**, 2013. doi:10.1371/journal.pone.0059084
- [104] Nicholas W. Calderone. Insect Pollinated Crops, Insect Pollinators and US Agriculture: Trend Analysis of Aggregate Data for the Period 1992–2009. *PLoS ONE*, **7(5)**, 2012. doi:10.1371/journal.pone.0037235
- [105] Suzanne M. O’Regan, John E. Vinson, and Andrew W. Park. Interspecific Contact and Competition May Affect the Strength and Direction of Disease-Diversity Relationships for Directly Transmitted Microparasites, *The American Naturalist*, **186(4)**, 480-494, 2015.
- [106] Marilyn J. Roossinck. Symbiosis versus competition in plant virus evolution, *Nature Review Microbiology*, **3**, 917-924, 2005.
- [107] Kirill S. Korolev, Joao B. Xavier, and Jeff Gore. Turning ecology and evolution against cancer, *Nature Reviews Cancer*, **14**, 371-380, 2014.
- [108] N.F. Britton. Aggregation and the competitive exclusion principle, *J. Theor. Biol.*, **136(1)**, 57-66, 1989.
- [109] Dylan Z. Childs, Michael Boots. The interaction of seasonal forcing and immunity and the resonance dynamics of malaria, *J. R. Soc. Interface*, **7**, 307-319, 2010.
- [110] Caroline W. Kabaria, Fabrizio Molteni, Renata Mandike, Frank Chacky, Abdisalan M. Noor, Robert W. Snow, and Catherine Linard. Mapping intra-urban malaria risk using high resolution satellite imagery: a case study of Dar es Salaam, *International Journal of Health Geographics*, 15-26, 2016. DOI 10.1186/s12942-016-0051-y
- [111] Jens M. Olesen. Constanti Stefanescu and Anna Traveset. Strong, Long-Term Temporal Dynamics of an Ecological Network, *PLoS One*, **6(11)**: e26455, 2011. DOI: 10.1371/journal.pone.0026455.

- [112] Jones, P., Harpham, C., Kilsby, C., Glenis, V., Burton, A., 2009. *Projections of Future Daily Climate for the UK from the Weather Generator. Technical Report.*
- [113] D. A. Ewing, C.A. Cobbold, B.V. Purse, M.A. Nunn, S.M. White. Modelling the effect of temperature on the seasonal population dynamics of temperate mosquitoes, *Journal of Theoretical Biology*, **400**, 65–79, 2016.
- [114] N.F. Britton. Spatial structures and periodic travelling waves in an integro-differential reaction-diffusion population model, *SIAM. J. Appl. Math.*, **50(6)**, 1663-1688, 1990.
- [115] M.A. Fuentes, M.N. Kuperman, and V.M. Kenkre. Nonlocal interaction effects on pattern formation in population dynamics, *Phys. Rev. Lett.*, **91(15)**, 158104, 2003.
- [116] M.A. Fuentes, M.N. Kuperman, and V.M. Kenkre. Analytical considerations in the study of spatial patterns arising from nonlocal interaction effects, *J. Phys. Chem. B*. **108(29)**, 10505-10508, 2004
- [117] S. Genieys, V. Volpert, and P. Auger. Pattern and waves for a model in population dynamics with nonlocal consumption of resources, *Math. Model. Nat. Phenom*, **1(1)**, 65-82, 2006.
- [118] S. Genieys, N. Bessonov, and V. Volpert. Mathematical model of evolutionary branching, *Math. Comput. Model*, **49**, 2109-2115, 2009.
- [119] B. Perthame, S. Genieys. Concentration in the nonlocal Fisher equation: the Hamilton-Jacobi limit, *Math. Model. nat. Phenom*, **2**, 135-151, 2007.
- [120] B.L. Segal, V. A. Volpert, and A. Bayliss. Pattern formation in a model of competing populations with nonlocal interactions, *Physica D*, **253**, 12-22, 2013.
- [121] M.C. Tanzy, V.A. Volpert, A. Baylis, M.E. Nehrkorn. Stability and pattern formation for competing populations with asymmetric nonlocal coupling, *Mathematical Biosciences*, **246**, 14-26, 2013.
- [122] Greaves M., Maley CC.. Clonal evolution in cancer, *Nature*, **481(7381)**, 3D6-13, 2012
- [123] Barcellos-Hoff MH, Lyden D, and Wang TC. The evolution of the cancer niche during multistage carcinogenesis, *Nat Rev Cancer*, **13(7)**, 511-8, 2013.
- [124] Niko Beerenwinkel, Roland F. Schwarz, Moritz Gerstung, and Florian Markowetz. Caner Evolution: Mathematical Models and Computational Inference, *System Biology*, **64(1)**: e1-e25, 2015.

